Interacting Elastic Rods

Colin Taylor

August 31, 2015

Abstract

This study presents a general theory of interacting elastic curves in two dimensions before moving into a more general model of interacting elastic rods in three dimensions. It begins by looking at methods of modelling a single continuous two dimensional curve, before making a first attempt at modelling interactions between such curves. Finding that a discrete model would be more appropriate, the theory of two dimensional discrete curves is introduced along with a definition of discrete curvature. This model is shown to provide a good approximation to the continuous case. With promising results in the case of a single curve we model the interaction between several discrete curves with great success. The general equations are then applied to a variety of interacting curve models, providing physically realistic results. Continuous space curves, curve framing, and the general theory of elastic rods is introduced in order to build discrete analogies to each, before moving on to build a discrete model of an elastic curve deforming in three dimensions.

This study provides the basis to support the eventual modelling of interacting elastic rods in three dimensions. Such a model can be applied to many bundle models, including but not limited to collagen type 1 fibrils.

Contents

List of Figures

1 Fibrous Polymers

The human body and that of other mammals is built up of a wide variety of proteins including fibrous proteins known as scleroproteins [1]. Scleroproteins form long fibrous polymers and are often structural proteins, providing strength and support to many connective tissues such as tendon, bone and muscle fibre. Some fibrous polymers are also formed from non-fibrous proteins. F-actin for example is a globular protein which can polymerize to form long, stiff fibers that make up the cytoskeleton.

We see in larger scale fibrous structures like rope or plywood, how the mechanical properties are largerly determined by the arrangement of the fibers within the material. In the same way, the mechanical properties of fibrous tissues are largely determined by the assembly of the fibrous polymers making up the tissue, rather than by a change in the chemical composition of the tissue [1, 2].

Of all proteins, collagen is the most abundant in mammals, making up about one third of the whole-body protein content. Collagen is mostly found in fibrous tissues such as tendon, ligament and skin, but is also abundant in cornea, cartilage, bone, blood vessels, the gut, and intervertebral disc.

Collagen refers to a family of proteins with common biochemical characteristics but which fulfil a variety of different mechanical functions within biological tissues: some, for example, are required to be flexible, whilst others must be tough and stiff.

To date, 28 types of collagen have been identified, however we will limit our attention to the fibrous type 1 collagen, the most abundent protein in the human body, providing tensile strength to tissues such as the dermis, bone, tendon and ligament.

1.1 Collagen Hierarchy

Like other biological protein materials, collagen-based tissues typically have a hierarchical structure [2]. At the lowest level are polypeptide chains referred to as α-chains, which contain a repeating triplet amino acid sequence of the form Gly-X-Y, where Gly represents glycine and X and Y typically represent proline and hydroxyproline [3]. Each polypeptide chain is coiled into a left-handed triple helix and three of these α-chains coil together into a right-handed triple helix stabilised by hydrogen bonds between adjacent α-chains, resulting in a stable rod-like structure [4] (Figure 1). This triple helix molecule is named tropocollagen and has a length of about 300nm and a diameter of about 1.5nm.

Figure 1: Tropocollagen molecule [4]

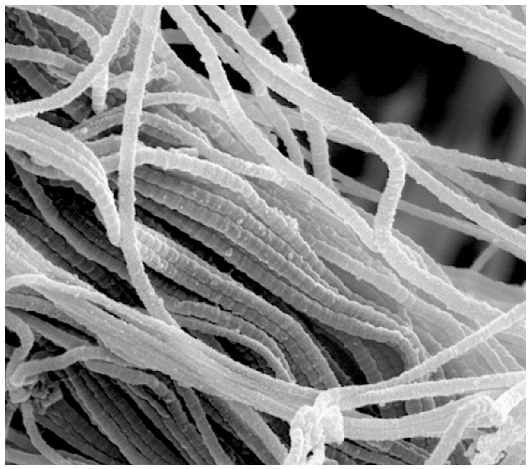

Figure 2: D-banding [5]

Tropocollagen molecules further assemble into fibrils, which are bundles of tropocollagen molecules with thicknesses varying from fifty to a few hundred nanometers.

Under an electron microscope, collagen fibrils appear to have a banded structure with a repeating pattern every 67nm (a unit referred to as 'D') [5] (Figure 2). Explaining this observation and advancing a model for the precise arrangement of the tropocollagen molecules within the fibril has proven elusive for decades despite the topic being heavily researched.

The most widely used, simplified (two dimensional) model of the fibril structure is the parallel, D-staggered arrangement, adapted from Petruska and Hodge [6], which has neighbouring molecules lining up in parallel, with regularly 'D-staggered' ends (see diagram below), meaning there is a gap of 67nm between the end of one molecule and the start of the next. This model introduces a repeating unit called the microfibril, consisting of a repeating axial series of five D-staggered tropocollagen molecules. Modelling in this way leads to four plus a fraction of tropocollagen molecules per D-period of the microfibril and therefore, in each D-period repeat of the microfibril, there is a part containing five molecules in cross-section, called the overlap, and a part containing only four molecules, called the gap.

Of major importance for the mechanical properties of the collagen fibril is the presence of various types of covalent and non-covalent chemical cross-links between the tropocollagen molecules within the fibril [1], which stabilise the different forms of supermolecular assembly. There are three types of cross-link present in collagen, but for fibrillar collagens it is predominently lysyl oxidise mediated [7], with experimental analysis of the molecular geometry suggesting that the intermolecular cross links primarily develop at the ends of the tropocollagen molecules [8].

With this in mind it is suggested that the cross-linking present in the end-end region of adjacent molecules leads to an increased intermolecular adhesion in these regions (indicated by the red links in figure 3(c)) and relatively weak (although still strong) intermolecular adhesion elsewhere [9].

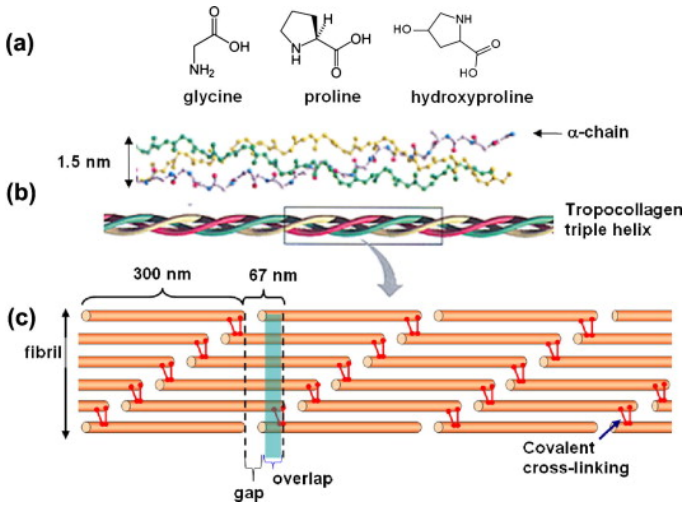

Figure 3: Collagen Hierarchy [10]

The most obvious way to extend this model from two to three dimensions is to simply coil the microfibril structure into a hollow-circular microfibril, consisting in cross section of five tropocollagen molecules, each laying on a common circle. This model proposes a microfibril diameter of 3.5nm [11].

Other structural models of the arrangement of the tropocollagen molecules within the microfibril have been proposed from X-ray diffraction and atomic force microscopy studies [12, 13, 14], posing various cross sectional arrangements of the molecular packing within the fibril, often displaying some degree of disorder. Such packing arrangements pose a geometrical restriction on subsequent mechanical models, which often assume the microfibril to consist of five naturally straight elastic rods connected by springs [15].

Other schematic models of the fibrillar structure have also been put forward, but the microfibrils are simply assumed to be elastic rods with very little attention paid to the arrangement of the tropocollagen molecules within the microfibril [16].

Orgel et al [17] present a crystallographic determination of the collagen type I supermolecular structure, identifying the molecular conformation of each collagen segment found within the naturally occurring crystallographic unit cell. This is the most up to date and widely accepted three dimensional structural arrangement of the tropocollagen molecules within type 1 collagen fibrils in situ, and has recently been verified by molecular dynamic simulations [18].

The structural model suggests that the molecular packing of the collagen molecules is such that packing neighbours are arranged to form a supertwisted, discontinuous and right-handed microfibril that interlocks with neighbouring unit cells, establishing that the fibril is formed of quasihexagonally packed collagen molecules.

Further analysis of the X-ray data provides more insight into the exact cross-sectional structure of the collagen fibril as the fibril axis is traversed. It can be observed that in the overlap region, the tropcollagen molecules are densely packed in a slightly distorted hexagonal fashion, whereas in the gap region the shape of the lattice varies substantially [19].

From this model we see that in reality the microfibril is formed from five D-staggered tropocollagen molecules winding around each other with the molecules tilted with respect

to the fibril axis in the overlap region. This leads to a crimped rope-like structure, but unlike a rope, each strand does not make contact with its nearest neighbours but rather interacts with them via the chemical cross-links.

1.2 Collagen as a Bundle of Interacting Elastic Rods

Collagen fibrils consist of many hundreds of microfibrils and so atomistic modelling is not a practical way to understand how the structure of the collagen fibril lends itself to the larger scale mechanical properties of collagen based tissues. The aim here is to develop a mechanical model of the fibrillar structure of collagen where the tropocollagen molecules are modelled as elastic rods.

There has been very little application of elastic rod theory to the structure and mechanics of collagen fibrils as compared to the relatively large volume of work applying the theory to DNA molecules [20].

Indeed, the first and only application of elastic rod theory to the collagen structure models collagen fibrils as nanoscale ropes and uses a multi-ply rod model to show the possibility of D-banding without the need for a staggered fibrillar arrangement [21]. This model, however, assumes a regular cross-sectional configuration and cross linking was not considered.

Our structural consideration is inspired by the most up to date three dimensional microfibrilar structure mentioned above but with two further assumptions.

Firstly, we take the repeating pattern of (tropocollagen molecule) - (increased adhesion zone) - (tropocollagen molecule) as a continuous elastic rod. In doing so we eliminate the problem of force transfer across the gap region and assume force is transferred along the fibril via the tropocollagen molecules and the strong end-end cross linking of neighbouring tropocollagen molecules.

Secondly, we model the covalent cross links in the weaker adhesion regions via elastic springs of varying stress-strain relationships. The particular choice of stress-strain relationship can be chosen to represent any type of cross-linking bond.

By working with the spring potential, we have the freedom to simulate interesting bonding characteristics such as bond breaking or 'no touch' conditions at the locations where the spring connects neighbouring rods.

By making such assumptions, we have reduced the the problem to modelling a system of interacting elastic rods and a successful model can be used to analyse the mechanical properties of any such structure, not only type 1 collagen fibrils. An example of note is F-actin, for which a similar model of interacting elastic rods was posed and named the wormlike bundle model [22] and is depicted in figure 4. Due to the uniform F-actin molecules (as opposed to the D-banding present in collagen) there is no need to make the force transferring assumption as is needed for collagen fibrils. However deformation of the rod bundle in this model leads to a shear deformation of the cross links rather than a stretching.

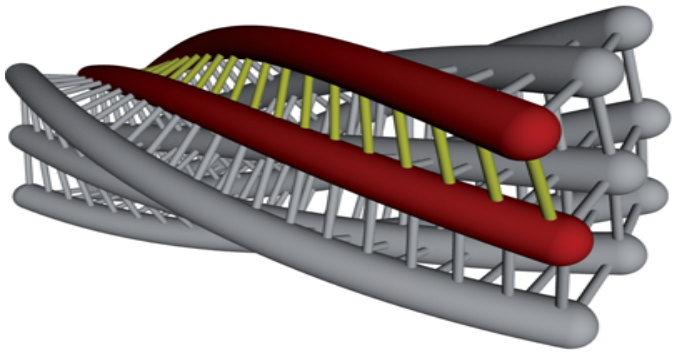

Figure 4: Bundle of interactng elastic rods [22]

Our final consideration is the pre-deformed configuration of the rods within the bundle. For collagen fibrils this could either be simplified by assuming a helical shape or could be matched up with the cross-sectional data provided by Orgel et al [17].

Once the model is developed, we wish to run three simulations in particular.

1. Compressing or stretching the bundle. Simply put, we aim to simulate the deformation of the fibril under some change in end displacement.

2. Plucking a single rod from the edge of the bundle. Here we aim to simulate plucking a single tropocollagen molecule from the edge of the fibril (on the boundary), in a direction perpendicular to the fibril axis (we must assume that the end-end cross links at either end do not break and the molecule does not break away at either end).

3. Plucking a single rod from within the fibril. Here we aim to simulate plucking a single tropocollagen molecule from within the fibril (not on the boundary), in the direction of the fibril axis (assuming the end-end cross links do not break).

As the mechanical constants will be left free within the modelling process, we can appeal to experimental data [23] in order to best simulate the deformation of collagen fibrils. Simulation one could provide some insight into how the mechanical properies of the molecule can effect its deformation under loading - for example in bone or tendon. Simulations two and three provide a possible model of experimental work as well as simulating damage and fatigue to the bundle [1].

This introductory study will present the beginnings of the interacting elastic rod model by focussing on a more simple, two dimensional model where we consider the various deformations of a bundle of interacting elastic curves. In particular, we will demonstrate the validity of the model by carrying out simplified two dimensional versions of the three simulations listed above.

2 Numerical Solutions using AUTO

Before we begin the modelling process it is convenient to introduce the software AUTO [24] used to numerically solve the equations which represent each of the physical systems considered in the chapters to follow. AUTO can perform a bifurcation analysis of systems of ordinary differential equations of the form

$$\mathbf{u}'(s) = \mathbf{f}(\mathbf{u}(s), p) \qquad \mathbf{u}, \mathbf{f}(\cdot, \cdot) \in \mathbb{R}^n \tag{1}$$

Subject to boundary or initial conditions and integral constraints.

AUTO can also perform a bifurcation analysis of algebraic systems of the form

$$\mathbf{g}(\mathbf{v}, p) = \mathbf{0} \qquad \mathbf{v}, \mathbf{g}(\cdot, \cdot) \in \mathbb{R}^n \tag{2}$$

Where p denotes one or more free parameters.

In either case AUTO requires a starting solution which solves the equation for some fixed starting parameter(s) $p = p_s$. Once this is known, the software then varies the parameter(s) p, updating the solution at each iteration and providing a solution at each step. AUTO is also able to locate branch points where multiple solutions exist, and then continue along the branches, calculating all possible solutions.

Choosing a parameter(s) and finding a suitable starting solution is usually relatively straight forward but as we shall see later, in some cases the choice of starting solution can dramatically affect the family of solutions generated by continuing in the parameter.

The software requires two input files: one defining the equations, parameters and starting solution and one defining various options such as the parameter step size. Once the family of solutions is calculated there may be some post processing to be undertaken in order to calculate further quantities of interest. Examples of the equation file and the post processing file can be found in the appendix.

3 Continuous Planar Elastic Curves

We start the modelling process by looking at the most simple model of slender elastic bodies. Such a model ignores the three dimensional structure of the body and does not allow for any twisting or shearing that would take place in a more realistic scenario. We model the elastic body as a planar curve, constraining the deformations to a plane which we take to be the $x - y$ plane.

3.1 Defining arclength and curvature

For a curve described parametrically by $x = x(t)$, $y = y(t)$, we define the arclength from $t = a$ to $t = b$ by

$$s := \int_a^b \sqrt{x'(t) + y'(t)}dt \tag{3}$$

We also define the signed curvature by

$$k := \frac{x'y'' - x''y'}{(x'^2 + y'^2)^{\frac{3}{2}}} \tag{4}$$

3.2 Inextensible Planar Elastica

Here we consider the classic (inextensible) planar elastica first studied by Euler [25] and often referred to as the 'Euler elastica'. An inextensible planar elastica is a planar curve which minimises the curvature dependent bending energy over the length of the curve, subject to various constraints [26].

Since the curve is taken to be inextensible, we can parameterise it by the arc length. That is, for a curve of length L, the position of each point of the curve is given by $\mathbf{r}(s) = (x(s), y(s))$ for some $s \in [0, L]$, such that $\mathbf{r}(0)$ and $\mathbf{r}(L)$ correspond to the start and end of the curve respectively.

The bending energy is defined to be

$$E_b[k(s)] := \int_0^L \frac{1}{2}B(s)k(s)^2 ds \tag{5}$$

Where $k(s)$ is the curvature and $B(s)$ is referred to as the bending stiffness.

We now introduce the angle $\theta(s)$, between the tangent vector and the x axis at the point $\mathbf{r}(s)$ by the relations

$$\frac{dx}{ds} = \cos\theta \tag{6}$$

$$\frac{dy}{ds} = \sin\theta \tag{7}$$

With this definition in place and denoting differentiation with respect to s by $(')$, we can define the curvature in terms of the angle θ by noting that by definition

$$k := \frac{x'y'' - y'x''}{(x'^2 + y'^2)^{\frac{3}{2}}} = \frac{\cos^2\theta\theta' + \sin^2\theta\theta'}{\cos^2\theta + \sin^2\theta} = \theta' \tag{8}$$

We can now write the bending energy in terms of θ and by further assuming $B(s)$ to be constant along the curve, we arrive at a final expression of the bending energy in terms of θ

$$E_b = \int_0^L \frac{1}{2} B\theta'^2 ds \tag{9}$$

We now wish to find stationary points (functions $\theta(s)$) of this functional subject to a variety of contraints on the curve.

Before we turn to specific constraints we also note that we wish impose boundary conditions on θ at each end of the curve.

The two most common boundary conditions are referred to as clamped and pinned boundary conditions.

Clamped

Clamped boundary conditions impose no deflection angle at the boundaries

$$\theta(0) = \theta(L) = 0 \tag{10}$$

Pinned

Pinned boundary conditions impose a stationary deflection angle at the boundaries

$$\theta'(0) = \theta'(L) = 0 \tag{11}$$

One may also take a mixture of the two conditions. For instance, clamped at the start of the curve and pinned at the end of the curve.

3.3 Inextensible Planar Elastica under an End Displacement

Here we aim to find stationary points of E_b such that the start of the curve is fixed at the origin and the end of the curve has coordinates (X, Y). This leads us to the conditions

$$\int_0^L \cos\theta ds = X \tag{12}$$

$$\int_0^L \sin\theta ds = Y \tag{13}$$

We solve this problem by using the Lagrange multiplier technique [27]. We thus consider the problem of finding stationary points of the Lagrangian functional defined by

$$\mathcal{L} = \int_0^L \frac{1}{2} B\theta'^2 ds + \lambda_1 \int_0^L \cos\theta ds + \lambda_2 \int_0^L \sin\theta ds \tag{14}$$

Where λ_1 and λ_2 are the Lagrange multipliers.

Applying the Euler-Lagrange equations to find stationary points of this functional we arrive at

$$B\theta'' + \lambda_1 \sin\theta - \lambda_2 \cos\theta = 0 \tag{15}$$

For any given (X, Y), together with two boundary conditions on θ, equations (12), (13) and (15) can be solved to give $\theta = \theta(s)$.

Along with the condition $\mathbf{r}(0) = 0$ already imposed, we can then solve equations (6) and (7) to give $x = x(s)$ and $y = y(s)$, providing us with the shape of the curve.

3.4 Inextensible Planar Elastica under an End Force

We now consider finding stationary values of E_b, such that the start of the curve is fixed at the origin and the end of the curve is subject to a force $\mathbf{F} = (-F, -G)$.

By taking the zero potential to be at the origin, the total energy of the system is given by the sum of the bending energy E_b and the potential energy due to the end force.

$$E = \int_0^L \left(\frac{1}{2} B\theta'^2 + F\cos\theta + G\sin\theta \right) ds \tag{16}$$

Finding stationary points of E leads to the equation

$$B\theta'' + F\sin\theta - G\cos\theta = 0 \tag{17}$$

Which for any given $(-F, -G)$, together with two boundary conditions on θ, can be solved to give $\theta = \theta(s)$ and then as before we can recover the shape of the curve.

With $\theta = \theta(s)$ we can further calculate the end coordinates of the curve (X, Y) using

$$\int_0^L \cos\theta ds = X \tag{18}$$

$$\int_0^L \sin\theta ds = Y \tag{19}$$

We see that this system is simply a reformulation of the previous one and that the Lagrange multipliers employed in the first formulation correspond to the forces (F, G) we apply to the end of the curve in order to impose the end point coordinates (X, Y).

3.5 Example One

Here we take a pinned inextensible curve of length L and bending stiffness B, lying along along the x axis with the start of the curve fixed at the origin. We then impose a force $\mathbf{F} = (-F, 0)$ to the end of the curve and increase F from zero.

This example of an inextensible curve under an increasing end force is solved using AUTO by first splitting equation (17) into two first order equations (conveniently chosen to include equation (7)), and also adding equation (6) to arrive at the following system

$$\frac{d\theta}{ds} = -\frac{Fy}{B} \tag{20}$$

$$\frac{dx}{ds} = \cos\theta \tag{21}$$

$$\frac{dy}{ds} = \sin\theta \tag{22}$$

We see that the boundary conditions $\theta'(0) = \theta'(L) = 0$, $x(0) = 0$, $y(0) = 0$ reduce to just three conditions and so by taking F as our parameter and the starting solution $(\theta, x, y; F) = (0, s, 0, 0)$, this system is of the form required for finding solutions using AUTO by increasing F in order to simulate the increasing end force.

AUTO locates the branch points which correspond to the curve buckling under the force F, which is known to occur at a set of discrete values [29].

$$F_n = \frac{n^2\pi^2 B}{L^2} \qquad n \in \mathbb{N} \tag{23}$$

We say the curve buckles into the n^{th} mode as we follow the branch which occurs at parameter value (Force) $F = F_n$. Note that each mode can exist in two forms with the curve buckling in one of two possible directions, one being a mirror image of the other.

The numerical results produced by AUTO match these values of F_n and with θ, x and y as functions of s together with the condition $\mathbf{r}(0) = \mathbf{0}$, we can further solve equations (21) and (22) to provide us with the shape of the curve for any given F.

Figures 5 and 6 show the curve buckling into the first and second modes respectively, for $L = B = 1$

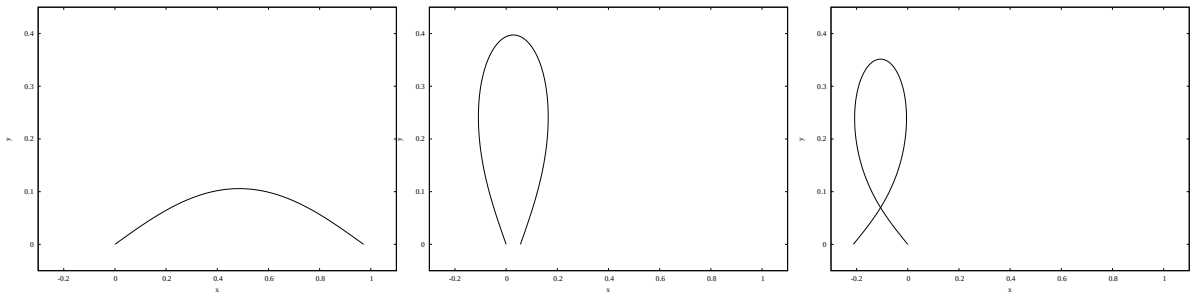

(a) $F = 10$ (b) $F = 20$ (c) $F = 30$

Figure 5: The curve buckling under increasing F in the first mode

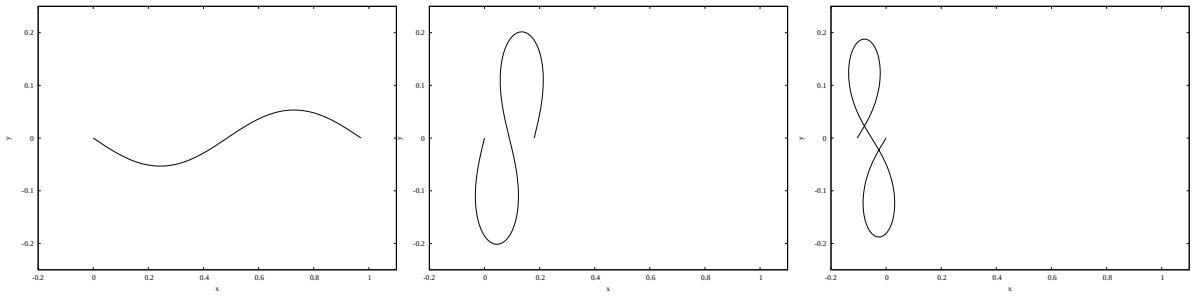

(a) $F = 40$ (b) $F = 70$ (c) $F = 100$

Figure 6: The curve buckling under increasing F in the second mode

Finally, we can calculate the end displacement d, given by $d = L - X$, or

$$d = L - \int_0^L \cos\theta ds \tag{24}$$

We can now plot a relationship between the applied end force and the resulting end displacment in each mode. Figure 7 shows this relationship for the first and second mode.

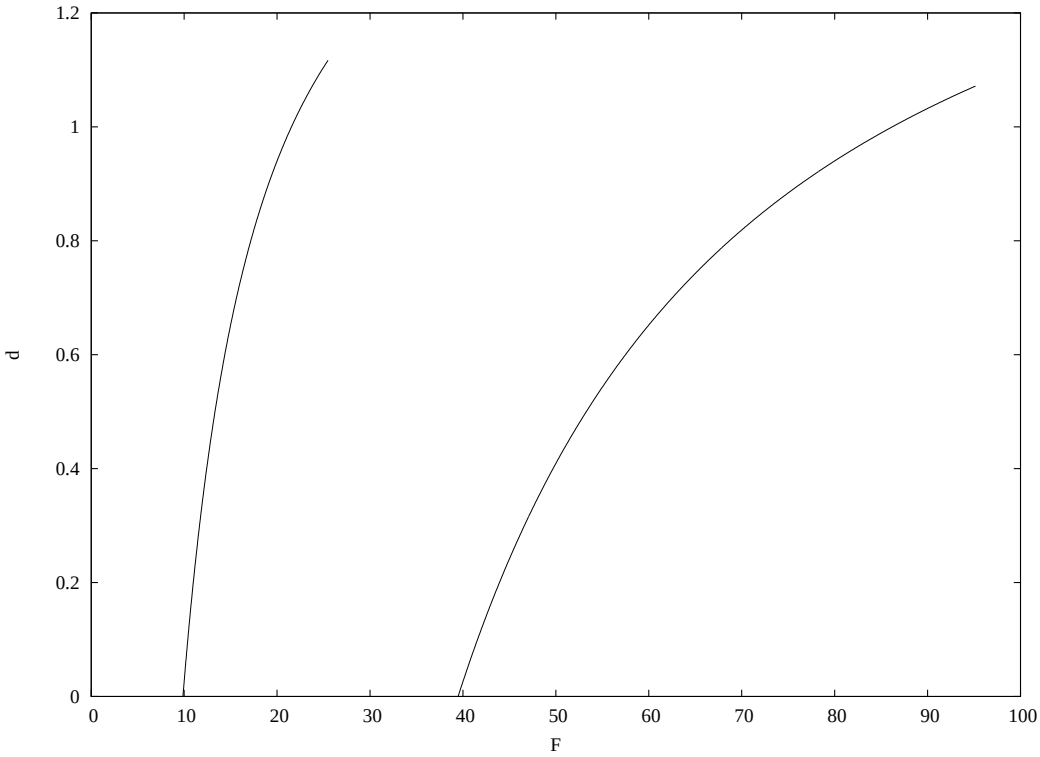

Figure 7: $F - d$ relationship

Before leaving this example notice that we used the end force as our parameter rather than the end displacement.

In the case of using the end force as the parameter we can have our starting solution $(\theta, x, y) = (0, s, 0)$. This solution can hold for any value of F and is the only solution for $F < F_1$.

However, using end displacement as a parameter would mean that we have $(\theta, x, y) = (0, s, 0)$ as solution only for $X = 0$. This results in the system needing to branch as soon as we start to vary the parameter X.

3.6 Extensible Planar Elastica under an End Displacement

We now extend the model introduced in section 3.4 to allow the curve to have variable length [29].

Take the curve in an unstretched state, parameterised by arclength S for $S \in [0, L]$. As the curve is deformed we must reparameterise by a new parameter $s \in [0, L_s]$ for some L_s such that

$$\frac{ds}{dS} = 1 + \varepsilon \tag{25}$$

Where ε is the extension of the curve in the positive x direction.

We now introduce the angle θ via the relations (4) and (5) and notice that

$$\frac{dx}{dS} = \frac{dx}{ds}\frac{ds}{dS} = (1 + \varepsilon)\cos\theta \tag{26}$$

$$\frac{dy}{dS} = \frac{dy}{ds}\frac{ds}{dS} = (1 + \varepsilon)\sin\theta \tag{27}$$

As before, we fix the start of the curve at the origin and subject the end of the curve to a force $\mathbf{F} = (-F, -G)$, so that by resolving these forces along the curve's tangent vector and appealing to Hooke's law (assuming the curve to be linearly elastic) we have

$$F\cos\theta + G\sin\theta = -C\varepsilon \tag{28}$$

For some constant C, known as the stretching stiffness.

Denoting differentiation with respect to S by $(\dot{})$ the total energy of the system is then a sum of the bending energy, stretching energy and potential energy of the end force

$$E = \int_0^L \left(\frac{1}{2}B\dot{\theta}^2 + \frac{1}{2}C\varepsilon^2 + F(1 + \varepsilon)\cos\theta + G(1 + \varepsilon)\sin\theta\right) dS \tag{29}$$

Substituting in ε leads to

$$E = \int_0^L \left(\frac{1}{2} B\dot{\theta}^2 - \frac{1}{2C}(F\cos\theta + G\sin\theta)^2 + F\cos\theta + G\sin\theta \right) dS \tag{30}$$

Finding stationary points of E using the Euler-Lagrange equations leads to the equation

$$B\ddot{\theta} + (F\sin\theta - G\cos\theta)\left[1 - \frac{F\cos\theta + G\sin\theta}{C}\right] = 0 \tag{31}$$

Which for any given $(-F, -G)$, together with two boundary conditions on θ, can be solved to give $\theta = \theta(S)$.

Substituting ε into equations (26) and (27) then leads to

$$\frac{dx}{dS} = \left(1 - \frac{F\cos\theta + G\sin\theta}{C}\right)\cos\theta \tag{32}$$

$$\frac{dy}{dS} = \left(1 - \frac{F\cos\theta + G\sin\theta}{C}\right)\sin\theta \tag{33}$$

Together with the condition that the start of the rod remains fixed at the origin, these equations can be solved to find the shape of the curve $x = x(S)$, $y = y(S)$.

3.7 Example Two

We now extend Example One by taking the same system but now assuming the curve is extensible, and of stretching stiffness C.

To solve this system using AUTO we again split the second order equation (31) into two first order equations and add equation (33). This leaves us with

$$\frac{d\theta}{dS} = -\frac{Fy}{B} \tag{34}$$

$$\frac{dx}{dS} = (1 - \frac{F\cos\theta}{C})\cos\theta \tag{35}$$

$$\frac{dy}{dS} = (1 - \frac{F\cos\theta}{C})\sin\theta \tag{36}$$

Once again the boundary conditions reduce to just three conditions. Taking F as our parameter we can take the same starting solution $(\theta, x, y; F) = (0, s, 0, 0)$

AUTO produces solutions to these equations in the same way as before and we again see buckling behaviour at a set of discrete values. However the values for the forces under which the curve buckles are higer than before. For $C = 1$, we find the buckling value for the first two modes are $F = 11.11$ and $F = 88.90$ respectively.

By further solving equations (305) and (36) along with the condition $\mathbf{r}(0) = \mathbf{0}$ we can find the shape of the curve. Figure 8 shows the curve buckled in the first mode for $L = B = C = 1$, under the same forces as the inextensible case. These figures can be compared to the corresponding figures in Example One.

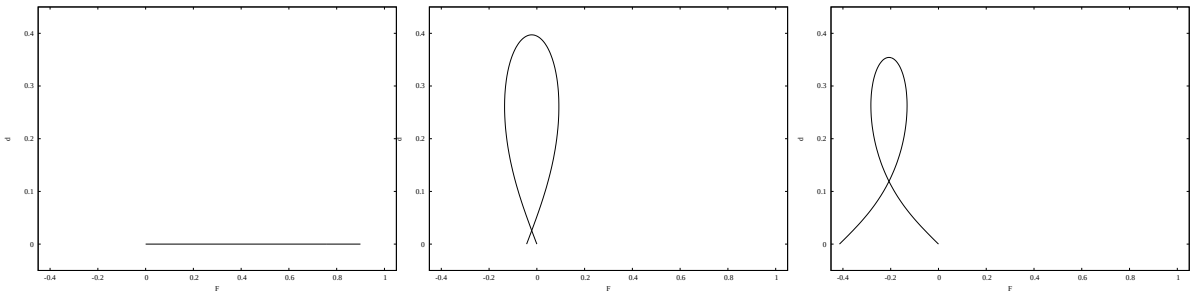

(a) $F = 10$ (b) $F = 20$ (c) $F = 30$

Figure 8: The curve buckling under increasing F in the first mode

The higher buckling values can be justified physically. As the force is applied, the curve energy can be minimised by either bending or shortening in length. For less rigid curves a shortening is preferable, at least for small values of F. As F increases and the curve gets shorter we reach a tipping point where it becomes preferable to bend, at which point the curve buckles at a comparatively greater force than the corresponding buckling of an inextensible curve. The extent to which the curve shortens before it buckles depends on the stretching stiffness C. Indeed as $C \to \infty$ we are left with the inextensible equations, confirming what we expect: as the curve becomes more rigid, it behaves more like an inextensible curve. By varying C one can varify that as $C \to \infty$, the forces under which the curve buckles approach those for an inextensible curve.

Although inextensibility is considered in the discrete models to follow, it is discarded when considering specific examples and so is left in the equations purely for the sake of completeness.

3.8 A First Look at Joining Curves Together

Consider now a very basic connected curve model. Take two inextensible planar elastic curves C_1 and C_2 of length L and of bending stiffness B_1 and B_2 respectively, one with the start fixed at $(0,0)$ and the other with the start fixed at a horizontal distance G below $(0,0)$ - that is at $(0,-G)$. We join the curves together at the midpoints by an elastic spring of natural length G and spring energy function f. Adopting subscripts 1 and 2 to differentiate between the curves, the length of the spring D is given by

$$D^2 = \left(G + \int_0^{\frac{L}{2}} \cos\theta_1 ds_1 - \int_0^{\frac{L}{2}} \cos\theta_2 ds_2 \right)^2 + \left(\int_0^{\frac{L}{2}} \sin\theta_1 ds_1 - \int_0^{\frac{L}{2}} \sin\theta_2 ds_2 \right)^2 \tag{37}$$

The sum of the bending energy and spring stretching energy is then

$$E = \int_0^L \frac{1}{2} B_1 \dot{\theta_1}^2 ds_1 + \int_0^L \frac{1}{2} B_2 \dot{\theta_2}^2 ds_2 + f(D-G) \tag{38}$$

We wish to minimise this functional such that the endpoints of curve 1 and 2 have coordinates $(X,0)$ and $(X,-G)$ respectively.

If we were to start with both curves parallel to the x axis, decreasing X from zero would simulate a simultaneous and equal end displacement of the curves. This is depicted in figure 9.

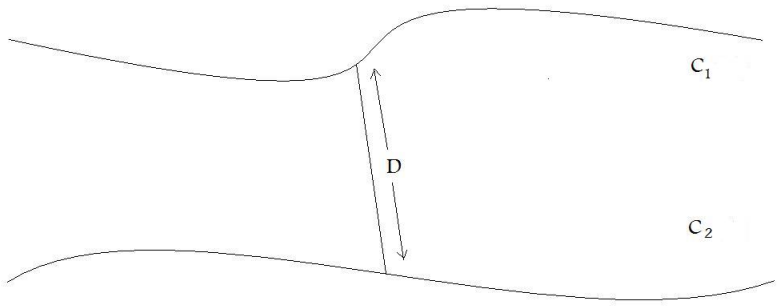

Figure 9: Joining two curves together

With the integral limits not matching throughout the functional and the complexity of such a simple example, a continuos model does not seem viable.

Additionaly, using the end displacement as a parameter renders AUTO unable to solve the equations. Therefore we must instead use the end force F as our parameter. However, the force-displacement relationship is mode dependent, so at a critical value of F one rod may buckle while the other does not: at this point they would evolve under the same end force but have a different end displacement.

This mismatch in the end displacement needs to be avoided if we wish to model simultaneous and equal end displacement, and so we are left in a position where we can neither use end displacement nor end force as a parameter.

To overcome these issues we look to modelling the curves as discrete instead of continuous [30]. Inspired by some of the ideas presented in this chapter we now move on to build up an analogous discrete model of planar elastic curves before again attempting to join such curves together.

4 Discrete Planar Elastic Curves

4.1 Discrete Planar Curves

A discrete planar curve is a map $\mathbf{x} : I \to \mathbb{R}^2$, where $I = \{0, ..., n+1\}$. The map defines a set of points $\{\mathbf{x}(0), ..., \mathbf{x}(n+1)\}$ in $\mathbb{R}^2$ which we will call vertices. These vertices are joined together by edges $\{\mathbf{e}(0), ..., \mathbf{e}(n)\}$ which in turn form the curve.

To simplify notation we denote $\mathbf{x}(j)$ by $\mathbf{x}_j$ and $\mathbf{e}(j)$ by $\mathbf{e}^j$, associating subscripts with the vertices and superscripts with the edges.

By construction we have $\mathbf{e}^j = \mathbf{x}_{j+1} - \mathbf{x}_j$ and so

$$\mathbf{x}_j = \mathbf{x}_0 + \sum_{k=0}^{j-1} \mathbf{e}^k \tag{39}$$

The length of the curve is given by

$$L = \sum_{j=0}^{n} |\mathbf{e}^j| \tag{40}$$

In the special case that $|\mathbf{e}^j| = l$ for some constant $l \in \mathbb{R}$, the length is given simply by $L = (n+1)l$.

We denote the signed angle between edge $\mathbf{e}^j$ and the positive x axis by θ_j, where $-\pi < \theta_j < \pi$. This then allows us to write

$$\mathbf{e}^j = |\mathbf{e}^j| \cos\theta_j \mathbf{i} + |\mathbf{e}^j| \sin\theta_j \mathbf{j} \tag{41}$$

We now define the turning angle at vertex $\mathbf{x}_j$ for $j = 1, ..., n$, to be the angle through which we must rotate edge $\mathbf{e}^{j-1}$ so that it becomes parallel to edge $\mathbf{e}^j$. We denote this angle by ψ_j and associate a positive angle with an anticlockwise rotation so that $-\pi < \psi_j < \pi$.

We can write ψ_j in terms of θ_{j-1} and θ_j by noting that

$$\mathbf{e}^{j-1} \cdot \mathbf{e}^j = \pm|\mathbf{e}^{j-1}||\mathbf{e}^j| \cos(|\psi_j|)$$

$$= |\mathbf{e}^{j-1}||\mathbf{e}^j| \cos\theta_{j-1} \cos\theta_j + |\mathbf{e}^{j-1}||\mathbf{e}^j| \sin\theta_{j-1} \sin\theta_j$$

$$\Rightarrow \pm\cos(\psi_j) = \cos\theta_{j-1} \cos\theta_j + \sin\theta_{j-1} \sin\theta_j = \cos(\theta_{j-1} - \theta_j)$$

$$\Rightarrow \psi_j = \pm(\theta_{j-1} - \theta_j)$$

depending on the orientation of the rotation.

In order to preserve our association of a positive ψ_j with an anticlockwise rotation we define

$$\psi_j := \theta_j - \theta_{j-1} \qquad j = 1, ..., n \tag{42}$$

Figure 10 depicts part of a discrete curve

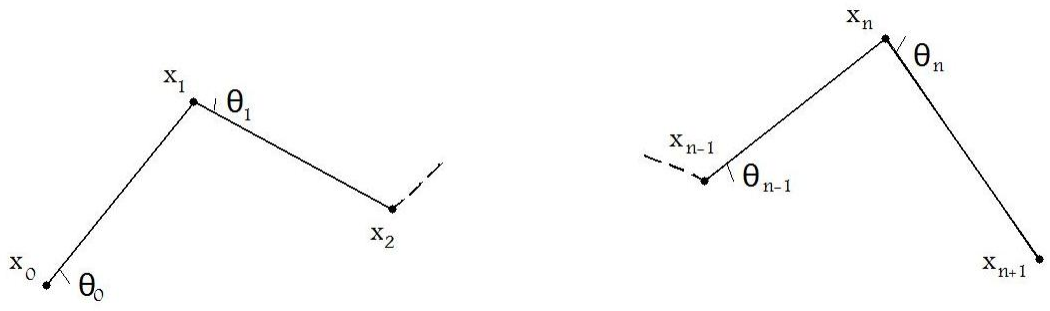

Figure 10: The discrete curve

4.2 Defining Curvature using a Discrete Derivative

In order to formulate an energy equation for discrete elastic curves analogous to the continuous case covered in section three, we must have a definition of discrete curvature. We start with the most basic approach using a discrete derivative.

For the continuous case we saw that the curvature of a continuous curve parameterised by arclength s is given by θ'. Motivated by this we define the domain of the curve from the mid point of edge $\mathbf{e}^{j-1}$ to edge $\mathbf{e}^{j}$ by Δ_j, that is

$$\Delta_j = \left\{ \mathbf{x}_j + (\lambda_1 - \frac{1}{2})\mathbf{e}^{j-1}, \lambda_1 \in [0, \frac{1}{2}] \right\} \bigcup \left\{ \mathbf{x}_j + \lambda_2 \mathbf{e}^{j}, \lambda_2 \in [0, \frac{1}{2}] \right\} \tag{43}$$

We then define the discrete curvature over this domain using a backwards divided difference, discrete derivative.

$$k_j = \frac{\theta_j - \theta_{j-1}}{D_j} \qquad j = 1, ..., n \tag{44}$$

Where D_j is the length of the domain Δ_j. That is

$$D_j = \frac{1}{2}(|\mathbf{e}^{j-1}| + |\mathbf{e}^{j}|) \tag{45}$$

Noting that the union of all the domains Δ_j for $j = 1, ...n$, together with the first half of edge $\mathbf{e}^0$ and the last half of $\mathbf{e}^n$, cover the curve completely.

By setting the curvature to be zero along these first and last half edges of the curve, we have a definition of curvature along the whole curve.

We could, in a simlar fashion, define the curvature using a forward or central divided difference derivative. However using a backwards divided difference derivative proves most useful as it ties in nicely with the definition of the turning angle.

Notice that we certainly have $k_j \to 0$ as $\psi_j \to 0$ as we would expect. However as $\psi_j \to \pi$ and the curve turns back on itself, we would expect the curvature to become infinitely large. Here this is not the case and we in fact have an upper bound on the curvature in each domain Δ_j.

4.3 Defining Curvature via a Discrete Osculating Circle

In the smooth case, the centre of curvature at a point P is defined as the intersection point of two infinitely close normals to the curve at P. The radius of curvature, r, is the distance from that point to the curve, and the curvature itself is the inverse of the radius of curvature [31]. The circle sketched out in this way is known as the osculating circle and plays a large part in several of the possible definitions of discrete curvature. Figure 11 depicts the osculating circle at the point P for a curve C.

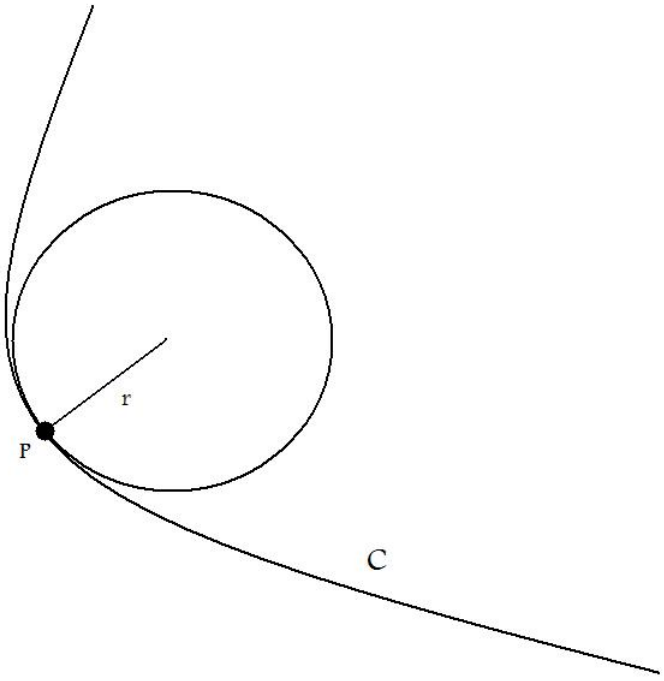

Figure 11: Osculating circle

If we try to adapt this idea in a discrete setting we have zero curvature along the straight sections and infinite curvature at the verticies. We therefore need an alternative way to define the osculating circle if we are to use it to define curvature. We now introduce two possible definitions of a discrete osculating circle with the associated definitions of curvature.

4.3.1 Definition One - Three Point Osculating Circle

We define the three point osculating circle C_j over the domain Δ_j of the curve to be the circle which passes through the vertex $\mathbf{x}_j$ and the mid points of edges $\mathbf{e}^{j-1}$ and $\mathbf{e}^j$. This circle is depicted in figure 12

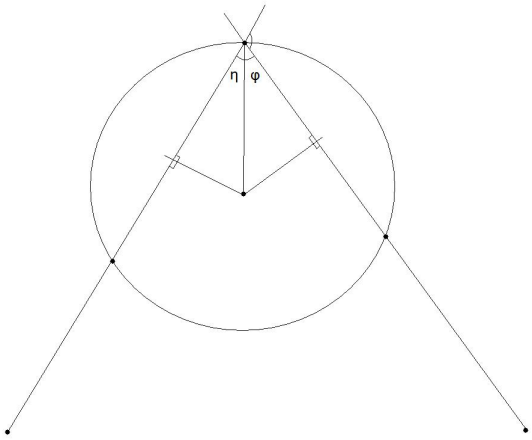

Figure 12: Three point osculating circle

By piecing together sections of these circles together with the straight half edges at either end of the curve we form a new curve along the length of the discrete curve, which we call the osculating circle curve. This is depicted in figure 13

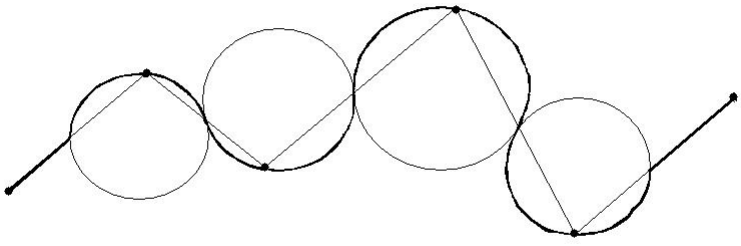

Figure 13: Osculating circle curve

We define the curvature of the discrete curve to be equal to the curvature of the osculating circle curve along its length. That is, equal to the inverse of the radius of the osculating circles over the domains Δ_j for $j = 1, ..., n$, and zero otherwise. This, once again, provides us with a definition of curvature along the whole curve.

We construct two right angled triangles as shown in figure 12 and denote the radius of C_j by r_j. We see that

$$\cos\eta = \frac{|\mathbf{e}^{j-1}|}{4r_j} \ , \cos\phi = \frac{|\mathbf{e}^{j}|}{4r_j} \ , |\psi_j| + \eta + \phi = \pi$$

We can then eliminate ϕ to provide us with

$$\cos(\eta + |\psi_j|) = -\frac{|\mathbf{e}^{j}|}{4r_j}$$

We therefore have

$$|\mathbf{e}^{j-1}|\cos(\eta + |\psi_j|) + |\mathbf{e}^{j}|\cos\eta = 0$$

After some rearranging we arrive at an expression for r_j^2

$$r_j^2 = \frac{|\mathbf{e}^{j-1}|^2 + |\mathbf{e}^{j}|^2 + 2|\mathbf{e}^{j-1}||\mathbf{e}^{j}|\cos\psi_j}{16\sin^2\psi_j} \tag{46}$$

By using the cosine rule we can can reduce this to

$$r_j^2 = \frac{|\mathbf{x}_{j+1} - \mathbf{x}_{j-1}|}{16\sin^2\psi_j} \tag{47}$$

By then associating a positive curvature to an anticlockwise rotation and rewriting the numerator in terms of the edges, we arrive at a definition of curvature over the domain Δ_j to be

$$k_j = \frac{4\sin(\theta_j - \theta_{j-1})}{|\mathbf{e}_{j-1} + \mathbf{e}_j|} \qquad j = 1, ..., n \tag{48}$$

4.3.2 Definition Two - Two Edge Osculating Circle

We first define

$$M_j = \min\left\{|\mathbf{e}^{j-1}|, |\mathbf{e}^j|\right\} \qquad j = 1, ..., n \tag{49}$$

Then denote the domain of the curve from the point $\mathbf{x}_j - \frac{M_j}{2|\mathbf{e}_{j-1}|}\mathbf{e}_{j-1}$ to the point $\mathbf{x}_j + \frac{M_j}{2|\mathbf{e}_j|}\mathbf{e}_j$ by Δ_j^*. That is

$$\Delta_j^* = \left\{\mathbf{x}_j + (\lambda_1 - \frac{1}{2})\frac{M_j}{|\mathbf{e}^{j-1}|}\mathbf{e}^{j-1}, \lambda_1 \in [0, \frac{1}{2}]\right\} \bigcup \left\{\mathbf{x}_j + \lambda_2 \frac{M_j}{|\mathbf{e}^j|}\mathbf{e}^j, \lambda_2 \in [0, \frac{1}{2}]\right\} \tag{50}$$

We define the two edge osculating circle C_j over the domain Δ_j^*, to be the circle which passes through the points $\mathbf{x}_j - \frac{M_j}{2|\mathbf{e}_{j-1}|}\mathbf{e}_{j-1}$ and $\mathbf{x}_j + \frac{M_j}{2|\mathbf{e}_j|}\mathbf{e}_j$ and has $\mathbf{e}^{j-1}$ and $\mathbf{e}^j$ as tangents. This is depicted in figure 14

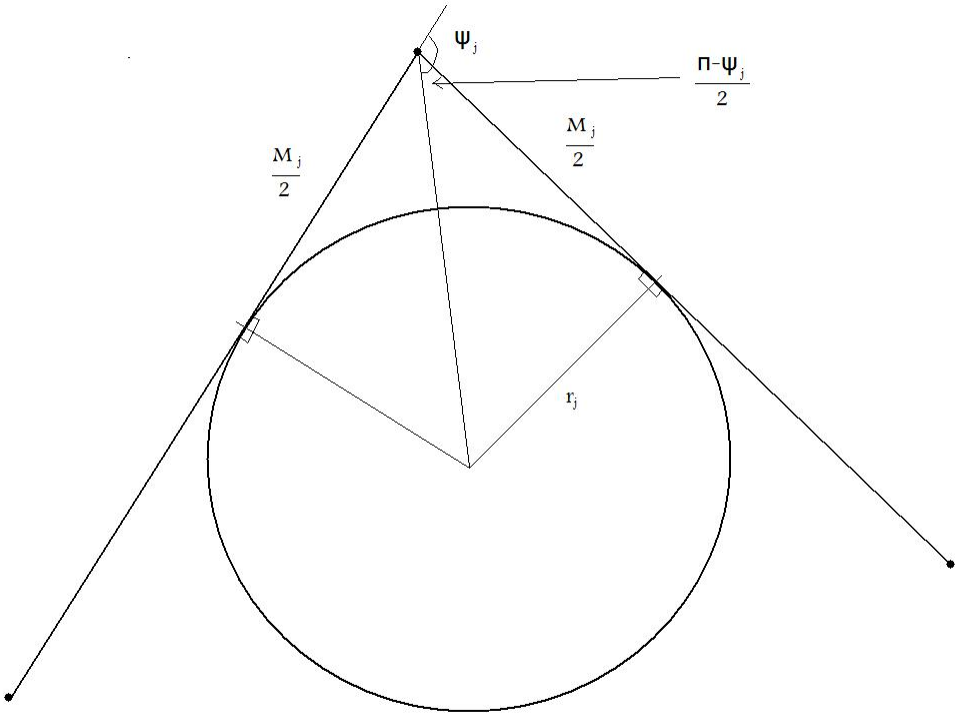

Figure 14: Two edge osculating circle

By piecing together the sections of these circles, along with the straight sections of the discrete curve which lay outside the domains Δ_j^*, we can form an osculating circle curve as depicted in figure 15

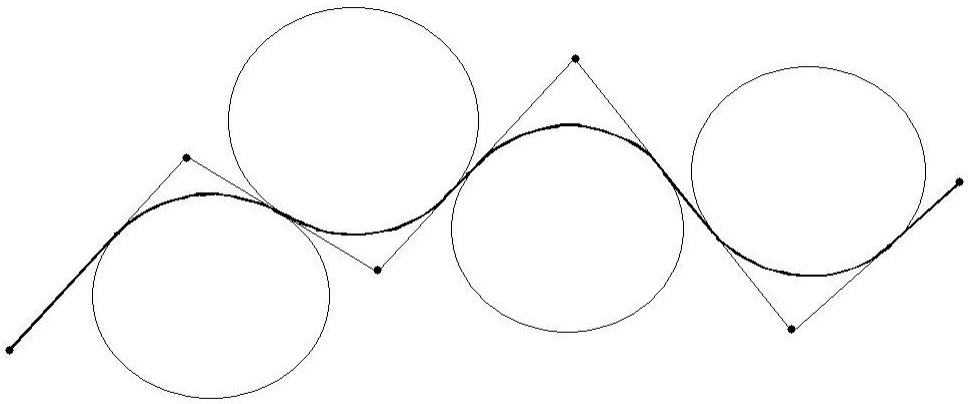

Figure 15: Forming a continuous curve

We now define the curvature of the discrete curve be equal to the curvature of the osculating circle curve we have constructed. That is, to be equal to the inverse of the radius of the osculating circles over the domain Δ_j^* for $j = 1, ..., n$, and zero otherwise, once again defining curvature along the whole curve.

Noticing that $|\Delta_j^*| = M_j$ we consider the right angled triangle constructed in figure 13, giving us

$$\tan\left(\frac{\pi}{2} - \frac{|\psi_j|}{2}\right) = \frac{r_j}{\frac{1}{2}M_j} \Rightarrow \frac{1}{r_j} = \frac{2}{M_j}\tan\left(\frac{\psi_j}{2}\right)$$

By continuing to associate a positive curvature with an anticlockwise rotation we arrive at a definition of curvature over the domain Δ_j^* to be

$$k_j = \frac{2}{M_j}\tan\left(\frac{\theta_j - \theta_{j-1}}{2}\right) \qquad j = 1, ..., n \tag{51}$$

Notice that for the special case of constant edge length, $|\mathbf{e}^j| = l$, there are no straight sections between osculating circles, and the domains Δ_j^* become equal to Δ_j. In this case $M_j = D_j = l$ and so

$$k_j = \frac{2}{l} \tan\left(\frac{\theta_j - \theta_{j-1}}{2}\right) \qquad j = 1, ..., n \tag{52}$$

Due to the awkward M_j term, we wish to extend our definition of curvature over the domain Δ_j^* to the domain Δ_j. We do this by first defining the dimensionless vertex curvature at the vertex $\mathbf{x}_j$ to be

$$k_j = 2 \tan\left(\frac{\theta_j - \theta_{j-1}}{2}\right) \tag{53}$$

We then associate this curvature with the domain Δ_j by defining the curvature over the domain Δ_j to be

$$k_j = \frac{2}{D_j} \tan\left(\frac{\theta_j - \theta_{j-1}}{2}\right) \qquad j = 1, ..., n \tag{54}$$

This is the definition we shall adopt and as $M_j = D_j$ for curves of constant edge length, this final definition is only relevant for curves of non constant edge length.

Also note that for constant edge length, definition one becomes:

$$k_j = \frac{4}{l} \sin\left(\frac{\theta_j - \theta_{j-1}}{2}\right) \qquad j = 1, ..., n \tag{55}$$

Which does not approximate the first divided difference as well as definition two.

4.4 Discrete Inextensible Planar Elastica

With the ideas presented so far in this section, we can now construct a discrete planar elastica which builds on the same principles as the corresponding continuous model.

We set up the discrete model by taking a discrete planar curve as defined in section 4.1. Since the curve is taken to be inextensible we define the edge length to be constant such that $|\mathbf{e}^j| = l$ for $j = 0, ..., n$.

The bending energy is then analogously defined by

$$E_b = \sum_{j=1}^{n} \frac{1}{2} B_j k_j^2 \cdot D_j \tag{56}$$

Taking our definition of discrete curvature and further assuming that the bending stiffness remains constant along the curve, we arrive at an expression for the bending energy in terms of the angles $\{\theta_j\}_{j=0,...,n}$

$$E_b = \sum_{j=1}^{n} \frac{2B}{l} \tan^2 \left(\frac{\theta_j - \theta_{j-1}}{2} \right) \tag{57}$$

We now wish to proceed as before by finding stationary points of this function subject to various constraints. Before turning to specific constraints we consider appropriate boundary conditions.

The boundary conditions considered in the continuous case can be imposed on a discrete curve, however because our definitions of curvature are over domains rather than at each point along the curve, analogous boundary conditions impose greater restrictions than are desirable.

First we note that by definition we have zero curvature at each end of the curve and so have constructed a curve that is in effect pinned.

In order to impose clamped boundary conditions we need to impose that $\theta_0 = \theta_n = 0$. In doing so we also force the start and end section of the curve to lay parallel to the x axis, a restriction that is 'more than' clamped, but one we cannot avoid.

4.5 Discrete Inextensible Planar Elastica under an End Displacement

Here we aim to find critical points of E_b such that the start of the curve is fixed at the origin and the end of the curve has coordinates (X, Y). This leads us to the conditions

$$\sum_{j=0}^{n} l \cos\theta_j = X \tag{58}$$

$$\sum_{j=0}^{n} l \sin\theta_j = Y \tag{59}$$

Using the Lagrange multiplier technique we consider the problem of finding stationary points of the Lagrangian function

$$\Lambda = E_b + \lambda_1 \left(\sum_{j=0}^{n} l \cos\theta_j - X \right) + \lambda_2 \left(\sum_{j=0}^{n} l \sin\theta_j - Y \right) \tag{60}$$

Stationary points of this sytem are given by differentiating with respect to each variable, giving us

$$\frac{\partial \Lambda}{\partial \lambda_1} = \frac{\partial \Lambda}{\partial \lambda_2} = \frac{\partial \Lambda}{\partial \theta_k} = 0 \qquad k = 0, ..., n \tag{61}$$

Noticing that the derivatives with respect to the Lagrange multipliers simply reproduces the contraints (55) and (56), as is typical.

For any given X and Y, equations (61) can be solved to give $\lambda_1, \lambda_2, \theta_0, ..., \theta_n$

As with the continuous case, the Lagrange multipliers are equal to the forces in the x and y direction of motion and along with the condition $\mathbf{x}_0 = \mathbf{0}$ already imposed, we can now solve equation (39)

$$\mathbf{x}_j = \sum_{k=0}^{j-1} l \left(\cos\theta_k, \sin\theta_k \right) \qquad j = 1, ..., n+1 \tag{62}$$

to provide us with the shape of the curve.

Notice that this discrete model now involves solving a system of algebraic equations rather than a system of ordinary differential equations. Recall that for the continuous case, it was not possible to use the curve end position as a parameter, as the need to instantly branch renders AUTO unable to solve the equations. In the discrete case we do not have this problem and can use X, Y as our parameters without issue, even if the branch point is at the starting solution.

4.6 Example Three

Here we wish to replicate the system introduced in Example One, but for a discrete curve and using end displacement instead of force as our parameter.

We take a discrete pinned curve of $(n+1)$ edges, length L and bending stiffness B lying along the x axis with the start of the curve fixed at the origin. We then impose a displacement (rather than a force) on the end of the curve so that the coordinates of the end are $(L-d, 0)$. We take d as our parameter and increase it from zero.

To solve this problem using AUTO we solve equations (61)

$$\frac{\partial \Lambda}{\partial \lambda_1} = \sum_{j=0}^{n} l\cos\theta_j - L + d = 0 \tag{63}$$

$$\frac{\partial \Lambda}{\partial \lambda_2} = \sum_{j=0}^{n} l\sin\theta_j = 0 \tag{64}$$

$$\frac{\partial \Lambda}{\partial \theta_k} =$$

$$\frac{2B}{l}\left(\tan\left(\frac{\theta_k-\theta_{k-1}}{2}\right)\sec^2\left(\frac{\theta_k-\theta_{k-1}}{2}\right) - \tan\left(\frac{\theta_{k+1}-\theta_k}{2}\right)\sec^2\left(\frac{\theta_{k+1}-\theta_k}{2}\right)\right) \tag{65}$$

$$-\lambda_1 l\sin\theta_k + \lambda_2 l\cos\theta_k = 0 \qquad k = 0, ..., n$$

Where, for sake of notation, we define $\theta_{-1} = \theta_0$ and $\theta_n = \theta_{n+1}$

The starting solution is $(\theta_0, ..., \theta_n, \lambda_1, \lambda_2; d) = (0, ..., 0, 0, 0; 0)$ and AUTO produces solutions to these equations, finding $\lambda_1, \lambda_2, \theta_k$ for $k = 0, ..., n$.

AUTO also picks up values for d under which the system branches (the curve buckles). As before, it is then possible to follow one of these branches, tracking how the system evolves along it.

With the values of θ_k we can further solve equation (62) to provide us with the shape of the curve for any given d.

Figures 16 and 17 show the curve buckled in the first and second modes respectively for $L = B = 1$ and $n = 19$ under the same force as in figures 5 and 6. We see by comparison to figures 5 and 6 that already at $n = 19$, this discrete model provides a good approximation to the continuous case.

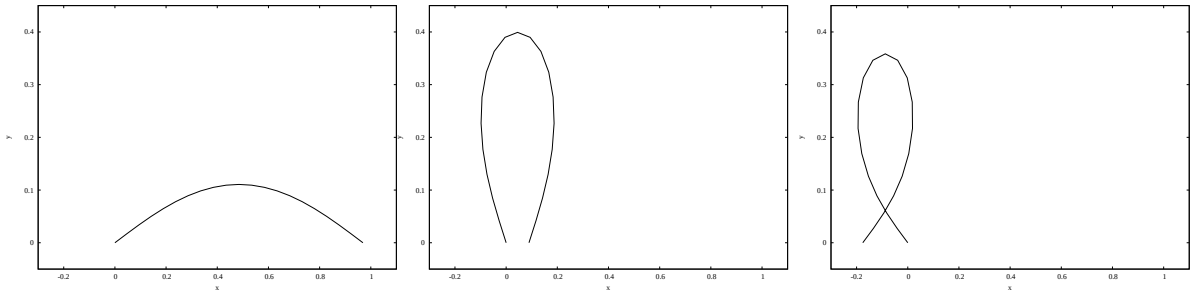

(a) $d = 0.03, \lambda_1 = 10$ (b) $d = 0.91, \lambda_1 = 20$ (c) $d = 1.18, \lambda_1 = 30$

Figure 16: The discrete curve buckling in the first mode

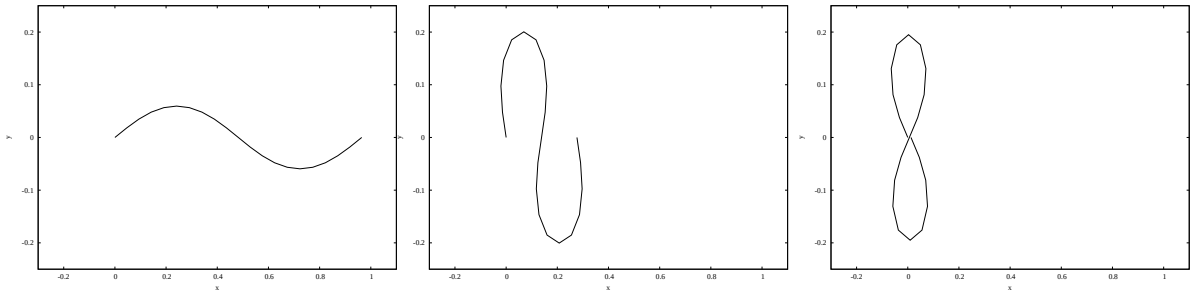

(a) $d = 0.04, \lambda = 40$ (b) $d = 0.72, \lambda = 70$ (c) $d = 0.99, \lambda = 100$

Figure 17: The discrete curve buckling in the second mode

Finally, by appealing to the value of the Lagrange multiplier λ_1, we can identify the end force required to impose a buckling into each mode. Here we find $F_1 = 9.85$ and $F_2 = 39.15$; good approximations to the continuous case. Through further calculations with increasing n we find that as $n \to \infty$, $F_n \to n^2\pi^2$, as we would expect.

4.7 Discrete Extensible Planar Elastica

We set up an extensible model in exactly the same manner as the inextensible case, except that we now allow the edge length to vary.

Denote $|\mathbf{e}^j|$ by r^j and assume that edge $\mathbf{e}^j$ has natural length l. Assuming the curve to be uniformly, linearly elastic with stretching stiffness C, we can write the total stretching energy as

$$E_s = \sum_{j=0}^{n} \frac{1}{2} C(r^j - l)^2 \tag{66}$$

Adding this to the bending energy then gives us the total energy of the curve

$$E = \sum_{j=1}^{n} \frac{2B}{D_j} \tan^2\left(\frac{\theta_j - \theta_{j-1}}{2}\right) + \sum_{j=0}^{n} \frac{1}{2} C(r^j - l)^2 \tag{67}$$

We can then proceed as usual, by finding stationary values of this function subject to various constraints by differentiating with respect to each variable and taking note of the added equations

$$\frac{\partial \Lambda}{\partial r^j} = 0 \qquad j = 0, ..., n$$

Although we take note of this extensible case, the specific examples introduced in the chapters to follow will all be considered inextensible. The extensibility is included for completeness.

4.8 Discrete Inextensible Planar Elastica under a Central Vertex Displacement

With the freedom to use displacement as a parameter we can easily simulate more interesting problems in a discrete setting. We now set up a slightly different model of a discrete elastic curve such that the mid point of the curve has coordinates (X, Y) and the start and end points lie along the x-axis. Because now the start and end points of the curve will be displaced along the axis, we must consider this in the model.

We take n to be odd, and set the start position of the curve to be $\mathbf{x}_0 = (x_0, 0)$. We wish to find stationary points of E_b such that

$$x_0 + \sum_{j=0}^{\frac{n+1}{2}} \cos\theta_j = X \tag{68}$$

$$\sum_{j=0}^{\frac{n+1}{2}} \sin\theta_j = Y \tag{69}$$

$$\sum_{j=0}^{n} \sin\theta_j = 0 \tag{70}$$

As before we consider the problem of finding stationary points of the Lagrangian

$$\Lambda = E_b + \lambda_1 \left(x_0 + \sum_{j=0}^{\frac{n+1}{2}} \cos\theta_j - X \right) + \lambda_2 \left(\sum_{j=0}^{\frac{n+1}{2}} \sin\theta_j - Y \right) + \lambda_3 \left(\sum_{j=0}^{n} \sin\theta_j \right) \tag{71}$$

Stationary points of this system are given by differentiating with respect to each variable, giving us

$$\frac{\partial\Lambda}{\partial\lambda_1} = \frac{\partial\Lambda}{\partial\lambda_2} = \frac{\partial\Lambda}{\partial\lambda_3} = \frac{\partial\Lambda}{\partial x_0} = \frac{\partial\Lambda}{\partial\theta_k} = 0 \qquad\qquad k = 0, ..., n \tag{72}$$

and the shape of the curve is then given by a slightly altered form of equation (39)

$$\mathbf{x}_j = \left(x_0 + \sum_{k=0}^{j-1} \cos\theta_k, \sum_{k=0}^{j-1} \sin\theta_k \right) \tag{73}$$

4.9 Example Four

Here we wish to simulate plucking the mid point of the curve directly upwards by a distance d. In this case the the central vertex of the curve has coordinates $((\frac{n+1}{2})l, d)$. This provides us with the system of equations

$$\frac{\partial \Lambda}{\partial \lambda_1} = x_0 + \sum_{j=0}^{\frac{n+1}{2}} \cos\theta_j - \left(\frac{n+1}{2}\right) l = 0 \tag{74}$$

$$\frac{\partial \Lambda}{\partial \lambda_2} = \sum_{j=0}^{\frac{n+1}{2}} \sin\theta_j - d = 0 \tag{75}$$

$$\frac{\partial \Lambda}{\partial \lambda_3} = \sum_{j=0}^{n} \sin\theta_j = 0 \tag{76}$$

$$\frac{\partial \Lambda}{\partial x_0} = \lambda_1 \tag{77}$$

$$\frac{\partial \Lambda}{\partial \theta_k} = \frac{\partial E_b}{\partial \theta_k} - I_A(k)\lambda_1 \sin\theta_k + I_A(k)\lambda_2 \cos\theta_k + \lambda_3 \cos\theta_k \qquad k = 0, ..., n \tag{78}$$

Where I_A is the indicator function and $A = \left\{0, ..., \frac{n+1}{2}\right\}$

Using d as our parameter, this system of $(n+5)$ equations can be solved using AUTO and Figure 18 shows the shape of the curve under increasing d.

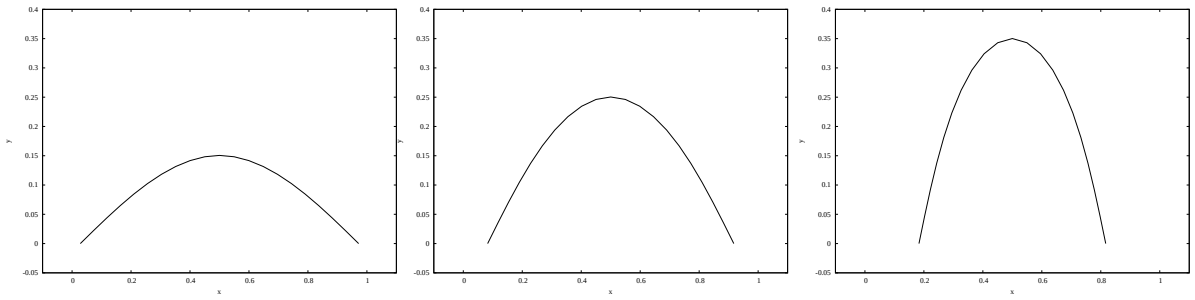

(a) $d = 0.15$ (b) $d = 0.25$ (c) $d = 0.35$

Figure 18: The discrete curve under an increasing central displacement

5 Interacting Discrete Planar Elastic Curves

5.1 Outlining the Model

Using the theory of discrete planar elastic curves outlined in section 4, we are in a position to model the behaviour of interacting planar elastic curves as was first attempted for continuous curves at the end of section three. We take m discrete planar elastic curves made up of equal number of edges. The curves are joined together at their respective vertices by elastic springs; in doing so we construct a system consisting of m discrete elastic curves with each curve connected to its nearest neighbours such that the j^{th} vertex of the i^{th} curve is connected to the j^{th} vertex of the $(i-1)^{th}$ and $(i+1)^{th}$ curve.

We denote the vertices of the i^{th} curve of the system by $\{\mathbf{x}_{i,j} = (x_{i,j}, y_{i,j})\}_{j=0}^{n+1}$ and the edges by $\{\mathbf{e}^{i,j}\}_{j=0}^{n}$. We denote $|\mathbf{e}^{i,j}|$ by $r^{i,j}$ and take the natural length of $\mathbf{e}^{i,j}$ to be l, so that the total natural length of each curve is $L = (n+1)l$. Constraining each curve to lie in the $x-y$ plane, we denote the angle between edge $\mathbf{e}^{i,j}$ and the positive x axis by $\theta_{i,j}$. We take the bending stiffness and stretching stiffness to be constant along the i^{th} curve and of values B_i and C_i respectively.

We now define the vector connecting vertex $\mathbf{x}_{i,j}$ to vertex $\mathbf{x}_{i+1,j}$ by

$$\mathbf{Z}_{i,j} = \mathbf{x}_{i,j} - \mathbf{x}_{i+1,j} \qquad i = 1, ..., m-1, \qquad j = 0, ..., n+1 \tag{79}$$

We take this vector to define the length of the connecting spring and set the spring to have natural length G and strain energy function $f_{i,j}(Z_{i,j})$, where $Z_{i,j} = |\mathbf{Z}_{i,j}|$.

We can thus write the total energy of the system as

$$E = \sum_{i=1}^{m}\sum_{j=1}^{n} \frac{4B_i}{r^{i,j} + r^{i,j-1}} \tan^2\left(\frac{\theta_{i,j} - \theta_{i,j-1}}{2}\right) + \sum_{i=1}^{m}\sum_{j=0}^{n} \frac{1}{2} C_i (r^{i,j} - l)^2 + \sum_{i=1}^{m-1}\sum_{j=0}^{n+1} f_{i,j}(Z_{i,j}) \tag{80}$$

We associate the first term with the bending energy E_b, the second with the stretching energy E_s and the final term with the stretching energy of the connecting springs E_c.

Once again we set up an optimisation problem by finding stationary points of E subject to various constraints. The nature of the constraints depends on the system we are attempting to model and will be covered in detail when each model is considered separately in the following sections. As always we set up a Lagrangian function in order to consider any such constraints.

Once we have solved the equations, we can find the shape of the curve by solving

$$x_{i,j} = x_{i,0} + \sum_{k=0}^{j-1} r^{i,k} \cos\theta_{i,k} \tag{81}$$

$$y_{i,j} = y_{i,0} + \sum_{k=0}^{j-1} r^{i,k} \sin\theta_{i,k} \tag{82}$$

Before we can set up this optimisation problem we look at the derivatives of E with respect to each variable.

5.2 Derivatives

We must first write $Z_{i,j}$ in terms of $x_{i,0}$, $y_{i,0}$, $\theta_{i,j}$ and $r^{i,j}$. We do this by writing

$\mathbf{Z}_{i,j} = (X_{i,j}, Y_{i,j})$, where

$$X_{i,j} = x_{i,0} - x_{i+1,0} + \sum_{k=0}^{j-1}(r^{i,k}\cos\theta_{i,k} - r^{i+1,k}\cos\theta_{i+1,k}) \tag{83}$$

$$Y_{i,j} = y_{i,0} - y_{i+1,0} + \sum_{k=0}^{j-1}(r^{i,k}\sin\theta_{i,k} - r^{i+1,k}\sin\theta_{i+1,k}) \tag{84}$$

So that we have

$$Z_{i,j}^2 = X_{i,j}^2 + Y_{i,j}^2 \tag{85}$$

5.2.1 The Derivative of $\mathbf{E}_b$

E_b depends on $\theta_{i,j}$ and $r_{i,j}$. We find that

$$\frac{\partial E_b}{\partial \theta_{\alpha,\beta}} = \sum_{j=\beta}^{\beta+1}(-1)^{j-\beta}\frac{4B_\alpha}{r^{\alpha,j} + r^{\alpha,j-1}}\tan\left(\frac{\theta_{\alpha,j} - \theta_{\alpha,j-1}}{2}\right)\sec^2\left(\frac{\theta_{\alpha,j} - \theta_{\alpha,j-1}}{2}\right) \tag{86}$$

$$\frac{\partial E_b}{\partial r^{\alpha,\beta}} = -\sum_{j=\beta}^{\beta+1}\frac{4B_\alpha}{(r^{\alpha,j} + r^{\alpha,j-1})^2}\tan^2\left(\frac{\theta_{\alpha,j} - \theta_{\alpha,j-1}}{2}\right) \tag{87}$$

5.2.2 The Derivative of $\mathbf{E}_s$

E_s depends on $r_{i,j}$. We find that

$$\frac{\partial E_s}{\partial r^{\alpha,\beta}} = C_\alpha(r^{\alpha,\beta} - l) \tag{88}$$

5.2.3 The Derivative of $\mathbf{E}_c$

Unfortunately, the derivative of E_c is a lot more complex. E_c depends on $x_{i,0}, y_{i,0}, \theta_{i,j}$ and $r_{i,j}$ via the dependence on $Z_{i,j}$

First note that $Z_{i,j}$ is a function of $x_{i,0}, x_{i+1,0}, y_{i,0}, y_{i+1,0}, \theta_{i,0}, ..., \theta_{i,j-1}, \theta_{i+1,0}, ..., \theta_{i+1,j-1}$, $r^{i,0}, ..., r^{i,j-1}$ and $r^{i+1,0}, ..., r^{i+1,j-1}$. With this in mind we pick out the relevant terms for each of our particular derivatives. This allows us to write

$$\begin{aligned}\frac{\partial E_c}{\partial x_{\alpha,0}} &= \frac{\partial}{\partial x_{\alpha,0}} \sum_{j=0}^{n+1} \left(f_{\alpha,j}(Z_{\alpha,j}) + f_{\alpha-1,j}(Z_{\alpha-1,j})\right) \\ &= \sum_{j=0}^{n+1} \left(f'_{\alpha,j}(Z_{\alpha,j}) \frac{\partial Z_{\alpha,j}}{\partial x_{\alpha,0}} + f'_{\alpha-1,j}(Z_{\alpha-1,j}) \frac{\partial Z_{\alpha-1,j}}{\partial x_{\alpha,0}} \right)\end{aligned} \tag{89}$$

And similarly for $y_{\alpha,0}$

We can also write

$$\begin{aligned}\frac{\partial E_c}{\partial \theta_{\alpha,\beta}} &= \frac{\partial}{\partial \theta_{\alpha,\beta}} \sum_{j=\beta+1}^{n+1} \left(f_{\alpha,j}(Z_{\alpha,j}) + f_{\alpha-1,j}(Z_{\alpha-1,j})\right) \\ &= \sum_{j=\beta+1}^{n+1} \left(f'_{\alpha,j}(Z_{\alpha,j}) \frac{\partial Z_{\alpha,j}}{\partial \theta_{\alpha,\beta}} + f'_{\alpha-1,j}(Z_{\alpha-1,j}) \frac{\partial Z_{\alpha-1,j}}{\partial \theta_{\alpha,\beta}} \right)\end{aligned} \tag{90}$$

And similarly for $r^{\alpha,\beta}$

We defined $Z_{i,j}$ such that $Z_{i,j}^2 = X_{i,j}^2 + Y_{i,j}^2$. Giving us, for any variable, v

$$Z_{i,j} \frac{\partial Z_{i,j}}{\partial v} = X_{i,j} \frac{\partial X_{i,j}}{\partial v} + Y_{i,j} \frac{\partial Y_{i,j}}{\partial v} \tag{91}$$

Using this result together with the definitions of $X_{i,j}$ and $Y_{i,j}$ we can calculate some intermediate derivatives.

For $j = 0, ..., n+1$

$$\frac{\partial Z_{\alpha,j}}{\partial x_{\alpha,0}} = \frac{X_{\alpha,j}}{Z_{\alpha,j}}$$
$$\frac{\partial Z_{\alpha-1,j}}{\partial x_{\alpha,0}} = -\frac{X_{\alpha-1,j}}{Z_{\alpha-1,j}}$$
$$\frac{\partial Z_{\alpha,j}}{\partial y_{\alpha,0}} = \frac{Y_{\alpha,j}}{Z_{\alpha,j}}$$
$$\frac{\partial Z_{\alpha-1,j}}{\partial y_{\alpha,0}} = -\frac{Y_{\alpha-1,j}}{Z_{\alpha-1,j}}$$

And for $j = \beta+1, ..., n+1$

$$\frac{\partial Z_{\alpha,j}}{\partial \theta_{\alpha,\beta}} = \frac{r^{\alpha,\beta}}{Z_{\alpha,j}}(-X_{\alpha,j}\sin\theta_{\alpha,\beta} + Y_{\alpha,j}\cos\theta_{\alpha,\beta})$$
$$\frac{\partial Z_{\alpha-1,j}}{\partial \theta_{\alpha,\beta}} = -\frac{r^{\alpha,\beta}}{Z_{\alpha-1,j}}(-X_{\alpha-1,j}\sin\theta_{\alpha,\beta} + Y_{\alpha-1,j}\cos\theta_{\alpha,\beta})$$
$$\frac{\partial Z_{\alpha,j}}{\partial r^{\alpha,\beta}} = \frac{1}{Z_{\alpha,j}}(X_{\alpha,j}\cos\theta_{\alpha,\beta} + Y_{\alpha,j}\sin\theta_{\alpha,\beta})$$
$$\frac{\partial Z_{\alpha-1,j}}{\partial r^{\alpha,\beta}} = -\frac{1}{Z_{\alpha-1,j}}(X_{\alpha-1,j}\cos\theta_{\alpha,\beta} + Y_{\alpha-1,j}\sin\theta_{\alpha,\beta})$$

Substituting these derivatives into equations (89) and (90) give us

$$\frac{\partial E_c}{\partial x_{\alpha,0}} = \sum_{i=\alpha-1}^{\alpha}\sum_{j=0}^{n+1}(-1)^{i-\alpha}\frac{X_{i,j}f'_{i,j}(Z_{i,j})}{Z_{i,j}} \tag{92}$$

$$\frac{\partial E_c}{\partial y_{\alpha,0}} = \sum_{i=\alpha-1}^{\alpha}\sum_{j=0}^{n+1}(-1)^{i-\alpha}\frac{Y_{i,j}f'_{i,j}(Z_{i,j})}{Z_{i,j}} \tag{93}$$

$$\frac{\partial E_c}{\partial \theta_{\alpha,\beta}} = r^{\alpha,\beta}\sum_{i=\alpha-1}^{\alpha}\sum_{j=\beta+1}^{n+1}(-1)^{i-\alpha}\frac{f'_{i,j}(Z_{i,j})}{Z_{i,j}}(-X_{i,j}\sin\theta_{\alpha,\beta} + Y_{i,j}\cos\theta_{\alpha,\beta}) \tag{94}$$

$$\frac{\partial E_c}{\partial r^{\alpha,\beta}} = r^{\alpha,\beta}\sum_{i=\alpha-1}^{\alpha}\sum_{j=\beta+1}^{n+1}(-1)^{i-\alpha}\frac{f'_{i,j}(Z_{i,j})}{Z_{i,j}}(X_{i,j}\sin\theta_{\alpha,\beta} + Y_{i,j}\cos\theta_{\alpha,\beta}) \tag{95}$$

Putting all these derivatives together we have for $(\alpha, \beta) \in \{1, ..., m\} \times \{0, ..., n\}$

$$\frac{\partial E}{\partial x_{\alpha,0}} = \sum_{i=\alpha-1}^{\alpha} \sum_{j=0}^{n+1} (-1)^{i-\alpha} \frac{X_{i,j} f'_{i,j}(Z_{i,j})}{Z_{i,j}} \tag{96}$$

$$\frac{\partial E}{\partial y_{\alpha,0}} = \sum_{i=\alpha-1}^{\alpha} \sum_{j=0}^{n+1} (-1)^{i-\alpha} \frac{Y_{i,j} f'_{i,j}(Z_{i,j})}{Z_{i,j}} \tag{97}$$

$$\begin{aligned} \frac{\partial E}{\partial \theta_{\alpha,\beta}} = & \sum_{j=\beta}^{\beta+1} (-1)^{j-\beta} \frac{4B_\alpha}{r^{\alpha,j} + r^{\alpha,j-1}} \tan\left(\frac{\theta_{\alpha,j} - \theta_{\alpha,j-1}}{2}\right) \sec^2\left(\frac{\theta_{\alpha,j} - \theta_{\alpha,j-1}}{2}\right) \\ & + r^{\alpha,\beta} \sum_{i=\alpha-1}^{\alpha} \sum_{j=\beta+1}^{n+1} (-1)^{i-\alpha} \frac{f'_{i,j}(Z_{i,j})}{Z_{i,j}} (-X_{i,j} \sin\theta_{\alpha,\beta} + Y_{i,j} \cos\theta_{\alpha,\beta}) \end{aligned} \tag{98}$$

$$\begin{aligned} \frac{\partial E}{\partial r^{\alpha,\beta}} = & -\sum_{j=\beta}^{\beta+1} \frac{4B_\alpha}{(r^{\alpha,j} + r^{\alpha,j-1})^2} \tan^2\left(\frac{\theta_{\alpha,j} - \theta_{\alpha,j-1}}{2}\right) + C_\alpha(r^{\alpha,\beta} - l) \\ & + r^{\alpha,\beta} \sum_{i=\alpha-1}^{\alpha} \sum_{j=\beta+1}^{n+1} (-1)^{i-\alpha} \frac{f'_{i,j}(Z_{i,j})}{Z_{i,j}} (X_{i,j} \sin\theta_{\alpha,\beta} + Y_{i,j} \cos\theta_{\alpha,\beta}) \end{aligned} \tag{99}$$

Where, for the sake of notation, we define for $i = 1, ..., m$, $\theta_{i,-1} = \theta_{i,0}$, $\theta_{i,n} = \theta_{i,n+1}$, $r^{i,-1} = r^{i,0}$, $r^{i,n} = r^{i,n+1}$ and for $j = 0, ..., n$, $X_{0,j} = Y_{0,j} = Z_{0,j} = f'_{0,j} = 0$ and $X_{m,j} = Y_{m,j} = Z_{m,j} = f'_{m,j} = 0$.

5.3 Simultaneous End Displacement of Interacting Elastic Curves

Here we wish set up a system of m pinned, inextensible curves of length L and bending stiffness B_i, lying side by side, parallel to the x axis and a distance G apart. We impose that the start of the i^{th} curve is fixed at $(0,(1-i)G)$ and the end point has coordinates $(L-d,(1-i)G)$. Taking d as our parameter, we increase it from zero to simulate a simultaneous and equal end displacement of the curves from the initial state.

We have here, $x_{i,0}=0$ and $y_{i,0}=(1-i)G$ with the constraints

$$\sum_{j=0}^{n} l\cos\theta_{i,j} = L-d \qquad i=1,...,m \tag{100}$$

$$\sum_{j=0}^{n} l\sin\theta_{i,j} = 0 \qquad i=1,...,m \tag{101}$$

We consider the problem of finding stationary points of the Lagrangian

$$\begin{aligned}\Lambda = &\sum_{i=1}^{m}\sum_{j=1}^{n}\frac{2B_i}{l}\tan^2\left(\frac{\theta_{i,j}-\theta_{i,j-1}}{2}\right)+\sum_{i=1}^{m-1}\sum_{j=0}^{n+1}f_{i,j}(Z_{i,j})\\ &+\sum_{i=1}^{m}\lambda_{1,i}\sum_{j=0}^{n}\left(l\cos\theta_{i,j}-L+d\right)+\sum_{i=1}^{m}\lambda_{2,i}\sum_{j=0}^{n}l\sin\theta_{i,j}\end{aligned} \tag{102}$$

Stationary points of this system are given by differentiating with respect to each variable

$$\frac{\partial\Lambda}{\partial\lambda_{1,\alpha}}=\frac{\partial\Lambda}{\partial\lambda_{2,\alpha}}=\frac{\partial\Lambda}{\partial\theta_{\alpha,\beta}}=0 \qquad (\alpha,\beta)\in\{1,...,m\}\times\{0,...,n\} \tag{103}$$

Giving us a system of $m(n+3)$ equations.

$$\frac{\partial \Lambda}{\partial \lambda_{1,\alpha}} = \sum_{j=0}^{n} l \cos\theta_{i,j} - L + d = 0 \qquad i = 1, ..., m \tag{104}$$

$$\frac{\partial \Lambda}{\partial \lambda_{2,\alpha}} = \sum_{j=0}^{n} l \sin\theta_{i,j} = 0 \qquad i = 1, ..., m \tag{105}$$

$$\frac{\partial \Lambda}{\partial \theta_{\alpha,\beta}} = \frac{2}{l} \sum_{j=\beta}^{\beta+1} (-1)^{j-\beta} B_\alpha \tan\left(\frac{\theta_{\alpha,j} - \theta_{\alpha,j-1}}{2}\right) \sec^2\left(\frac{\theta_{\alpha,j} - \theta_{\alpha,j-1}}{2}\right)$$

$$+ l \sum_{i=\alpha-1}^{\alpha} \sum_{j=\beta+1}^{n+1} (-1)^{i-\alpha} \frac{f'_{i,j}(Z_{i,j})}{Z_{i,j}} (-X_{i,j} \sin\theta_{\alpha,\beta} + Y_{i,j} \cos\theta_{\alpha,\beta}) \tag{106}$$

$$- \lambda_{1,\alpha} l \sin\theta_{\alpha,\beta} + \lambda_{2,\alpha} l \cos\theta_{\alpha,\beta} = 0 \qquad (\alpha, \beta) \in \{1, ..., m\} \times \{0, ..., n\}$$

Our starting solution is

$\lambda_{1,j} = \lambda_{2,j} = \theta_{i,j} = 0$ for $(i, j) \in \{1, ..., m\} \times \{0, ..., n\}$

We now have a system of the required form to solve using AUTO.

On first attempting to solve this problem numerically we see that all the curves buckle together in the same mode and direction, leaving the springs at natural length, thereby not contributing to the energy of the system at all. As we wish to understand how cross linking effects the deformation of the system, where the springs come into play because of the curves deforming away or towards each other, or indeed into different modes, we must reconsider our starting solution.

Because we know how a single curve will buckle when subject to an end displacement, the idea is to construct a starting solution such that the system has already and will continue to buckle into any combination of modes we choose. We can force this to occur by first taking a combination of single curve solutions in a buckled state for very small end displacement, $d = \epsilon << 1$. This combination of solutions is taken as our initial values of $\lambda_{1,i}$,$\lambda_{2,i}$ and $\theta_{i,j}$ for $(i, j) \in \{1, ..., m\} \times \{0, ..., n\}$ and also for the parameter d.

We then take the connecting springs to all be at natural length in this state, denoting the length of spring $Z_{i,j}$ by $G_0(i, j)$.

By defining

$$Z_{i,j} = (1 - \mu)G_0(i, j) + \mu G \tag{107}$$

We now have a valid solution to equations (103) and aim to find further solutions as we increase the paramer μ from zero and stopping when $\mu = 1$. This process allows the system to evolve into a state where the springs now have natural length G and we can read off a valid solution to the equations.

At this point we have our sought after starting solution: values for $\lambda_{1,i}$,$\lambda_{2,i}$ and $\theta_{i,j}$ for $(i, j) \in \{1, ..., m\} \times \{0, ..., n\}$, such that the system has already buckled into our chosen modes with $d = \epsilon$.

Finally we solve the equations once again, but now using d as the parameter, increasing d from ϵ, and thus tracking how the system evolves under an increasing end displacement.

This problem is very general, as picking which combination of buckled single curve solutions we take in order to construct the initial solution leads to many possibilities. Even if we only consider curves that have buckled in the first mode (they can either buckle up

or down) we have two possibilities for a system of two curves (1 up, 2 down or 1 down, 2 up), six for a system of three, fourteen for a system of four, and so on.

5.3.1 Example Five

Take the case of two curves laying side by side, with a Hookean spring of natural length G connecting the central vertex of each rod. We do this by taking $m = 2$, n odd and $f_{i,j}(x) = \frac{1}{2}k_{i,j}(x - G)^2$, where $k_{i,j}$ is the elastic constant of the springs such that $k_{i,j} = k\delta_{1,i}\delta_{\frac{n+1}{2},j}$. For the initial solution we take the two curves in the first mode, but buckled in opposite directions with curve $i = 1$ buckling in the positive x direction and the curve $i = 2$ buckling in the negative x direction.

For $n = 19$, $B_1 = B_2 = B = 1$, we take a very stiff spring by setting $k = 10,000$. Figure 19(a) shows the curves laying side by side in the buckled states with $d = 8.26 \times 10^{-5}$, before we vary the parameter μ. Figure 19(b) shows the curves once we reach $\mu = 1$.

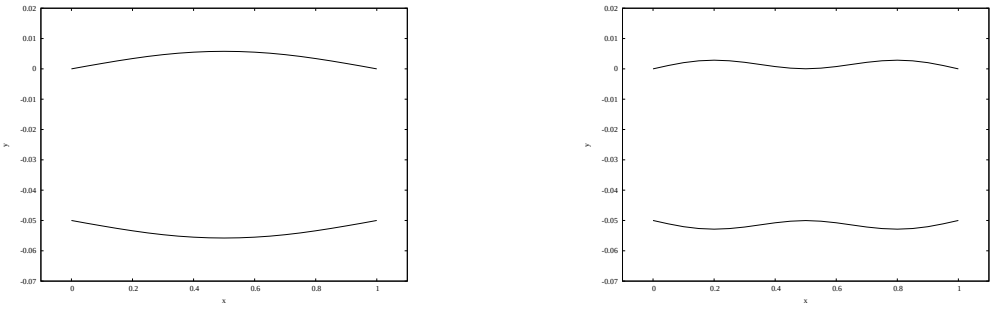

(a) $\mu = 0$ (b) $\mu = 1$

Figure 19: The system at $\mu = 0$ and $\mu = 1$

Taking this as our initial solution, figure 20 shows how the system evolves under an increasing end displacement d.

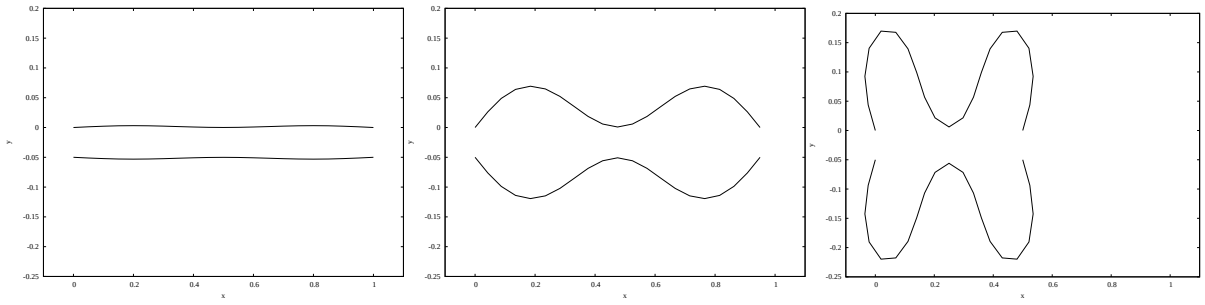

(a) $d = 8.26 \times 10^{-5}$ (b) $d = 0.05$ (c) $d = 0.5$

Figure 20: Two interacting curves buckling together in opposite directions

There are many more interesting examples we can investigate, varying the spring constants and positions of the connecting springs. In particular we can use a three dimensional version of this model to represent an end displacement the collagen fibril, while enforcing certain buckling modes on each of the (molecule)-(end-end corss-link)-(molecule) rod structure. Alternatively we could begin with the curves in a bent shape and then stretch the curves in the axial direction to simulate an extension of the collagen fibril.

5.4 Single End Displacement of Interacting Elastic Curves

We now wish to set up a system of m pinned, inextensible curves of length L and bending stiffness B_i, laying side by side, parallel to the x axis and a distance G apart. We impose that the start and end points of the i^{th} curve lay on the line $y = (1-i)G$ and for $i \neq a$ $x_{i,0} = 0$, where $a \in \{2, ..., m-1\}$. We then impose that the end coordinates of rod $i = a$ are $(L+d, (1-a)G)$. Taking d as our parameter, we increase it from zero to simulate a single end displacement of one of the central curves in the positive x direction.

Here we have $x_{i,0} = \delta_{i,a}(L+d)$ and $y_{i,0} = (1-i)G$, with the constraints

$$x_{a,0} + \sum_{j=0}^{n} l\cos\theta_{a,j} = (n+1)l + d \tag{108}$$

$$\sum_{j=0}^{n} l\sin\theta_{i,j} = 0 \qquad i = 1, ..., m \tag{109}$$

We consider the problem of finding stationary points of the Lagrangian

$$\Lambda = \sum_{i=1}^{m}\sum_{j=1}^{n} \frac{2B_i}{l}\tan^2\left(\frac{\theta_{i,j} - \theta_{i,j-1}}{2}\right) + \sum_{i=1}^{m-1}\sum_{j=0}^{n+1} f_{i,j}(Z_{i,j})$$

$$+ \mu\left(x_{a,0} + \sum_{j=0}^{n} l\cos\theta_{a,j} - (n+1)l - d\right) \tag{110}$$

$$+ \sum_{i=1}^{m}\lambda_i \sum_{j=0}^{n} l\sin\theta_{i,j}$$

Stationary values of this system are given by differentiating with respect to each variable

$$\frac{\partial\Lambda}{\partial\mu} = \frac{\partial\Lambda}{\partial\lambda_\alpha} = \frac{\partial\Lambda}{\partial x_{a,0}} = \frac{\partial\Lambda}{\partial\theta_{\alpha,\beta}} = 0 \qquad (\alpha,\beta) \in \{1, ..., m\} \times \{0, ..., n\} \tag{111}$$

Giving us a system of $m(n+2)+2$ equations.

$$\frac{\partial \Lambda}{\partial \mu} = x_{a,0} + \sum_{j=0}^{n} l \cos\theta_{a,j} - (n+1)l - d = 0 \tag{112}$$

$$\frac{\partial \Lambda}{\partial \lambda_\alpha} = \sum_{j=0}^{n} l \sin\theta_{\alpha,j} = 0 \qquad \alpha = 1, ..., m \tag{113}$$

$$\frac{\partial \Lambda}{\partial x_{a,0}} = \sum_{i=a-1}^{a} \sum_{j=0}^{n+1} (-1)^{i-a} \frac{X_{i,j} f'_{i,j}(Z_{i,j})}{Z_{i,j}} + \mu = 0 \tag{114}$$

$$\frac{\partial \Lambda}{\partial \theta_{\alpha,\beta}} = \frac{2}{l} \sum_{j=\beta}^{\beta+1} (-1)^{j-\beta} B_\alpha \tan\left(\frac{\theta_{\alpha,j} - \theta_{\alpha,j-1}}{2}\right) \sec^2\left(\frac{\theta_{\alpha,j} - \theta_{\alpha,j-1}}{2}\right)$$

$$+ l \sum_{i=\alpha-1}^{\alpha} \sum_{j=\beta+1}^{n+1} (-1)^{i-\alpha} \frac{f'_{i,j}(Z_{i,j})}{Z_{i,j}} (-X_{i,j} \sin\theta_{\alpha,\beta} + Y_{i,j} \cos\theta_{\alpha,\beta}) \tag{115}$$

$$- \delta_{\alpha,a} \mu l \sin\theta_{\alpha,\beta} + \lambda_\alpha l \sin\theta_{\alpha,\beta} = 0 \qquad (\alpha, \beta) \in \{1, ..., m\} \times \{0, ..., n\}$$

Our starting solution is

$\mu = \lambda_\alpha = x_{a,0} = \theta_{\alpha,\beta} = 0$ for $(\alpha, \beta) \in \{1, ..., m\} \times \{0, ..., n\}$

We now have a system of the required form to solve using AUTO.

5.4.1 Example Six

Take the case of three curves laying side by side with an even number of sections. We connect vertices $\mathbf{x}_{1,\frac{n+1}{4}}$ to $\mathbf{x}_{2,\frac{n+1}{4}}$ and $\mathbf{x}_{2,\frac{n+1}{2}}$ to $\mathbf{x}_{3,\frac{n+1}{2}}$, via Hookean springs of natural length G. We do this by taking $m = 3$, n odd and $f_{i,j}(x) = \frac{1}{2}k_{i,j}(x - G)^2$, where $k_{i,j}$ is the elastic constant of the springs such that $k_{i,j} = k_1\delta_{1,i}\delta_{\frac{n+1}{4},j} + k_2\delta_{2,i}\delta_{\frac{n+1}{2},j}$.

For $n = 19$, $B_1 = B_2 = B_3 = B = 1$, Figure 21 shows the curves evolving under the increasing end displacement of the central curve, while the other two have their starting coordinate fixed. d for $k_1 = 100$ and $k_2 = 10$

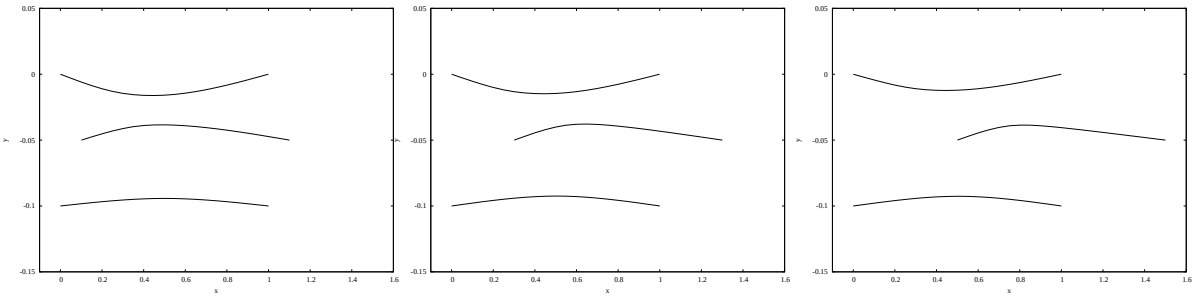

(a) $d = 0.1$ (b) $d = 0.3$ (c) $d = 0.5$

Figure 21: Central curve being pulled out of the bunch

There is no branching in this system. The curves simply deform as the central curve is pulled out of the bundle.

There are many more interesting examples we can investigate, varying the spring constants and positions of the connecting springs. In particular we can use a three dimensional version of this model to represent plucking a single tropocollagen molecule in the axial direction, from within the fibril.

5.5 Plucking the Top Curve

We now wish set up a system of m pinned, inextensible curves of length L and bending stiffness B_i, laying side by side, parallel to the x axis and a distance G apart. We impose that the start and end points of the i^{th} curve lay on the line $y = (1-i)G$, and that the coordinates of vertex $\mathbf{x}_{1,b}$ $(0 < b < n+1)$ are (X, Y), simulating a displacement of this vertex.

We have $y_{i,0} = (1-i)G$ and the constraints

$$x_{1,0} + \sum_{j=0}^{b-1} l \cos\theta_{1,j} = X \tag{116}$$

$$\sum_{j=0}^{b-1} l \sin\theta_{1,j} = Y \tag{117}$$

$$\sum_{j=0}^{n} l \sin\theta_{i,j} = 0 \qquad i = 1, ..., m \tag{118}$$

We consider finding stationary points of the Lagrange function

$$\begin{aligned}\Lambda = &\sum_{i=1}^{m}\sum_{j=1}^{n} \frac{2B_i}{l} \tan^2\left(\frac{\theta_{i,j} - \theta_{i,j-1}}{2}\right) + \sum_{i=1}^{m-1}\sum_{j=0}^{n+1} f_{i,j}(Z_{i,j}) \\ &+ \mu\left(x_{1,0} + \sum_{j=0}^{b-1} l\cos\theta_{1,j} - X\right) + \eta\left(\sum_{j=0}^{b-1} l\sin\theta_{1,j} - Y\right) + \sum_{i=1}^{m}\lambda_i \sum_{j=0}^{n} l\sin\theta_{i,j}\end{aligned} \tag{119}$$

Stationary values of this system are given by differentiating with respect to each variable

$$\frac{\partial\Lambda}{\partial\mu} = \frac{\partial\Lambda}{\partial\eta} = \frac{\partial\Lambda}{\partial\lambda_\alpha} = \frac{\partial\Lambda}{\partial x_{\alpha,0}} = \frac{\partial\Lambda}{\partial\theta_{\alpha,\beta}} = 0 \qquad (\alpha,\beta) \in \{1,...,m\} \times \{0,...,n\} \tag{120}$$

Giving us a system of $m(n+3)+2$ equations.

$$\frac{\partial \Lambda}{\partial \mu} = x_{1,0} + \sum_{j=0}^{b-1} l \cos\theta_{1,j} - X = 0 \tag{121}$$

$$\frac{\partial \Lambda}{\partial \eta} = \sum_{j=0}^{b-1} l \sin\theta_{1,j} - Y = 0 \tag{122}$$

$$\frac{\partial \Lambda}{\partial \lambda_\alpha} = \sum_{j=0}^{n} l \sin\theta_{\alpha,j} = 0 \qquad \alpha = 1, ..., m \tag{123}$$

$$\frac{\partial \Lambda}{\partial x_{\alpha,0}} = \sum_{i=\alpha-1}^{\alpha} \sum_{j=0}^{n+1} (-1)^{i-\alpha} \frac{X_{i,j} f'_{i,j}(Z_{i,j})}{Z_{i,j}} + \delta_{1,\alpha}\mu = 0 \qquad \alpha = 1, ..., m \tag{124}$$

$$\begin{aligned} \frac{\partial \Lambda}{\partial \theta_{\alpha,\beta}} &= \frac{2}{l} \sum_{j=\beta}^{\beta+1} (-1)^{j-\beta} B_\alpha \tan\left(\frac{\theta_{\alpha,j} - \theta_{\alpha,j-1}}{2}\right) \sec^2\left(\frac{\theta_{\alpha,j} - \theta_{\alpha,j-1}}{2}\right) \\ &+ l \sum_{i=\alpha-1}^{\alpha} \sum_{j=\beta+1}^{n+1} (-1)^{i-\alpha} \frac{f'_{i,j}(Z_{i,j})}{Z_{i,j}} (-X_{i,j} \sin\theta_{\alpha,\beta} + Y_{i,j} \cos\theta_{\alpha,\beta}) \\ &- \delta_{1,\alpha} I_A(\beta) \mu l \sin\theta_{\alpha,\beta} + \delta_{1,\alpha} I_A(\beta) \eta l \cos\theta_{\alpha,\beta} + \lambda_\alpha l \cos\theta_{\alpha,\beta} = 0 \end{aligned} \tag{125}$$

$(\alpha, \beta) \in \{1, ..., m\} \times \{0, ..., n\}$

Where $A = \{0, ..., b-1\}$

Our starting solution is

$\mu = \eta = \lambda_\alpha = x_{\alpha,0} = \theta_{\alpha,\beta} = 0$ for $(\alpha, \beta) \in \{1, ..., m\} \times \{0, ..., n\}$

We now have a system of the required form to solve using AUTO.

5.5.1 Example Seven

Take the case of three curves laying side by side with an even number of sections. We connect curve one to curve two by a spring one quarter along their length and curve two to curve three by a spring three quarters along their length. We impose this condition by connecting vertex $\mathbf{x}_{1,\frac{n+1}{4}}$ to $\mathbf{x}_{2,\frac{n+1}{4}}$ and vertex $\mathbf{x}_{2,\frac{3(n+1)}{4}}$ to $\mathbf{x}_{3,\frac{3(n+1)}{4}}$ by Hookean springs of natural length G. We do this by taking $m = 3$, n odd and $f_{i,j}(x) = \frac{1}{2}k_{i,j}(x - G)^2$, where $k_{i,j}$ is the elastic constant of the springs such that $k_{i,j} = k_1\delta_{1,i}\delta_{\frac{n+1}{4},j} + k_2\delta_{2,i}\delta_{\frac{3(n+1)}{2},j}$.

We then displace the central vertex of the curve $i = 1$ in the positive y direction by setting $(X, Y) = ((\frac{n+1}{2})l, d)$ and increasing d from zero.

For $n = 19$, $B_1 = B_2 = B_3 = B = 1$, Figure 22 shows the curves evolving under the increasing displacement d for $k_1 = 100$ and $k_2 = 10$

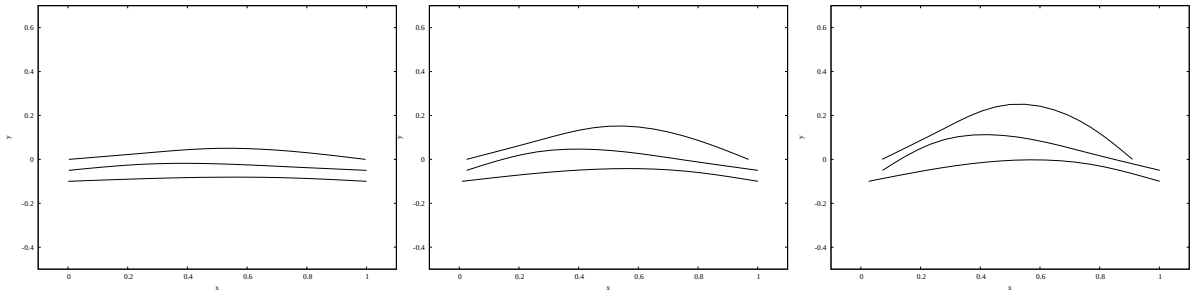

(a) $d = 0.05$ (b) $d = 0.15$ (c) $d = 0.25$

Figure 22: Plucking the top curve

We can clearly see how the springs affect the deformation of the system as the top curve is plucked in the positive y direction.

There are many more interesting examples we can investigate, varying the spring constants and positions of the connecting springs. In particular we can use a three dimensional version of this model to represent plucking a single tropocollagen molecule in a direction perpendicular to the axial direction, from the edge of the collagen fibril.

6 Continuous Space Curves

6.1 Space Curves

A parameterised differentiable space curve (henceforth referred to as a space curve, or simply, curve), is a three times, continuously differentiable map $\mathbf{r} : I \to \mathbb{R}^3$, where $I = [p_A, p_B] \subset \mathbb{R}$, and the parameter p maps to the point $\mathbf{r}(p)$.

The curve is said to be regular if $\mathbf{r}'(p) \neq \mathbf{0}$ for all $p \in I$

For such regular curves we can define the tangent vector to the curve at $\mathbf{r}(p)$ by

$$\mathbf{t}(p) = \mathbf{r}'(p) \tag{126}$$

For any $p_0 \in I$, the arclength of the curve from p_0 to p is given by

$$s(p) = \int_{p_0}^{p} |\mathbf{t}(u)| du \tag{127}$$

From which it follows that

$$\frac{ds}{dp} = |\mathbf{t}(p)| \tag{128}$$

We can reparameterise the curve by the arclength by setting $s(p) = p$, and as a consequence $|\mathbf{t}(s)| = 1$.

Thus for finite curves of length L we can always parameterise the curve by arclength such that $\mathbf{r} : [0, L] \to \mathbb{R}^3$

6.2 Curve Framing

We now wish to define an orthonormal coordinate frame at each point along the space curve. Such frames are not unique and we introduce two especially important frames below, the Frenet frame and the natural frame. The latter is also called the parallel transport or Bishop frame, after [32]. When we assign a frame to each point of the curve we refer to a framed curve. If we further take one of the orthonormal coordinate vectors defining the frame to be in the direction of the tangent to the curve at all points, then we say that the frame is adapted to the curve, and we refer to an adapted framed curve. Figure 23 depicts an adapted orthonormal frame at various points along a curve.

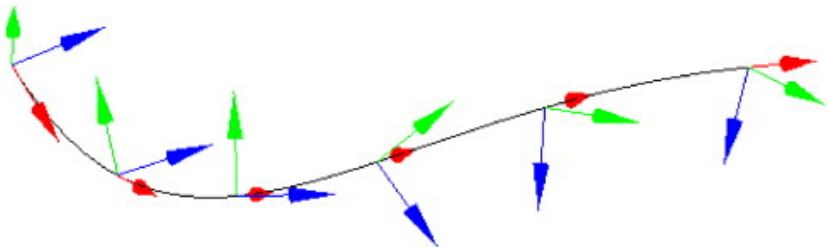

Figure 23: Moving frame

6.2.1 The Darboux Vector

Before going on to discuss these frames we note that the evolution of any orthonormal frame $\{\mathbf{e}_1(s), \mathbf{e}_2(s), \mathbf{e}_3(s)\}$ as we traverse a space curve parameterised by arclength s, is given in terms of the Darboux vector $\mathbf{\Omega}(s)$, by

$$\mathbf{e}_i' = \mathbf{\Omega} \times \mathbf{e}_i \qquad i = 1, 2, 3 \tag{129}$$

Where, $\mathbf{\Omega} = \Omega_1\mathbf{e}_1 + \Omega_2\mathbf{e}_2 + \Omega_3\mathbf{e}_3$ [33]

And so we have the skew-symmetric system

$$\begin{aligned}
\mathbf{e}_1' &= \qquad\quad \Omega_3\mathbf{e}_2 - \Omega_2\mathbf{e}_3 \\
\mathbf{e}_2' &= -\Omega_3\mathbf{e}_1 \qquad\quad + \Omega_1\mathbf{e}_3 \\
\mathbf{e}_3' &= \quad \Omega_2\mathbf{e}_1 - \Omega_1\mathbf{e}_2
\end{aligned}$$

Or in matrix form

$$\begin{pmatrix} \mathbf{e}_1' \\ \mathbf{e}_2' \\ \mathbf{e}_3' \end{pmatrix} = \begin{pmatrix} 0 & \Omega_3 & -\Omega_2 \\ -\Omega_3 & 0 & \Omega_1 \\ \Omega_2 & -\Omega_1 & 0 \end{pmatrix} \begin{pmatrix} \mathbf{e}_1 \\ \mathbf{e}_2 \\ \mathbf{e}_3 \end{pmatrix}$$

Which we use to write

$$\begin{aligned}
\Omega_1 &= \mathbf{e}_2' \cdot \mathbf{e}_3 = -\mathbf{e}_3' \cdot \mathbf{e}_2 = \tfrac{1}{2}\left(\mathbf{e}_2' \cdot \mathbf{e}_3 - \mathbf{e}_3' \cdot \mathbf{e}_2\right) \\
\Omega_2 &= -\mathbf{e}_1' \cdot \mathbf{e}_3 = \mathbf{e}_3' \cdot \mathbf{e}_1 = \tfrac{1}{2}\left(-\mathbf{e}_1' \cdot \mathbf{e}_3 + \mathbf{e}_3' \cdot \mathbf{e}_1\right) \\
\Omega_3 &= \mathbf{e}_1' \cdot \mathbf{e}_2 = -\mathbf{e}_2' \cdot \mathbf{e}_1 = \tfrac{1}{2}\left(\mathbf{e}_1' \cdot \mathbf{e}_2 - \mathbf{e}_2' \cdot \mathbf{e}_1\right)
\end{aligned}$$

That is

$$\Omega_i = \frac{1}{2}\varepsilon_{ijk}\mathbf{e}_j' \cdot \mathbf{e}_k \tag{130}$$

6.2.2 The Frenet Frame

For an arc length parameterised curve, we define the unit tangent vector to the curve at $\mathbf{r}(s)$ as before

$$\mathbf{t}(s) = \mathbf{r}'(s) \tag{131}$$

Differentiating $\mathbf{t}(s) \cdot \mathbf{t}(s) = 1$ with respect to s shows that $\mathbf{t} \cdot \mathbf{t}' = 0$ (the vectors are orthogonal). We then define the curvature at $\mathbf{r}(s)$ by

$$k(s) = |\mathbf{t}'(s)| \tag{132}$$

This measures the turning rate of the tangent along the curve and is geometrically given by the inverse of the radius of the best fitting circle at s, just as in the two dimensional case. If this is non zero, we then define the unit normal vector to the curve at $\mathbf{r}(s)$ by

$$\mathbf{n}(s) = \frac{\mathbf{t}'(s)}{k(s)} \tag{133}$$

Finally we define the unit binormal vector to the curve at $\mathbf{r}(s)$ in terms of the unit tangent and unit normal vectors.

$$\mathbf{b}(s) = \mathbf{t}(s) \times \mathbf{n}(s) \tag{134}$$

Now since $\mathbf{b}$ is a unit vector, $\mathbf{b}'$ is orthogonal to $\mathbf{b}$. Also, by differentiating the definition of $\mathbf{b}$ and using the definition of $\mathbf{n}$, we have

$$\mathbf{b}' = \mathbf{t}' \times \mathbf{n} + \mathbf{t} \times \mathbf{n}' = k\mathbf{n} \times \mathbf{n} + \mathbf{t} \times \mathbf{n}' = \mathbf{t} \times \mathbf{n}'$$

Hence $\mathbf{b}'$ is also orthogonal to $\mathbf{t}$.

It follows that there exists a scalar (called the torsion of the curve at $\mathbf{r}(s)$) such that

$$\mathbf{b}'(s) = -\tau(s)\mathbf{n}(s) \tag{135}$$

The frame $\{\mathbf{t}, \mathbf{n}, \mathbf{b}\}$ is an orthonormal frame, called the Frenet frame [33,34,35]. It is one of many frames which are adapted to the space curve.

We also have $\mathbf{n} = \mathbf{b} \times \mathbf{t}$. Differentiating this and using the results above, we have:

$$\mathbf{n}'(s) = \mathbf{b}' \times \mathbf{t} + \mathbf{b} \times \mathbf{t}' = -\tau \mathbf{n} \times \mathbf{t} + k\mathbf{b} \times \mathbf{n} = \tau \mathbf{b} - k\mathbf{t}$$

We have now put together the equations known as the Frenet formulas

$$\mathbf{t}' = k\mathbf{n}$$

$$\mathbf{n}' = -k\mathbf{t} + \tau \mathbf{b} \tag{136}$$

$$\mathbf{b}' = -\tau \mathbf{n}$$

Or in matrix from

$$\begin{pmatrix} \mathbf{t}' \\ \mathbf{n}' \\ \mathbf{b}' \end{pmatrix} = \begin{pmatrix} 0 & k & 0 \\ -k & 0 & \tau \\ 0 & -\tau & 0 \end{pmatrix} \begin{pmatrix} \mathbf{t} \\ \mathbf{n} \\ \mathbf{b} \end{pmatrix} \tag{137}$$

Notice then, that for the Frenet frame we have the Darboux vector given by

$$\mathbf{\Omega}_F = \tau \mathbf{t} + k\mathbf{b} \tag{138}$$

It is very typical to treat moving frames using the Frenet frame, but we note that it is undefined when the curve has vanishing curvature ($|\mathbf{t}'| = 0$).

As the Frenet frame may be completely different along sections of the curve that do not have vanishing curvature it is not possible to uniquely define a frame that varies continuously along the curve, being equal to the Frenet frame where it is defined.

6.2.3 Parallel Vector Fields

Given an arc length parameterised space curve $\mathbf{r} = \mathbf{r}(s)$, we define a vector field $\mathbf{u}(s)$ to be normal to the curve, if it is everywhere perpendicular to the curve's tangent vector $\mathbf{t}(s)$, that is $\mathbf{u}(s) \cdot \mathbf{t}(s) = 0$. We further define a vector field to be parallel to the curve if its derivative is tangential along the curve (the vector only varies in the tangential direction), that is $\mathbf{u}'(s) = \alpha(s)\mathbf{t}(s)$ for some function $\alpha(s)$

For such a curve and vector field we have the following properties [36]:

1. $\mathbf{u}(s)$ has constant length.

2. An initial vector $\mathbf{u}_0$ normal to the curve at a point $\mathbf{r}(s_0)$ generates a unique, parallel vector field $\mathbf{u}(s)$ along the curve, such that $\mathbf{u}(s_0) = \mathbf{u}_0$.

The vector field $\mathbf{u}(s)$ generated by $\mathbf{u}_0$ is called the parallel transport of $\mathbf{u}_0$ along $\mathbf{r}(s)$

3. If initial vectors $\mathbf{u}_0$ and $\mathbf{v}_0$ normal to the curve at a point $\mathbf{r}(s_0)$ generate parallel fields $\mathbf{u}(s)$ and $\mathbf{v}(s)$ respectively, the angle between $\mathbf{u}(s)$ and $\mathbf{u}(s)$ is constant along the curve. That is $\mathbf{u}(s) \cdot \mathbf{v}(s) = \mathbf{u}_0 \cdot \mathbf{v}_0$.

6.2.4 The Bishop Frame

We now introduce an alternative approach to defining a moving frame that is well-defined even when the curve has vanishing curvature. The frame is called the natural, parallel transport or Bishop frame [37].

This frame relies on the observation that while the tangent vector $\mathbf{t}$ for a given curve is unique, we may choose any arbitrary basis $\{\mathbf{u}, \mathbf{v}\}$ for the remainder of the orthonormal frame so long as these vectors remain in the normal plane, perpendicular to $\mathbf{t}$.

The Bishop frame is constructed using property three above. That is, given two orthonormal vectors laying in the normal plane to the curve at some point, we can parallel transport these two vectors along the curve, which together with the tangent vector, will form an orthonormal frame at each point along the curve.

Specifically, for an arclength parameterised curve, take the unique, normal tangent vector $\mathbf{t}(s)$ along curve, together with two normal vectors $\mathbf{u}(0)$ and $\mathbf{v}(0)$ such that $\{\mathbf{t}(0), \mathbf{u}(0), \mathbf{v}(0)\}$ forms an orthonormal frame. We define the Bishop frame to be $\{\mathbf{t}, \mathbf{u}, \mathbf{v}\}$, where $\mathbf{u}$ and $\mathbf{v}$ are the parallel transport of $\mathbf{u}(0)$ and $\mathbf{v}(0)$ along the curve.

We can parallel transport the vector $\mathbf{u}(0)$ along the curve by integrating the equation $\mathbf{u}' = \mathbf{\Omega}_B \times \mathbf{u}$ with the initial condition $\mathbf{u}(0) = \mathbf{u}_0$. Where $\mathbf{\Omega}_B$ is the Darboux vector for the Bishop frame.

Now, as $\mathbf{u}$ and $\mathbf{v}$ are parallel normal vector fields, we know that their derivatives are tangential along the curve. That is, $\mathbf{u}' \cdot \mathbf{v} = -\mathbf{v}' \cdot \mathbf{u} = 0$. This is equivalent to $\Omega_1 = 0$.

We therefore have $\mathbf{\Omega}_B = \Omega_2 \mathbf{u} + \Omega_3 \mathbf{v}$ and the alternative frame equations

$$\begin{pmatrix} \mathbf{t}' \\ \mathbf{u}' \\ \mathbf{v}' \end{pmatrix} = \begin{pmatrix} 0 & \Omega_3 & -\Omega_2 \\ -\Omega_3 & 0 & 0 \\ \Omega_2 & 0 & 0 \end{pmatrix} \begin{pmatrix} \mathbf{t} \\ \mathbf{u} \\ \mathbf{v} \end{pmatrix} \tag{139}$$

6.2.5 The Relationship Between the Frenet and Bishop Frames

As the orthonormal pairs $\{\mathbf{n}, \mathbf{b}\}$ and $\{\mathbf{u}, \mathbf{v}\}$ both lie in the normal plane to the tangent vector $\mathbf{t}$, we can relate the vectors by a rotation about an angle θ in this plane.

$$\mathbf{u} = \cos\theta\mathbf{n} + \sin\theta\mathbf{b} \tag{140}$$

$$\mathbf{v} = -\sin\theta\mathbf{n} + \cos\theta\mathbf{b} \tag{141}$$

Differentiating with respect to s and using the Frenet equations gives:

$$\mathbf{u}' = -\theta'\sin\theta\mathbf{n} + \cos\theta\mathbf{n}' + \theta'\cos\theta\mathbf{b} + \sin\theta\mathbf{b}'$$

$$= -\theta'\sin\theta\mathbf{n} + \cos\theta(-k\mathbf{t} + \tau\mathbf{b}) + \theta'\cos\theta\mathbf{b} + \sin\theta(-\tau\mathbf{n})$$

$$= (-k\cos\theta)\mathbf{t} + (-\theta'\sin\theta - \tau\sin\theta)\mathbf{n} + (-\tau\cos\theta + \theta'\cos\theta)\mathbf{b}$$

$$= -\Omega_3\mathbf{t}$$

$$\mathbf{v}' = -\theta'\cos\theta\mathbf{n} - sin\theta\mathbf{n}' - \theta' sin\theta\mathbf{b} + cos\theta\mathbf{b}'$$

$$= -\theta'\cos\theta\mathbf{n} - \sin\theta(-k\mathbf{t} + \tau\mathbf{b}) - \theta'\sin\theta\mathbf{b} + \cos\theta(-\tau\mathbf{n})$$

$$= (k\sin\theta)\mathbf{t} + (-\theta'\cos\theta - \tau\cos\theta)\mathbf{n} + (-\tau\sin\theta + \theta'\sin\theta)\mathbf{b}$$

$$= \Omega_2\mathbf{t}$$

Comparing terms we find that

$$\Omega_2 = k\sin\theta \tag{142}$$

$$\Omega_3 = k\cos\theta \tag{143}$$

$$\tau = -\theta' \tag{144}$$

Which we use to write

$$k = \sqrt{\Omega_2^2 + \Omega_3^2} \tag{145}$$

Noting also that $\tan\theta = \dfrac{\Omega_2}{\Omega_3}$ we can deduce that

$$\tau = \frac{\Omega_2'\Omega_3 - \Omega_3'\Omega_2}{\Omega_2^2 + \Omega_3^2} \tag{146}$$

Finally we notice that as $\mathbf{\Omega}_B$ has no tangential component ($\mathbf{\Omega}_B \cdot \mathbf{t} = 0$), we can write

$$k\mathbf{b} = \mathbf{t} \times k\mathbf{n} = \mathbf{t} \times \mathbf{t}' = \mathbf{t} \times (\mathbf{\Omega}_B \times \mathbf{t}) = (\mathbf{t} \cdot \mathbf{t})\,\mathbf{\Omega}_B - (\mathbf{t} \cdot \mathbf{\Omega}_B)\,\mathbf{t} = \mathbf{\Omega}_B$$

Therefore we have the important relationship

$$\mathbf{\Omega}_B = k\mathbf{b} \tag{147}$$

We see that parallel transporting a vector $\mathbf{x}$ along the curve infinitesimally corresponds to a rotation about the binormal.

7 Continuous Elastic Rod Theory

7.1 Introduction

We now wish to develop a theory that allows us to model the behaviour of a slender elastic body in three dimensions. As well as considering the extra spatial dimension, we wish to allow the body to bend, extend, twist and shear. Bending and stretching were considered in the two dimensional case of deforming elastic curves but we have yet to consider twist and shear as it is not applicable for planar curves.

So far we have modelled the bodies as one dimensional curves deforming in two dimensions. A first attempt to move the model into three dimensions may be to simply allow the one dimensional curves to deform in three dimensions. Consider then, a cylinder of elastic material lying along the x axis, $[0, L]$ subject to a twist on one end, relative to the other. If we were to model this body by an elastic space curve, this case would be indistinguishable from the case of an untwisted rod in the same configuration.

In order to include the behaviour of twisting and shearing (even in planar motion) we need to generalise the notion of space curves to geometric rods, that is, a long and slender length of elastic material whose lateral dimensions are very small compared to its length.

There are two approaches to the mathematical theory of rods. The first treats the rod as a three dimensional elastic body and uses the methods of three dimensional elasticity theory to find the deformation configuration [38,39]. The second approach (which we will use) is one dimensional rod theory and is often referred to as the director theory of rods [41,41,42,43]. In such a model, stretching and bending is captured by deformation of a curve called the centreline, whilst twisting and shearing is captured by the rotation of a material frame associated to each point on the centreline and its deviation from the normal plane to the centreline.

In this section we look at the general theory of shearable, extensible, hyperelastic (not linearly elastic) rods via the general theory of Kirchhoff rods. The theory and analysis of such rod models is covered extensively in the continuous case, but discrete models are far less common in the literature [44,45]. The two major difficulties in developing a discrete theory are defining the material frames and defining the curvature (a problem we also faced in the case of planar discrete elastic curves).

7.2 General Elastic Rod Theory

Using the theory of space curves and curve framing introduced above, we introduce the theory of elastic rods.

A Kirchhoff rod, R, is represented by its centreline, a curve $\mathbf{r}(S) : \mathbb{R} \to \mathbb{R}^3$. Where S is a material parameter taken to be the arc length in the stress free configuration $S \in [0, L]$. With the curvature, torsion and curve frames of the centreline defined in section 6, we can now introduce further theory to allow for twisting and shearing.

Along with $\mathbf{r}(S)$ we define two orthonormal material vector fields $\mathbf{m}_1(S)$ and $\mathbf{m}_2(S)$, representing the orientation of the material cross section at S. Note that these vectors are often denoted $\mathbf{d}_1(S)$ and $\mathbf{d}_2(S)$.

The stretch is defined as

$$\alpha = \frac{ds}{dS} \tag{148}$$

where $s = s(S)$ is the arclength from 0 to S

With these vector fields defined we now assume that after deformation the position $\mathbf{p}$ of the deformed material points can be described by

$$\mathbf{p}(S, \xi^1, \xi^2) = \mathbf{r}(S) + \xi^1 \mathbf{m}_1(S) + \xi^2 \mathbf{m}_2(S) \qquad (\xi^1, \xi^2) \in \Omega \tag{149}$$

Where Ω defines the shape of the cross section of the rod.

By defining $\mathbf{m}_0(s) = \mathbf{m}_1(s) \times \mathbf{m}_2(s)$ (often denoted $\mathbf{d}_3$) we have a local orthonormal material basis $\{\mathbf{m}_0, \mathbf{m}_1, \mathbf{m}_2\}$

We are now in a position to describe the strains on the rod.

Shearing and stretching

By defining $\mathbf{v} = v_0\mathbf{m}_0 + v_1\mathbf{m}_1 + v_2\mathbf{m}_2$ the shearing and stretching on the rod is captured by

$$\frac{d\mathbf{r}}{dS} = \mathbf{v} \tag{150}$$

Where v_1 and v_2 represent transverse shearing and v_0 represents stretching or compression, $v_0 < 1$ for compression and $v_0 > 1$ for stretching

Bending and twisting

We also know there exists a Darboux vector, $\mathbf{u} = u_0\mathbf{m}_0 + u_1\mathbf{m}_1 + u_2\mathbf{m}_2$, such that

$$\frac{d\mathbf{m}_i}{dS} = \mathbf{u} \times \mathbf{m}_i \tag{151}$$

Where u_1 and u_2 represent bending and u_0 represents twisting (rotation of the basis) around the $\mathbf{m}_0$ vector.

7.2.1 Inextensible, Unshearable Rods

By taking $v_1 = v_2 = 0$, $v_0 = 1$, that is, $\mathbf{v} = \mathbf{m}_0$, we define the special case of an inextensible, unshearable rod. Limiting the deformations such that the rods can not stretch or shear does limit our model but should provide an acceptable approximation to read world problems.

We have that

$$\frac{d\mathbf{r}}{dS} = \frac{d\mathbf{r}}{ds} \cdot \frac{ds}{dS} = \alpha \mathbf{t}(s) = \mathbf{m}_0$$

Thus there is no stretch, $\alpha = 1$ or equivalently $s = S$. This shows us that the material parameter can be regarded as the arc length of both the deformed and undeformed centreline both of which we take to have length L.

We now have the orthonormal material frame $\{\mathbf{t}, \mathbf{m}_1, \mathbf{m}_2\}$, so that $\mathbf{m}_1$ and $\mathbf{m}_2$ lie in the normal plane to the axis and deformations are restricted so that cross-sections remain orthogonal to the centre line.

The configuration of the rod is now described by an adapted framed curve $R = \{\mathbf{r}; \mathbf{t}, \mathbf{m}_1, \mathbf{m}_2\}$, where $\mathbf{r}(s)$ is the centreline of the rod and $\{\mathbf{t}, \mathbf{m}_1, \mathbf{m}_2\}$ forms an adapted orthonormal material frame along $\mathbf{r}$.

The evolution of the material frame is described the Darboux vector, which we now write as $\mathbf{u} = m\mathbf{t} + \omega_1 \mathbf{m}_1 + \omega_2 \mathbf{m}_2$. Thus we have

$$\mathbf{t}' = \omega_2 \mathbf{m}_1 - \omega_1 \mathbf{m}_2$$
$$\mathbf{m}_1' = -\omega_2 \mathbf{t} + m\mathbf{m}_2$$
$$\mathbf{m}_2' = \omega_1 \mathbf{t} - m\mathbf{m}_1$$

And

$$m = \mathbf{m}_1' \cdot \mathbf{m}_2 = -\mathbf{m}_2' \cdot \mathbf{m}_1$$
$$\omega_1 = -\mathbf{t}' \cdot \mathbf{m}_2 = \mathbf{m}_2' \cdot \mathbf{t}$$
$$\omega_2 = \mathbf{t}' \cdot \mathbf{m}_1 = -\mathbf{m}_1' \cdot \mathbf{t}$$

7.3 The Relationship Between the Material Frame and the Centreline Frames

The material frame $\{\mathbf{t}, \mathbf{m}_1, \mathbf{m}_2\}$ is, in general, different to the Frenet or Bishop frames $\{\mathbf{t}, \mathbf{n}, \mathbf{b}\}$ or $\{\mathbf{t}, \mathbf{u}, \mathbf{v}\}$. As the material frame is adapted to the curve in the same way as both the Frenet and Bishop frames, we know that $\mathbf{m}_1$ and $\mathbf{m}_2$ must lie in the normal plane to the tangent vector and can be related to the normal components of the other frames $\{\mathbf{n}, \mathbf{b}\}$ or $\{\mathbf{u}, \mathbf{v}\}$, via a rotation in this plane. In a similar fashion to the way we related the Bishop frame to the Frenet frame, we now relate the material frame to both of these frames.

7.3.1 Frenet Frame and Material Frame

Denoting the rotation angle by ϕ we write

$$\mathbf{m}_1 = \cos\phi\mathbf{n} + \sin\phi\mathbf{b} \tag{152}$$

$$\mathbf{m}_2 = -\sin\phi\mathbf{n} + \cos\phi\mathbf{b} \tag{153}$$

Differentiating with respect to s and using the Frenet equations gives

$$\mathbf{m}_1' = -\phi'\sin\phi\mathbf{n} + \cos\phi\mathbf{n}' + \phi'\cos\phi\mathbf{b} + \sin\phi\mathbf{b}'$$

$$= -\phi'\sin\phi\mathbf{n} + \cos\phi(-k\mathbf{t} + \tau\mathbf{b}) + \phi'\cos\phi\mathbf{b} + \sin\phi(-\tau\mathbf{n})$$

$$= (-k\cos\phi)\mathbf{t} + (-\phi'\sin\phi - \tau\sin\phi)\mathbf{n} + (\tau\cos\phi + \phi'\cos\phi)\mathbf{b}$$

$$= -\omega_2\mathbf{t} + m\mathbf{m}_2$$

$$= -\omega_2\mathbf{t} + (-m\sin\phi)\mathbf{n} + (m\cos\phi)\mathbf{b}$$

$$\mathbf{m}_2' = -\phi' \cos\phi \mathbf{n} - \sin\phi \mathbf{n}' - \phi' \sin\phi \mathbf{b} + \cos\phi \mathbf{b}'$$

$$= -\phi' \cos\phi \mathbf{n} - \sin\phi(-k\mathbf{t} + \tau\mathbf{b}) - \phi' \sin\phi \mathbf{b} + \cos\phi(-\tau\mathbf{n})$$

$$= (k\sin\phi)\mathbf{t} + (-\phi'\cos\phi - \tau\cos\phi)\mathbf{n} + (-\tau\sin\phi - \phi'\sin\phi)\mathbf{b}$$

$$= \omega_1 \mathbf{t} - m\mathbf{m}_1$$

$$= \omega_1 \mathbf{t} + (-m\cos\phi)\mathbf{n} + (-m\sin\phi)\mathbf{b}$$

Comparing terms we see that

$$\omega_1 = k\sin\phi \tag{154}$$

$$\omega_2 = k\cos\phi \tag{155}$$

$$m = \tau + \phi' \tag{156}$$

Inverting these equations in a similar way to before yields

$$k^2 = \omega_1^2 + \omega_2^2 \tag{157}$$

And noting that $\tan\phi = \dfrac{\omega_1}{\omega_2}$ we deduce that

$$\tau = m + \frac{\omega_2'\omega_1 - \omega_1'\omega_2}{\omega_1^2 + \omega_2^2} \tag{158}$$

Notice that the terms τ, ϕ' and m play related but distinctive roles. The torsion τ is a property of the centreline alone. ϕ' is the excess twist, and a property of the rod alone, representing the rotation of the material axes relative to the Frenet axes. An untwisted rod is characterised by $\phi' = 0$ and is such that the angle between the material axes and the Frenet axes remains constant. m is a property of both the centreline and the rod, measuring the total rotation of the material basis around the centreline as the curve is traversed.

7.3.2 Bishop Frame and Material Frame

Denoting the rotation angle by ψ we write

$$\mathbf{m}_1 = \cos\psi\mathbf{u} + \sin\psi\mathbf{v} \tag{159}$$

$$\mathbf{m}_2 = -\sin\psi\mathbf{u} + \cos\psi\mathbf{v} \tag{160}$$

Differentiating with respect to s and using the Frenet equations gives

$$\mathbf{m}_1' = -\psi'\sin\phi\mathbf{u} + \cos\psi\mathbf{u}' + \psi'\cos\psi\mathbf{v} + \sin\psi\mathbf{v}'$$

$$= -\psi'\sin\psi\mathbf{u} + \cos\psi(-\Omega_3\mathbf{t}) + \psi'\cos\psi\mathbf{v} + \sin\psi(\Omega_2\mathbf{t})$$

$$= (-\Omega_3\cos\psi + \Omega_2\sin\psi)\mathbf{t} + (-\psi'\sin\psi)\mathbf{u} + (\psi'\cos\psi)\mathbf{v}$$

$$= -\omega_2\mathbf{t} + m\mathbf{m}_2$$

$$= -\omega_2\mathbf{t} + (-m\sin\psi)\mathbf{u} + (m\cos\psi)\mathbf{v}$$

$$\mathbf{m}_2' = -\psi'\cos\psi\mathbf{u} - \sin\psi\mathbf{u}' - \psi'\sin\psi\mathbf{v} + \cos\psi\mathbf{v}'$$

$$= -\psi'\cos\psi\mathbf{u} - \sin\psi(-\Omega_3\mathbf{t}) - \psi'\sin\psi\mathbf{v} + \cos\psi(\Omega_2\mathbf{t})$$

$$= (\Omega_3\sin\psi + \Omega_2\cos\psi)\mathbf{t} + (-\psi'\cos\psi)\mathbf{u} + (-\psi'\sin\psi)\mathbf{v}$$

$$= \omega_1\mathbf{t} - m\mathbf{m}_1$$

$$= \omega_1\mathbf{t} + (-m\cos\psi)\mathbf{u} + (-m\sin\psi)\mathbf{v}$$

Comparing terms we see that

$$\omega_1 = \Omega_3 \sin\psi + \Omega_2 \cos\psi \tag{161}$$

$$\omega_2 = \Omega_3 \cos\psi - \Omega_2 \sin\psi \tag{162}$$

$$m = \psi' \tag{163}$$

Inverting, yields

$$\Omega_2^2 + \Omega_3^2 = \omega_1^2 + \omega_2^2 \tag{164}$$

This formulation yields a very convenient expression for the twist.

7.4 The Elastic Energy

The total elastic energy of the rod is given as a sum of the bending energy and twisting energy.

$$E = E_{bend} + E_{twist} \tag{165}$$

Assuming the rod is linearly elastic and the undeformed configuration is straight, the bending energy takes the form

$$E_{bend} = \frac{1}{2} \int_R \left(B_1 \omega_1^2 + B_2 \omega_2^2 \right) ds \tag{166}$$

and the twisting energy takes the form

$$E_{bend} = \frac{1}{2} \int_R C m^2 ds \tag{167}$$

Where B_1, B_2, C are the bending and twisting stiffnesses, respectively.

With this elastic energy and the various relationships above, we are now in a position to construct a discrete model of elastic rods in a similar way to section 4.

8 Discrete Space Curves

8.1 Space Curves

Much like the planar case, a discrete space curve is a map $\mathbf{x} : I \to \mathbb{R}^3$, where $I = \{0, ..., n+1\}$. This map defines vertices $\{\mathbf{x}(0), ..., \mathbf{x}(n+1)\}$ in $\mathbb{R}^3$. The vertices are joined together by edges $\{\mathbf{e}(0), ..., \mathbf{e}(n)\}$, which in turn form the curve.

As before we denote $\mathbf{x}(j) = \mathbf{x}_j$ and $\mathbf{e}(j) = \mathbf{e}^j$, associating subscripts with the vertices and superscripts with the edges.

We also have by construction $\mathbf{e}^j = \mathbf{x}_{j+1} - \mathbf{x}_j$, and equations (39) and (40) also hold here.

We denote the spherical polar angles of edge $\mathbf{e}^j$ relative to the fixed frame $\{\mathbf{i}, \mathbf{j}, \mathbf{k}\}$ by ψ_j and θ_j, so that

$$\mathbf{e}^j = |\mathbf{e}^j| \cos\psi_j \sin\theta_j \mathbf{i} + |\mathbf{e}^j| \sin\psi_j \sin\theta_j \mathbf{j} + |\mathbf{e}^j| \cos\theta_j \mathbf{k} \tag{168}$$

The turning angle at vertex $\mathbf{x}_j$ is defined exactly as before but now we denote this angle by ξ_j and can write

$$\mathbf{e}^{j-1} \times \mathbf{e}^j = |\mathbf{e}^{j-1}||\mathbf{e}^j| \sin\xi_j \boldsymbol{\beta}_j$$

Where $\boldsymbol{\beta}_j$ is a unit vector perpendicular to the plane containing $\mathbf{e}^{j-1}$ and $\mathbf{e}^j$ in the direction given by the right hand rule. That is

$$\boldsymbol{\beta}_j = \frac{\mathbf{e}^{j-1} \times \mathbf{e}^j}{|\mathbf{e}^{j-1} \times \mathbf{e}^j|} \tag{169}$$

Curvature is then defined in exactly the same way as for the two dimensional case. That is, by denoting the curvature over the domain Δ_j to be

$$k_j = \frac{2}{D_j} \tan\left(\frac{\xi_j}{2}\right) \tag{170}$$

And zero otherwise.

8.2 Discrete Parallel Transport and Bishop Frame

Firstly, the discrete unit tangent vector is defined along edge $\mathbf{e}^j$ in the obvious way

$$\mathbf{t}^j = \frac{\mathbf{e}^j}{|\mathbf{e}^j|} \tag{171}$$

We now define the unit binormal at vertex $\mathbf{x}_j$ to be $\boldsymbol{\beta}_j$ and by further defining

$$\mathbf{b}_j = \mathbf{t}^{j-1} \times \mathbf{t}^j \tag{172}$$

We can write $\boldsymbol{\beta}_j$ as

$$\boldsymbol{\beta}_j = \frac{\mathbf{b}_j}{|\mathbf{b}_j|} \tag{173}$$

We now define discrete parallel transport in analogy to the smooth case, that is, we parallel transport a vector from the edge $\mathbf{e}^{j-1}$ to the edge $\mathbf{e}^j$ by a rotation R_j about the binormal at the vertex $\mathbf{x}_j$. With that in mind, we define the rotation matrices by

$$\begin{aligned} R_j\left(\mathbf{t}^{j-1}\right) &= \mathbf{t}^j \\ R_j\left(\mathbf{t}^{j-1} \times \mathbf{t}^j\right) &= \mathbf{t}^{j-1} \times \mathbf{t}^j \end{aligned} \tag{174}$$

Also imposing that, R_j is the identity if $\mathbf{t}^{j-1} = \mathbf{t}^j$, and is not defined if $\mathbf{t}^{j-1} = -\mathbf{t}^j$.

In order to define a discrete Bishop frame along the curve we take an initial set of orthonormal unit vectors $\mathbf{u}^0$ and $\mathbf{v}^0$ which lie in the normal plane to $\mathbf{t}^0$. We then parallel transport these vectors along the curve by rotating the frame at each vertex using our rotation operators R_j. In doing this we iteratively define for $j = 1, ..., n$

$$\begin{aligned} \mathbf{u}^j &= R_j\left(\mathbf{u}^{j-1}\right) \\ \mathbf{v}^j &= R_j\left(\mathbf{v}^{j-1}\right) \end{aligned} \tag{175}$$

Now we have

$$\mathbf{t}^0 = \cos\psi_0 \sin\theta_0 \mathbf{i} + \sin\psi_0 \sin\theta_0 \mathbf{j} + \cos\theta_0 \mathbf{k} \tag{176}$$

So we can choose the following unit vectors normal to the curve along edge $\mathbf{e}^0$

$$\begin{aligned} \mathbf{u}^0 &= \cos\psi_0 \cos\theta_0 \mathbf{i} + \sin\psi_0 \cos\theta_0 \mathbf{j} - \sin\theta_0 \mathbf{k} \\ \mathbf{v}^0 &= -\sin\psi_0 \mathbf{i} + \cos\psi_0 \mathbf{j} \end{aligned} \tag{177}$$

We then have three vectors which form an initial orthonormal frame $B^0 = \{\mathbf{t}^0, \mathbf{u}^0, \mathbf{v}^0\}$ along $\mathbf{e}^0$.

By discrete parallel transporting this frame along the curve via a series of roations we can define a discrete Bishop frame $B^j = \{\mathbf{t}^j, \mathbf{u}^j, \mathbf{v}^j\}$, where

$$\mathbf{t}^j = \cos\psi_j \sin\theta_j \mathbf{i} + \sin\psi_j \sin\theta_j \mathbf{j} + \cos\theta_j \mathbf{k}$$

$$\begin{aligned} \mathbf{u}^j &= R_j \mathbf{u}^{j-1} = P_j \mathbf{u}^0 \\ \mathbf{v}^j &= R_j \mathbf{v}^{j-1} = P_j \mathbf{v}^0 \end{aligned} \tag{178}$$

Where the rotation matrix P_j is the product of frame rotations up to the frame B^{j-1}. That is

$$P_j = \prod_{k=0}^{j-1} R_{j-k} = R_j R_{j-1} ... R_1, \qquad P_0 = I \tag{179}$$

8.3 The Rotation Matrices R_j

Using the result from [47] our rotation matrices R_j, which rotate the vector $\mathbf{t}^{j-1}$ into $\mathbf{t}^j$ is given by

$$R_j = \begin{pmatrix} c_j + h_j b_{j,1}^2 & h_j b_{j,1} b_{j,2} - b_{j,3} & h_j b_{j,1} b_{j,3} + b_{j,2} \\ h_j b_{j,1} b_{j,2} + b_{j,3} & c_j + h_j b_{j,2}^2 & h_j b_{j,2} b_{j,3} - b_{j,1} \\ h_j b_{j,1} b_{j,3} - b_{j,2} & h_j b_{j,2} b_{j,3} + b_{j,1} & c_j + h_j b_{j,3}^2 \end{pmatrix} \tag{180}$$

where

$$\begin{aligned} \mathbf{b}_j &= (b_{j1}, b_{j2}, b_{j3})^T = \mathbf{t}^{j-1} \times \mathbf{t}^j \\ c_j &= \mathbf{t}^{j-1} \cdot \mathbf{t}^j \\ h_j &= \frac{1}{1 + c_j} \end{aligned} \tag{181}$$

That is, in terms of the angles,

$$\begin{aligned} b_{j,1} &= \sin\psi_{j-1} \sin\theta_{j-1} \cos\theta_j - \cos\theta_{j-1} \sin\psi_j \sin\theta_j \\ b_{j,2} &= -\cos\psi_{j-1} \sin\theta_{j-1} \cos\theta_j + \cos\theta_{j-1} \cos\psi_j \sin\theta_j \\ b_{j,3} &= \cos\psi_{j-1} \sin\theta_{j-1} \sin\psi_j \sin\theta_j - \sin\psi_{j-1} \sin\theta_{j-1} \cos\psi_j \sin\theta_j \\ c_j &= \cos\psi_{j-1} \sin\theta_{j-1} \cos\psi_j \sin\theta_j + \sin\psi_{j-1} \sin\theta_{j-1} \sin\psi_j \sin\theta_j + \cos\theta_{j-1} \cos\theta_j \end{aligned} \tag{182}$$

8.4 The Discrete Bishop Frame Darboux Vector

For a continuous Bishop frame we noted the important result, $\mathbf{\Omega}_B = k\mathbf{b}$, which we now deploy in a discrete setting by defining the discrete Bishop Darboux vector at vertex $\mathbf{x}_j$ by

$$\mathbf{\Omega}_j = k_j \boldsymbol{\beta}_j \tag{183}$$

This can be rewritten as

$$\frac{2}{D_j}\frac{\sin\xi_j}{1+\cos\xi_j}\boldsymbol{\beta}_j = \frac{2}{D_j}\frac{|\mathbf{t}^{j-1}||\mathbf{t}^j|\sin\xi_j\boldsymbol{\beta}_j}{|\mathbf{t}^{j-1}||\mathbf{t}^j| + |\mathbf{t}^{j-1}||\mathbf{t}^j|\cos\xi_j} = \frac{2}{D_j}\frac{\mathbf{t}^{j-1}\times\mathbf{t}^j}{1+\mathbf{t}^{j-1}\cdot\mathbf{t}^j} = \frac{2}{D_j}\frac{\mathbf{b}_j}{1+c_j}$$

Hence we have

$$\mathbf{\Omega}_j = \frac{2h_j}{D_j}\mathbf{b}_j \tag{184}$$

Notice that $|\mathbf{\Omega}_j| = |k_j|$, and by multiplying the top and bottom by $|\mathbf{e}^{j-1}||\mathbf{e}^j|$ we can write $\mathbf{\Omega}_j$ in terms of just the vectors $\mathbf{e}^{j-1}$ and $\mathbf{e}^j$

$$\mathbf{\Omega}_j = \frac{4}{|\mathbf{e}^{j-1}| + |\mathbf{e}^j|}\frac{\mathbf{e}^{j-1}\times\mathbf{e}^j}{|\mathbf{e}^{j-1}||\mathbf{e}^j| + \mathbf{e}^{j-1}\cdot\mathbf{e}^j} \tag{185}$$

9 Discrete Elastic Rods

Using the theory of discrete space curves and curve framing outlined above, we introduce the theory of discrete elastic rods. As we did in the continuous case, we focus on the case of inextensible, unshearable rods.

9.1 Inextensible, Unshearable, Discrete Elastic Rods

A discrete Kirchhoff rod is represented by its centerline, a discrete space curve $\mathbf{x} : I \to \mathbb{R}^3$ with the curvature and frames defined in section 8, together with two material vectors along edge $\mathbf{e}^j$, $\mathbf{m}_1^j$ and $\mathbf{m}_2^j$, representing the orientation of the material cross section along edge $\mathbf{e}^j$. For the inextensible, unshearable case, the final axis of the material frame is given by the tangent to the centerline and thus along edge $\mathbf{e}^j$, we have the material frame $M^j = \left\{\mathbf{t}^j, \mathbf{m}_1^j, \mathbf{m}_2^j\right\}$.

Looking back at the continuous case, we had the bending strains

$$\omega_1 = -\mathbf{t}' \cdot \mathbf{m}_2 = -\boldsymbol{\Omega} \times \mathbf{t} \cdot \mathbf{m}_2 = -\boldsymbol{\Omega} \cdot \mathbf{t} \times \mathbf{m}_2 = \boldsymbol{\Omega} \cdot \mathbf{m}_1$$

$$\omega_2 = \mathbf{t}' \cdot \mathbf{m}_1 = \boldsymbol{\Omega} \times \mathbf{t} \cdot \mathbf{m}_1 = \boldsymbol{\Omega} \cdot \mathbf{t} \times \mathbf{m}_1 = \boldsymbol{\Omega} \cdot \mathbf{m}_2$$

Where $\boldsymbol{\Omega}$ is the Darboux vector associated with either the Frenet or Bishop frame.

Inspired by this, we define equivalent discrete forms of the bending strains over the domain Δ_j for $j = 1, ..., n$ by

$$\begin{aligned} \omega_{1j} &= \frac{1}{2}\boldsymbol{\Omega}_j \cdot (\mathbf{m}_1^{j-1} + \mathbf{m}_1^j) \\ \omega_{2j} &= \frac{1}{2}\boldsymbol{\Omega}_j \cdot (\mathbf{m}_2^{j-1} + \mathbf{m}_2^j) \end{aligned} \tag{186}$$

As before, we can relate the material frame and Bishop frame along edge $\mathbf{e}^j$ via a rotation about an angle ϕ_j

$$\begin{aligned} \mathbf{m}_1^j &= \cos\phi_j \mathbf{u}^j + \sin\phi_j \mathbf{v}^j \\ & \qquad\qquad j = 0, ..., n \\ \mathbf{m}_2^j &= -\sin\phi_j \mathbf{u}^j + \cos\phi_j \mathbf{v}^j \end{aligned} \tag{187}$$

We now define

$$\begin{aligned} \mathbf{w}_{1,j} &= \cos\phi_j \mathbf{u}^0 + \sin\phi_j \mathbf{v}^0 \\ & \qquad\qquad j = 0, ..., n \\ \mathbf{w}_{2,j} &= -\sin\phi_j \mathbf{u}^0 + \cos\phi_j \mathbf{v}^0 \end{aligned} \tag{188}$$

So that

$$\begin{aligned} \mathbf{m}_1^j &= P_j \mathbf{w}_{1,j} \\ & \qquad\qquad j = 0, ..., n \\ \mathbf{m}_2^j &= P_j \mathbf{w}_{2,j} \end{aligned} \tag{189}$$

Now for constant edge length $|D_j| = l$, so we have

$$\mathbf{\Omega}_j = \frac{2}{l} h_j \mathbf{b}_j \qquad\qquad j = 1, ..., n \tag{190}$$

This gives the bending strains over the domain Δ_j

$$\begin{aligned} \omega_{1,j} &= \frac{h_j \mathbf{b}_j}{l} \cdot [P_{j-1}\mathbf{w}_{1,j-1} + P_j \mathbf{w}_{1,j}] \\ & \qquad\qquad j = 1, ..., n \\ \omega_{2,j} &= \frac{h_j \mathbf{b}_j}{l} \cdot [P_{j-1}\mathbf{w}_{2,j-1} + P_j \mathbf{w}_{2,j}] \end{aligned} \tag{191}$$

The twist strain is far more simple and is defined in analogy to the continuous case ($m = \psi'$) by backward divided difference.

We therefore define over the domain Δ_j

$$m_j = \frac{\phi_j - \phi_{j-1}}{l} \qquad j = 1, ..., n \tag{192}$$

9.2 Boundary Conditions

As with the two dimensional case, we have imposed pinned boundary conditions at the ends and we will take these boundary conditions in the models which follow.

We must also include conditions on the twist, which we do by fixing the total rotation of the material axes relative to the Bishop axes via the constraint

$\phi_n - \phi_0 = \text{constant}$

So if, for example, we wanted to twist the end of the rod by one full turn relative to the start, we would have the condition:

$\phi_n - \phi_0 = 2\pi$

9.3 The Discrete Elastic Energy

With the definitions above we can now write the bending energy as

$$E_{bend}(R) = \sum_{j=1}^{n} \left(\frac{1}{2} B_1 (\omega_{1j})^2 + \frac{1}{2} B_2 (\omega_{2j})^2 \right) l \tag{193}$$

And the twisting energy as

$$E_{twist}(R) = \sum_{j=1}^{n} \left(\frac{1}{2} C (m_j)^2 \right) l \tag{194}$$

And so the total elastic energy is

$$E(R) = \sum_{j=1}^{n} \left(\frac{1}{2} B_1 (\omega_{1j})^2 + \frac{1}{2} B_2 (\omega_{2j})^2 + \frac{1}{2} C (m_j)^2 \right) l \tag{195}$$

Thus, despite the complicated form of the functions ω_{1j} and ω_{2j}, we are now in a position to write the total energy as a function of $\psi_0, ..., \psi_n, \theta_0, ..., \theta_n, \phi_0, ..., \phi_n$ and are faced with the daunting task of finding stationary solutions by solving the equations

$$\frac{\partial E}{\partial \psi_j} = \frac{\partial E}{\partial \theta_j} = \frac{\partial E}{\partial \phi_j} = 0 \qquad j = 0, ..., n$$

Along with constraints depending on the problem we wish to solve.

9.4 The Derivatives

For A_k denoting any of the angles ψ_k, θ_k or ϕ_k we have

$$\frac{\partial E}{\partial A_k} = \sum_{j=1}^{n} \left(B_1 \omega_{1j} \frac{\partial \omega_{1j}}{\partial A_k} + B_2 \omega_{2j} \frac{\partial \omega_{2j}}{\partial A_k} + C m_j \frac{\partial m_j}{\partial A_k} \right) l \tag{196}$$

We now separate the cases for which A_k represents ψ_k or θ_k and the case where A_k represents ϕ_k

For the most simple case where A_k denotes the angle ϕ_k, we note that neither h_j, $\mathbf{b}_j$, P_{j-1} or P_j have any dependant on ϕ_k for any k. We therefore have

$$\begin{aligned} \frac{\partial \omega_{1,j}}{\partial \phi_k} &= \frac{h_j \mathbf{b}_j}{l} \cdot \left[P_{j-1} \frac{\partial \mathbf{w}_{1,j-1}}{\partial \phi_k} + P_j \frac{\partial \mathbf{w}_{1,j}}{\partial \phi_k} \right] \\ &= \frac{h_j \mathbf{b}_j}{l} \cdot \left[P_{j-1} \mathbf{w}_{2,k} \delta_{j-1,k} + P_j \mathbf{w}_{2,k} \delta_{j,k} \right] = \frac{h_j \mathbf{b}_j}{l} \cdot P_k \mathbf{w}_{2,k} (\delta_{j-1,k} + \delta_{j,k}) \end{aligned} \tag{197}$$

$$\begin{aligned} \frac{\partial \omega_{2,j}}{\partial \phi_k} &= \frac{h_j \mathbf{b}_j}{l} \cdot \left[P_{j-1} \frac{\partial \mathbf{w}_{2,j-1}}{\partial \phi_k} + P_j \frac{\partial \mathbf{w}_{2,j}}{\partial \phi_k} \right] \\ &= \frac{h_j \mathbf{b}_j}{l} \cdot \left[P_{j-1} (-\mathbf{w}_{1,k} \delta_{j-1,k}) + P_j (-\mathbf{w}_{1,k} \delta_{j,k}) \right] = -\frac{h_j \mathbf{b}_j}{l} \cdot P_k \mathbf{w}_{1,k} (\delta_{j-1,k} + \delta_{j,k}) \end{aligned} \tag{198}$$

$$\frac{\partial m_j}{\partial \phi_k} = \frac{\delta_{j,k} - \delta_{j-1,k}}{l} \tag{199}$$

Inserting these expressions into equation (196) gives us

$$\begin{aligned}\frac{\partial E}{\partial \phi_k} &= B_1(\omega_{1,k} h_k \mathbf{b}_k + \omega_{1,k+1} h_{k+1} \mathbf{b}_{k+1}) \cdot P_k \mathbf{w}_{2,k} \\ &- B_2(\omega_{2,k} h_k \mathbf{b}_k + \omega_{2,k+1} h_{k+1} \mathbf{b}_{k+1}) \cdot P_k \mathbf{w}_{1,k} \\ &+ C(m_k - m_{k+1})\end{aligned} \tag{200}$$

Where we define for the sake of notation

$\omega_{1,0} = \omega_{1,n+1} = 0$, $\omega_{2,0} = \omega_{2,n+1} = 0$, $m_0 = m_{n+1} = 0$, $\mathbf{b}_0 = \mathbf{b}_{n+1} = \mathbf{0}$ and $h_0 = h_{n+1} = 0$.

Now for A_k denoting the angles ψ_k or θ_k we have

$$\frac{\partial \omega_{1,j}}{\partial A_k} = \frac{1}{l}\frac{\partial (h_j \mathbf{b}_j)}{\partial A_k} \cdot \left[P_{j-1}\mathbf{w}_{1,j-1} + P_j \mathbf{w}_{1,j} \right]$$
$$+ \frac{h_j \mathbf{b}_j}{l} \cdot \left[P_{j-1}\frac{\partial \mathbf{w}_{1,j-1}}{\partial A_k} + \frac{\partial P_{j-1}}{\partial A_k}\mathbf{w}_{1,j-1} + P_j \frac{\partial \mathbf{w}_{1,j}}{\partial A_k} + \frac{\partial P_j}{\partial A_k}\mathbf{w}_{1,j} \right] \tag{201}$$

$$\frac{\partial \omega_{2,j}}{\partial A_k} = \frac{1}{l}\frac{\partial (h_j \mathbf{b}_j)}{\partial A_k} \cdot \left[P_{j-1}\mathbf{w}_{2,j-1} + P_j \mathbf{w}_{2,j} \right]$$
$$+ \frac{h_j \mathbf{b}_j}{l} \cdot \left[P_{j-1}\frac{\partial \mathbf{w}_{2,j-1}}{\partial A_k} + \frac{\partial P_{j-1}}{\partial A_k}\mathbf{w}_{2,j-1} + P_j \frac{\partial \mathbf{w}_{2,j}}{\partial A_k} + \frac{\partial P_j}{\partial A_k}\mathbf{w}_{2,j} \right] \tag{202}$$

$$\frac{\partial m_j}{\partial A_k} = 0 \tag{203}$$

Note first that

$$\frac{\partial h_j}{\partial A_k} = \frac{-1}{(1+c_j)^2}\frac{\partial c_j}{\partial A_k} = -h_j^2\frac{\partial c_j}{\partial A_k} \tag{204}$$

Noting also that $h_j\mathbf{b}_j$ is dependent only on A_{j-1} and A_j we can write

$$\frac{\partial(h_j\mathbf{b}_j)}{\partial A_k} = h_j\left(\frac{\partial \mathbf{b}_j}{\partial A_k} - h_j\frac{\partial c_j}{\partial A_k}\mathbf{b}_j\right)(\delta_{j,k} + \delta_{j,k+1}) \tag{205}$$

We also note that for $k > 0$ we have

$$\frac{\partial \mathbf{u}^0}{\partial A_k} = \frac{\partial \mathbf{v}^0}{\partial A_k} = 0 \tag{206}$$

And so for $k > 0$ we have for all j

$$\frac{\partial \mathbf{w}_{1,j}}{\partial A_k} = \frac{\partial \mathbf{w}_{2,j}}{\partial A_k} = 0 \tag{207}$$

With this in mind we calculate the following derivatives

$$\frac{\partial \mathbf{u}^0}{\partial \psi_0} = \cos\theta_0\mathbf{v}^0 \tag{208}$$

$$\frac{\partial \mathbf{v}^0}{\partial \psi_0} = -\cos\psi_0\mathbf{i} - \sin\psi_0\mathbf{j} \tag{209}$$

$$\frac{\partial \mathbf{u}^0}{\partial \theta_0} = -\mathbf{t}^0 \tag{210}$$

$$\frac{\partial \mathbf{v}^0}{\partial \theta_0} = \mathbf{0} \tag{211}$$

Hence we have

$$\frac{\partial \mathbf{w}_{1,j}}{\partial \psi_0} = \cos\phi_j\cos\theta_0\mathbf{v}_0 - \sin\phi_j(\cos\psi_0\mathbf{i} + \sin\psi_0\mathbf{j}) \tag{212}$$

$$\frac{\partial \mathbf{w}_{2,j}}{\partial \psi_0} = -\sin\phi_j\cos\theta_0\mathbf{v}_0 - \cos\phi_j(\cos\psi_0\mathbf{i} + \sin\psi_0\mathbf{j}) \tag{213}$$

$$\frac{\partial \mathbf{w}_{1,j}}{\partial \theta_0} = -\cos\phi_j\mathbf{t}^0 \tag{214}$$

$$\frac{\partial \mathbf{w}_{2,j}}{\partial \theta_0} = \sin\phi_j\mathbf{t}^0 \tag{215}$$

Now, as R_j depends only on $\psi_{j-1}, \psi_j, \theta_{j-1}, \theta_j$ we have for $j < k$

$$\frac{\partial P_j}{\partial A_k} = 0 \qquad k = 0, ..., n$$

Now

$$\frac{\partial P_k}{\partial A_k} = \frac{\partial}{\partial A_k}(R_k ... R_1) = \frac{\partial R_k}{\partial A_k} P_{k-1} \qquad k = 1, ..., n$$

And

$$\frac{\partial P_0}{\partial A_0} = 0$$

So we have

$$\frac{\partial P_{k+1}}{\partial A_k} = R_{k+1} \frac{\partial P_k}{\partial A_k} + \frac{\partial R_{k+1}}{\partial A_k} P_k \qquad k = 0, ..., n-1 \tag{216}$$

And finally,

$$\frac{\partial P_{k+\zeta}}{\partial A_k} = R_{k+\zeta} \frac{\partial P_{k+\zeta-1}}{\partial A_k} \qquad \zeta = 2, ..., n \qquad k = 0, ..., n-\zeta \tag{217}$$

We now need to take the derivative of each of the entries of the matrices R_{k+1} and R_k with respect to A_k

$$\frac{\partial (R_j)_{1,1}}{\partial A_k} = \left(1 - h_j^2 b_{j,1}^2\right) \frac{\partial c_j}{\partial A_k} + 2 h_j b_{j,1} \frac{\partial b_{j,1}}{\partial A_k}$$

$$\frac{\partial (R_j)_{1,2}}{\partial A_k} = h_j b_{j,1} \frac{\partial b_{j,2}}{\partial A_k} + h_j b_{j,2} \frac{\partial b_{j,1}}{\partial A_k} - h_j^2 b_{j,1} b_{j,2} \frac{\partial c_j}{\partial A_k} - \frac{\partial b_{j,3}}{\partial A_k}$$

$$\frac{\partial (R_j)_{1,3}}{\partial A_k} = h_j b_{j,1} \frac{\partial b_{j,3}}{\partial A_k} + h_j b_{j,3} \frac{\partial b_{j,1}}{\partial A_k} - h_j^2 b_{j,1} b_{j,3} \frac{\partial c_j}{\partial A_k} + \frac{\partial b_{j,2}}{\partial A_k}$$

$$\frac{\partial (R_j)_{2,1}}{\partial A_k} = h_j b_{j,1} \frac{\partial b_{j,2}}{\partial A_k} + h_j b_{j,2} \frac{\partial b_{j,1}}{\partial A_k} - h_j^2 b_{j,1} b_{j,2} \frac{\partial c_j}{\partial A_k} + \frac{\partial b_{j,3}}{\partial A_k}$$

$$\frac{\partial (R_j)_{2,2}}{\partial A_k} = \left(1 - h_j^2 b_{j,2}^2\right) \frac{\partial c_j}{\partial A_k} + 2 h_j b_{j,2} \frac{\partial b_{j,2}}{\partial A_k} \tag{218}$$

$$\frac{\partial (R_j)_{2,3}}{\partial A_k} = h_j b_{j,2} \frac{\partial b_{j,3}}{\partial A_k} + h_j b_{j,3} \frac{\partial b_{j,2}}{\partial A_k} - h_j^2 b_{j,2} b_{j,3} \frac{\partial c_j}{\partial A_k} - \frac{\partial b_{j,1}}{\partial A_k}$$

$$\frac{\partial (R_j)_{3,1}}{\partial A_k} = h_j b_{j,1} \frac{\partial b_{j,3}}{\partial A_k} + h_j b_{j,3} \frac{\partial b_{j,1}}{\partial A_k} - h_j^2 b_{j,1} b_{j,3} \frac{\partial c_j}{\partial A_k} - \frac{\partial b_{j,2}}{\partial A_k}$$

$$\frac{\partial (R_j)_{3,2}}{\partial A_k} = h_j b_{j,2} \frac{\partial b_{j,3}}{\partial A_k} + h_j b_{j,3} \frac{\partial b_{j,2}}{\partial A_k} - h_j^2 b_{j,2} b_{j,3} \frac{\partial c_j}{\partial A_k} + \frac{\partial b_{j,1}}{\partial A_k}$$

$$\frac{\partial (R_j)_{3,3}}{\partial A_k} = \left(1 - h_j^2 b_{j,3}^2\right) \frac{\partial c_j}{\partial A_k} + 2 h_j b_{j,3} \frac{\partial b_{j,3}}{\partial A_k}$$

We now fill in the final part for all the derivatives above; the specific derivatives in the case that A_k denotes ψ_k and in the case that A_k denotes θ_k.

We have for $A_k = \psi_k$

$$\begin{aligned}
\frac{\partial b_{k,1}}{\partial \psi_k} &= -\cos\theta_{k-1}\cos\psi_k\sin\theta_k \\
\frac{\partial b_{k,2}}{\partial \psi_k} &= -\cos\theta_{k-1}\sin\psi_k\sin\theta_k \\
\frac{\partial b_{k,3}}{\partial \psi_k} &= \cos\psi_{k-1}\sin\theta_{k-1}\cos\psi_k\sin\theta_k + \sin\psi_{k-1}\sin\theta_{k-1}\sin\psi_k\sin\theta_k \\
\frac{\partial c_k}{\partial \psi_k} &= -b_{k,3} \\
\frac{\partial b_{k+1,1}}{\partial \psi_k} &= \cos\psi_k\sin\theta_k\cos\theta_{k+1} \\
\frac{\partial b_{k+1,2}}{\partial \psi_k} &= \sin\psi_k\sin\theta_k\cos\theta_{k+1} \\
\frac{\partial b_{k+1,3}}{\partial \psi_k} &= -\sin\psi_k\sin\theta_k\sin\psi_{k+1}\sin\theta_{k+1} - \cos\psi_k\sin\theta_k\cos\psi_{k+1}\sin\theta_{k+1} \\
\frac{\partial c_{k+1}}{\partial \psi_k} &= b_{k+1,3}
\end{aligned} \tag{219}$$

And similarly for $A_k = \theta_k$

$$\begin{aligned}
\frac{\partial b_{k,1}}{\partial \theta_k} &= -\sin\psi_{k-1}\sin\theta_{k-1}\sin\theta_k - \cos\theta_{k-1}\sin\psi_k\cos\theta_k \\
\frac{\partial b_{k,2}}{\partial \theta_k} &= \cos\psi_{k-1}\sin\theta_{k-1}\sin\theta_k + \cos\theta_{k-1}\cos\psi_k\cos\theta_k \\
\frac{\partial b_{k,3}}{\partial \theta_k} &= \cos\psi_{k-1}\sin\theta_{k-1}\sin\psi_k\cos\theta_k - \sin\psi_{k-1}\sin\theta_{k-1}\cos\psi_k\cos\theta_k \\
\frac{\partial c_k}{\partial \theta_k} &= \cos\psi_{k-1}\sin\theta_{k-1}\cos\psi_k\cos\theta_k + \sin\psi_{k-1}\sin\theta_{k-1}\sin\psi_k\cos\theta_k - \cos\theta_{k-1}\sin\theta_k \\
\frac{\partial b_{k+1,1}}{\partial \theta_k} &= \sin\psi_k\cos\theta_k\cos\theta_{k+1} + \sin\theta_k\sin\psi_{k+1}\sin\theta_{k+1} \\
\frac{\partial b_{k+1,2}}{\partial \theta_k} &= \cos\psi_k\cos\theta_k\cos\theta_{k+1} + \sin\theta_k\cos\psi_{k+1}\sin\theta_{k+1} \\
\frac{\partial b_{k+1,3}}{\partial \theta_k} &= \cos\psi_k\cos\theta_k\sin\psi_{k+1}\sin\theta_{k+1} - \sin\psi_k\cos\theta_k\cos\psi_{k+1}\sin\theta_{k+1} \\
\frac{\partial c_{k+1}}{\partial \theta_k} &= \cos\psi_k\cos\theta_k\cos\psi_{k+1}\sin\theta_{k+1} + \sin\psi_k\cos\theta_k\sin\psi_{k+1}\sin\theta_{k+1} - \sin\theta_k\cos\theta_{k+1}
\end{aligned} \tag{220}$$

Feeding these results back into equations (218) gives us all 9 entries of the matrices

$$\frac{\partial R_{k+1}}{\partial A_k} \text{ and } \frac{\partial R_k}{\partial A_k}$$

for A_k representing either ψ_k or θ_k.

With these in hand we can feed the expressions into equations (216) and (217) to give an expression for $\frac{\partial P_j}{\partial A_k}$ in terms of the angles for $j = 1.,,,n$ and $k = 0.,,,n$

Putting all these results together gives us an expression for $\frac{\partial E}{\partial A_k}$ in terms of the angles.

9.5 Reduction to the Two Dimensional Model

To check the theory above, we aim to reproduce the two dimensional theory of an elastic curve by setting the angles $\psi_j = \phi_j = 0$ for all j above.

Firstly we have $\mathbf{t}^j = (\sin\theta_j, 0, \cos\theta_j)$ which we can use to find:

$\mathbf{b}_j = (0, \sin(\theta_j - \theta_{j-1}), 0)^T$

$c_j = \cos(\theta_j - \theta_{j-1})$

and thus

$$R_j = \begin{pmatrix} \cos(\theta_j - \theta_{j-1}) & 0 & \sin(\theta_j - \theta_{j-1}) \\ 0 & 1 & 0 \\ -\sin(\theta_j - \theta_{j-1}) & 0 & \cos(\theta_j - \theta_{j-1}) \end{pmatrix}$$

$$\mathbf{\Omega}_j = \left(0, \frac{2}{l}\tan\left(\frac{\theta_j - \theta_{j-1}}{2}\right), 0\right)^T$$

We also have

$\mathbf{u}^0 = (\cos\theta_0, 0, -\sin\theta_0)^T \qquad \text{and} \qquad \mathbf{v}^0 = (0, 1, 0)^T$

From which we can find

$\mathbf{u}^j = (X, 0, X)^T \qquad \text{and} \qquad \mathbf{v}^j = (0, 1, 0)^T$

We also notice that

$\mathbf{m}_1^j = \mathbf{u}^j \qquad \text{and} \qquad \mathbf{m}_2^j = \mathbf{v}^j$

From which we find

$$\omega_{1j} = 0 \qquad \text{and} \qquad \omega_{2j} = \frac{2}{l}\tan\left(\frac{\theta_j - \theta_{j-1}}{2}\right)$$

Now we clearly have $m_j = 0$ so we can write:

$$E(R) = \sum_{j=1}^{n} \frac{B_2}{2l} \tan^2 \left(\frac{\theta_j - \theta_{j-1}}{2} \right)$$

This result is exactly as in chapter 4, verifying that this three dimensional model does indeed reduce to two dimensions when we limit the motion to a deformation in the $y - z$ plane.

9.6 Example Eight

We now reproduce the same simulation as in example three but this time in three dimensions with a thin rod rather than a curve.

We again set up an optimisation problem by minimising E, such that the start of the rod is fixed at the origin and the end of the rod has coordinates (X, Y, Z). That is

$$\sum_{j=0}^{n} l \cos\psi_j \sin\theta_j = X \tag{221}$$

$$\sum_{j=0}^{n} l \sin\psi_j \sin\theta_j = Y \tag{222}$$

$$\sum_{j=0}^{n} l \cos\theta_j = Z \tag{223}$$

Using the Lagrange multiplier technique we consider the problem of minimising the Lagrangian function defined by

$$\Lambda(\theta_0, ..., \theta_n, \psi_0, ..., \psi_n, \phi_0, ..., \phi_n, \lambda_1, \lambda_2, \lambda_3) = E(R)$$

$$+ \lambda_1 \left(\sum_{j=0}^{n} l \cos\psi_j \sin\theta_j - X \right) + \lambda_2 \left(\sum_{j=0}^{n} l \sin\psi_j \sin\theta_j - Y \right) + \lambda_3 \left(\sum_{j=0}^{n} l \cos\theta_j - Z \right) \tag{224}$$

We must now solve the system of $3(n+2)$ equations

$$\frac{\partial E}{\partial \psi_j} - \lambda_1 l \sin\psi_j \sin\theta_j + \lambda_2 l \cos\psi_j \sin\theta_j = 0$$

$$\frac{\partial E}{\partial \theta_j} + \lambda_1 l \cos\psi_j \cos\theta_j + \lambda_2 l \sin\psi_j \cos\theta_j - \lambda_3 l \sin\theta_j = 0 \tag{225}$$

$$\frac{\partial E}{\partial \phi_j} = 0$$

10 Concluding Remarks

Unfortunately I was unable to run example eight in AUTO and it became an insurmountable obstacle to moving onto the final model of a connected system of interacting elastic rods. Despite many rewrites, my code would not produce the expected results (or at times, any results at all) which prevented me from progressing beyond this point.

I attempted to trouble shoot the code in several ways:

1. Run the most simple example - A two section rod deforming with no end twist constraint- Neither writing new code for this model, nor adapting the more general code with $n = 2$ produced results (in both cases the rod would not buckle).

2. A starting solution for θ_j, obtained from the two dimensional model - The rod would not deviate from the starting solution as the parameter increased.

3. Simulating the two dimensional problem using the three dimensional code, that is, running the code with $\psi_j = \phi_j = 0$ - Again the rod would not deviate from the starting solution as the parameter increased.

The question remains whether the problem lies in the model or the code. As my model does reduce the the two dimensional case, I feel the problem lies in my attempt to produce code which can numerically solve the equations of example eight.

Had the code produced solutions, I would have been able to connect neighbouring rods via springs, as was done in the two dimensional case. The length of each connecting spring would be expressable in terms of the variables θ_j, ψ_j, ϕ_j and so the total spring enery would be too. Extending the model in this way would have allowed similar simulations to those seen in chapter five.

From [19], we have data on the relative positions of each triple helix as the fibril is traversed. It would be possible to choose a starting solution and a value for n such that the coorinates of each vertex match those in the experimental data, providing a starting configuration motivated by the structure of a collagen fibril. From this point, deformation simulations would represent the deformation of a collagen fibril, given suitable spring constants.

11 Appendix

11.1 Two dimensional bundle model code

```
SUBROUTINE FUNC(NDIM,U,ICP,PAR,IJAC,F,DFDU,DFDP)
!     ---------- ----

      IMPLICIT DOUBLE PRECISION (A-H,Q-Z)
      PARAMETER (m=2,n=19)
      INTEGER NDIM, ICP(*)
      DOUBLE PRECISION U(NDIM),PAR(*),F(NDIM)
      DIMENSION xB(m),xkappa(0:m,0:n+1),xGs(m-1,0:n+1)
      DIMENSION xlambda1(m),xlambda2(m),th(m,-1:n+1)
      DIMENSION xG(0:m,0:n+1)
      DIMENSION xinc(0:n),yinc(0:n)
      DIMENSION x(0:m,0:n+1),y(0:m,0:n+1),z(0:m,0:n+1)
      DIMENSION xinc1(0:n),dldxlambda1(m)
      DIMENSION xinc2(0:n),dldxlambda2(m)
      DIMENSION xinc3(n+1),dldth(m,0:n)

!system dimension = m(n+3)

!parameters:

!xd = end displacement = par(1)
!xmu = homotopy parameter = par(2)

!constants:

!xl = natural length of curve sections
!xB(i) = bending stiffness of curve i
!xkappa(i,j) = spring constant of connecting spring z(i,j)
!xG0 = initial gap between rods in a fresh run from straight rods and at j=0 and j=n
!xGs(i,j) = initial gap between rod verticies (before springs are tightened)

!variables:

!xlambda1(i) = lagrange multiplier 1 of curve i
!xlambda2(i) = lagrange multiplier 2 of curve i
!th(i,j) = system angles

!-----------------------------------------------------------------------

!parameters

      xd = par(1)

      xmu = par(2)

!constants

      xl = 1d0/(n+1d0)

      do i=1,m
      xB(i)=1d0
      enddo

      do i=0,m
      do j=0,n+1
      xkappa(i,j)=0d0
      enddo
      enddo

      xkappa(1,10)=10000d0

      xG0 = 1d0/(n+1d0)

      do i=1,m-1
      do j=0,n+1
      read(30,*) xGs(i,j)
      enddo
```

```
      enddo
      rewind(30)

!continuation in mu

      do i=0,m
      do j=0,n+1
      xG(i,j)=xG0
      enddo
      enddo

      do i=1,m-1
      do j=0,n+1
      xG(i,j)=(1-xmu)*xGs(i,j)+xmu*xG0
      enddo
      enddo

!variables

      do i=1,m
      xlambda1(i)=u(i)
      enddo

      do i=1,m
      xlambda2(i)=u(m+i)
      enddo

      do i=1,m
      do j=0,n
      th(i,j)=u(2*m+(i-1)*n+i+j)
      enddo
      enddo

!for the sake of notation

      do i=1,m
      th(i,-1)=th(i,0)
      th(i,n+1)=th(i,n)
      enddo

!define the spring lengths and their components z,x,y

      do i=0,m
      do j=0,n+1
      x(i,j)=0d0
      y(i,j)=xG(i,j)
      z(i,j)=xG(i,j)
      enddo
      enddo

      do i=1,m-1
      x(i,0)=0d0
      do j=1,n+1
      sum=0d0
      do k=0,j-1
      xinc(k)=xl*dcos(th(i,k))-xl*dcos(th(i+1,k))
      sum=sum+xinc(k)
      enddo
      x(i,j)=sum
      enddo
      enddo

      do i=1,m-1
      y(i,0)=xG0
      do j=1,n+1
      sum=0d0
      do k=0,j-1
      yinc(k)=xl*dsin(th(i,k))-xl*dsin(th(i+1,k))
      sum=sum+yinc(k)
      enddo
      y(i,j)=xG0+sum
      enddo
      enddo
```

```
      do i=1,m-1
      do j=0,n+1
      z(i,j)=dsqrt(x(i,j)**2+y(i,j)**2)
      enddo
      enddo

!Lagrangian derivative wrt lambda1(i)

      do i=1,m
      sum=0d0
      do j=0,n
      xinc1(j)=xl*dcos(th(i,j))
      sum=sum+xinc1(j)
      enddo
      dldxlambda1(i)=sum-(n+1d0)*xl+xd
      enddo

!Lagrangian derivative wrt lambda2(i)

      do i=1,m
      sum=0d0
      do j=0,n
      xinc2(j)=xl*dsin(th(i,j))
      sum=sum+xinc2(j)
      enddo
      dldxlambda2(i)=sum
      enddo

!Lagrangian derivative wrt th(i,j)

      do i=1,m
      do j=0,n

      sum=0d0

      do k=j+1,n+1

      xinc3(k)= &

      -xl*(xkappa(i-1,k))*(z(i-1,k)-xG(i-1,k))*(1d0/z(i-1,k))*(-x(i-1,k)*dsin(th(i,j))+y(i-1,k)*dcos(th(i,j))) &

      +xl*(xkappa(i,k))*(z(i,k)-xG(i,k))*(1d0/z(i,k))*(-x(i,k)*dsin(th(i,j))+y(i,k)*dcos(th(i,j)))

      sum=sum+xinc3(K)

      enddo

      dldth(i,j) = &

      2*xB(i)*(1/xl)*dtan((th(i,j)-th(i,j-1))/2d0)/((dcos((th(i,j)-th(i,j-1))/2d0))*(dcos((th(i,j)-th(i,j-1))/2d0))) &

      -2*xB(i)*(1/xl)*dtan((th(i,j+1)-th(i,j))/2d0)/((dcos((th(i,j+1)-th(i,j))/2d0))*(dcos((th(i,j+1)-th(i,j))/2d0))) &

      +sum &

      -xlambda1(i)*xl*dsin(th(i,j)) &

      +xlambda2(i)*xl*dcos(th(i,j))

      enddo
      enddo

!equations

      do i=1,m
      F(i) = dldxlambda1(i)
      enddo

      do i=1,m
      F(m+i) = dldxlambda2(i)
      enddo
```

```
      do i=1,m
      do j=0,n
      F(2*m+(i-1)*n+i+j) = dldth(i,j)
      enddo
      enddo

      END SUBROUTINE FUNC

      SUBROUTINE STPNT(NDIM,U,PAR,T)
!     ---------- -----

      IMPLICIT DOUBLE PRECISION (A-H,Q-Z)
      PARAMETER (m=2,n=19)
      INTEGER NDIM
      DOUBLE PRECISION T, U(NDIM), PAR(*)

      read(20,*) par(1), u(1), u(2), u(3), u(4)

      do j=0,n
      read(21,*) u(2*m+1+j)
      enddo

      do j=0,n
      read(22,*) u(2*m+n+2+j)
      enddo

      END SUBROUTINE STPNT

      SUBROUTINE BCND
      END SUBROUTINE BCND

      SUBROUTINE ICND(NDIM,U,PAR,T)
      END SUBROUTINE ICND

      SUBROUTINE FOPT
      END SUBROUTINE FOPT

      SUBROUTINE PVLS
      END SUBROUTINE PVLS
```

11.2 Three dimensional single rod code

```
SUBROUTINE FUNC(NDIM,U,ICP,PAR,IJAC,F,DFDU,DFDP)

      IMPLICIT DOUBLE PRECISION (A-H,O-Z)

      integer xalpha,xbeta,xgamma,xzeta

      PARAMETER (n=4)
      INTEGER NDIM, ICP(*)
      DOUBLE PRECISION U(NDIM), PAR(*), F(NDIM)

      DIMENSION psi(0:n),th(0:n),phi(0:n)

      DIMENSION t(0:n,3)

      DIMENSION b(0:n+1,3),c(n),h(0:n+1)

      DIMENSION R(n,3,3)

      DIMENSION xincP(3),P(0:n,3,3)

      DIMENSION xincxu(3),xu(0:n,3)

      DIMENSION xincxv(3),xv(0:n,3)

      DIMENSION bigomega(n,3)

      DIMENSION w1(0:n,3),w2(0:n,3)

      DIMENSION xm1(0:n,3),xm2(0:n,3)

      DIMENSION xincomega1(3),omega1(0:n+1)

      DIMENSION xincomega2(3),omega2(0:n+1)

      DIMENSION xm(0:n+1)

      DIMENSION dbdpsi(n,0:n,3),dcdpsi(n,0:n)

      DIMENSION dbdth(n,0:n,3),dcdth(n,0:n)

      DIMENSION dRdpsi(n,0:n,3,3),dRdth(n,0:n,3,3)

      DIMENSION xincdPdpsi0(3),xincdPdpsi1(3),xincdPdpsixzeta(3),dPdpsi(0:n,0:n,3,3)

      DIMENSION xincdPdth0(3),xincdPdth1(3),xincdPdthxzeta(3),dPdth(0:n,0:n,3,3)

      DIMENSION du0dpsi(0:n,3),du0dth(0:n,3)

      DIMENSION dv0dpsi(0:n,3),dv0dth(0:n,3)

      DIMENSION dbigomegadpsi(n,0:n,3)

      DIMENSION dbigomegadth(n,0:n,3)

      DIMENSION dw1dpsi(0:n,0:n,3),dw1dth(0:n,0:n,3)

      DIMENSION dw2dpsi(0:n,0:n,3),dw2dth(0:n,0:n,3)

      DIMENSION xincdm1dpsi(3),dm1dpsi(0:n,0:n,3)

      DIMENSION xincdm1dth(3),dm1dth(0:n,0:n,3)

      DIMENSION xincdm2dpsi(3),dm2dpsi(0:n,0:n,3)

      DIMENSION xincdm2dth(3),dm2dth(0:n,0:n,3)

      DIMENSION xincdomega1dpsi(3),domega1dpsi(n,0:n)

      DIMENSION xincdomega1dth(3),domega1dth(n,0:n)

      DIMENSION xincdomega2dpsi(3),domega2dpsi(n,0:n)
```

```
      DIMENSION xincdomega2dth(3),domega2dth(n,0:n)

      DIMENSION xincdEdpsi(n),dEdpsi(0:n)

      DIMENSION xincdEdth(n),dEdth(0:n)

      DIMENSION xincdEdphi(3),dEdphi(0:n)

      DIMENSION xincsumone(0:n),xincsumtwo(0:n),xincsumthree(0:n)

!system dimension = 3n+6

!constants

!xl = natural length of rod sections
!xB1 = bending stiffness
!xB2 = bending stiffness
!xC =  twisting stiffness

!parameters

!xd = end displacement (in the negative z direction)

!variables

!lagrange multipliers

!xlambda1 = end force (x)
!xlambda2 = end force (y)
!xlambda3 = end force (z)
!xlambda4 = spin controll

!euler angles

!psi(k)
!th(k)
!phi(k)

!-----------------------------------------------------------------------

!constants

      xl = 1d0/(n+1d0)

      xB1 = 4d0

      xB2 = 1d0

      xC  = 2d0

!parameters

      xd = par(1)

!variables

      xlambda1 = u(1)

      xlambda2 = u(2)

      xlambda3 = u(3)

      do j=0,n

      psi(j) = u(4+j)

      enddo

      do j=0,n

      th(j) = u(n+5+j)
```

```
      enddo

      do j=0,n

      phi(j) = u(2*n+6+j)

      enddo

!define t^{j} for j=0,...,n

      do j=0,n

      t(j,1) = dcos(psi(j))*dsin(th(j))

      t(j,2) = dsin(psi(j))*dsin(th(j))

      t(j,3) = dcos(th(j))

      enddo

!define b_{j} for j=0,...,n+1

      do xalpha=1,3
      b(0,xalpha) = 0d0
      b(n+1,xalpha) = 0d0
      enddo

      do j=1,n

      b(j,1) = t(j-1,2)*t(j,3)-t(j-1,3)*t(j,2)

      b(j,2) =-t(j-1,1)*t(j,3)+t(j-1,3)*t(j,1)

      b(j,3) = t(j-1,1)*t(j,2)-t(j-1,2)*t(j,1)

      enddo

!define c_{j} for j=1,...,n

      do j=1,n

      c(j) = t(j-1,1)*t(j,1)+t(j-1,2)*t(j,2)+t(j-1,3)*t(j,3)

      enddo

!define h_{j} for j=0,...,n+1

      h(0) = 0d0
      h(n+1) = 0d0

      do j=1,n

      h(j) = 1d0/(1d0+c(j))

      enddo

!define R_{j} for j=1,...,n

      do j=1,n

      R(j,1,1) = c(j)+h(j)*b(j,1)*b(j,1)

      R(j,1,2) = h(j)*b(j,1)*b(j,2)-b(j,3)

      R(j,1,3) = h(j)*b(j,1)*b(j,3)+b(j,2)

      R(j,2,1) = h(j)*b(j,1)*b(j,2)+b(j,3)

      R(j,2,2) = c(j)+h(j)*b(j,2)*b(j,2)

      R(j,2,3) = h(j)*b(j,2)*b(j,3)-b(j,1)

      R(j,3,1) = h(j)*b(j,1)*b(j,3)-b(j,2)
```

```
      R(j,3,2) = h(j)*b(j,2)*b(j,3)+b(j,1)

      R(j,3,3) = c(j)+h(j)*b(j,3)*b(j,3)

      enddo

      do i=1,3
      write(1,'(45(1x,e17.8e3))') (R(1,i,j) ,j=1,3)
      enddo

!define P_{j} for j=0,...,n

      P(0,1,1) = 1d0
      P(0,1,2) = 0d0
      P(0,1,3) = 0d0
      P(0,2,1) = 0d0
      P(0,2,2) = 1d0
      P(0,2,3) = 0d0
      P(0,3,1) = 0d0
      P(0,3,2) = 0d0
      P(0,3,3) = 1d0

      do j=1,n

      do xalpha=1,3
      do xbeta=1,3
      sum=0d0
      do xgamma=1,3
      xincP(xgamma) = R(j,xalpha,xgamma)*P(j-1,xgamma,xbeta)
      sum = sum + xincP(xgamma)
      enddo
      P(j,xalpha,xbeta) = sum
      enddo
      enddo

      enddo

!define u^{j} for j=0,...,n

      xu(0,1) = dcos(psi(0))*dcos(th(0))

      xu(0,2) = dsin(psi(0))*dcos(th(0))

      xu(0,3) =-dsin(th(0))

      do j=1,n

      do xalpha=1,3
      sum=0d0
      do xgamma=1,3
      xincxu(xgamma) = P(j,xalpha,xgamma)*xu(0,xgamma)
      sum = sum + xincxu(xgamma)
      enddo
      xu(j,xalpha) = sum
      enddo

      enddo

!define v^{j} for j=0,...,n

      xv(0,1) =-dsin(psi(0))

      xv(0,2) = dcos(psi(0))

      xv(0,3) = 0d0

      do j=1,n

      do xalpha=1,3
      sum=0d0
      do xgamma=1,3
      xincxv(xgamma) = P(j,xalpha,xgamma)*xv(0,xgamma)
```

```
      sum = sum + xincxv(xgamma)
      enddo
      xv(j,xalpha) = sum
      enddo

      enddo

!define bigomega_{j} for j=1,...,n

      do j=1,n

      do xalpha=1,3
      bigomega(j,xalpha) = (2d0/xl)*h(j)*b(j,xalpha)
      enddo

      enddo

!define w1^{j} for j=0,...,n

      do j=0,n

      do xalpha=1,3
      w1(j,xalpha) = dcos(phi(j))*xu(0,xalpha)+dsin(phi(j))*xv(0,xalpha)
      enddo

      enddo

!define w2^{j} for j=0,...,n

      do j=0,n

      do xalpha=1,3
      w2(j,xalpha) =-dsin(phi(j))*xu(0,xalpha)+dcos(phi(j))*xv(0,xalpha)
      enddo

      enddo

!define m1^{j} for j=0,...,n

      do j=0,n

      do xalpha=1,3
      xm1(j,xalpha) = dcos(phi(j))*xu(j,xalpha)+dsin(phi(j))*xv(j,xalpha)
      enddo

      enddo

!define m2^{j} for j=0,...,n

      do j=0,n

      do xalpha=1,3
      xm2(j,xalpha) =-dsin(phi(j))*xu(j,xalpha)+dcos(phi(j))*xv(j,xalpha)
      enddo

      enddo

!define omega1_{j} for j=0,...,n+1

      omega1(0) = 0d0
      omega1(n+1) = 0d0

      do j=1,n

      sum=0d0
      do xgamma=1,3
      xincomega1(xgamma) = bigomega(j,xgamma)*(xm1(j-1,xgamma)+xm1(j,xgamma))
      sum = sum + xincomega1(xgamma)
      enddo
      omega1(j) = (sum)/(2d0)

      enddo
```

```
!define omega2_{j} for j=0,...,n+1

      omega2(0) = 0d0
      omega2(n+1) = 0d0

      do j=1,n

      sum=0d0
      do xgamma=1,3
      xincomega2(xgamma) = bigomega(j,xgamma)*(xm2(j-1,xgamma)+xm2(j,xgamma))
      sum = sum + xincomega2(xgamma)
      enddo
      omega2(j) = (sum)/(2d0)

      enddo

!define m for j=0,..,n+1

      xm(0) = 0d0
      xm(n+1) = 0d0

      do j=1,n

      xm(j) = (phi(j)-phi(j-1))/(xl)

      enddo

!define derivatives of b_{k,1},b_{k,2},b_{k,3},c_{k} wrt psi(k) for k=1,...,n

      do k=1,n

      dbdpsi(k,k,1) =-dcos(th(k-1))*dcos(psi(k))*dsin(th(k))

      dbdpsi(k,k,2) =-dcos(th(k-1))*dsin(psi(k))*dsin(th(k))

      dbdpsi(k,k,3) = dcos(psi(k-1))*dsin(th(k-1))*dcos(psi(k))*dsin(th(k)) &
     +dsin(psi(k-1))*dsin(th(k-1))*dsin(psi(k))*dsin(th(k))

      dcdpsi(k,k) =-b(k,3)

      enddo

!define derivatives of b_{k+1,1},b_{k+1,2},b_{k+1,3},c_{k+1} wrt psi(k) for k=0,...,n-1

      do k=0,n-1

      dbdpsi(k+1,k,1) = dcos(psi(k))*dsin(th(k))*dcos(th(k+1))

      dbdpsi(k+1,k,2) = dsin(psi(k))*dsin(th(k))*dcos(th(k+1))

      dbdpsi(k+1,k,3) =-dsin(psi(k))*dsin(th(k))*dsin(psi(k+1))*dsin(th(k+1)) &
                       -dcos(psi(k))*dsin(th(k))*dcos(psi(k+1))*dsin(th(k+1))

      dcdpsi(k+1,k) = b(k+1,3)

      enddo

!define derivatives of b_{k,1},b_{k,2},b_{k,3},c_{k} wrt th(k) for k=1,...,n

      do k=1,n

      dbdth(k,k,1) =-dsin(psi(k-1))*dsin(th(k-1))*dsin(th(k))-dcos(th(k-1))*dsin(psi(k))*dcos(th(k))

      dbdth(k,k,2) = dcos(psi(k-1))*dsin(th(k-1))*dsin(th(k))+dcos(th(k-1))*dcos(psi(k))*dcos(th(k))

      dbdth(k,k,3) = dcos(psi(k-1))*dsin(th(k-1))*dsin(psi(k))*dcos(th(k)) &
    -dsin(psi(k-1))*dsin(th(k-1))*dcos(psi(k))*dcos(th(k))

      dcdth(k,k) = dcos(psi(k-1))*dsin(th(k-1))*dcos(psi(k))*dcos(th(k)) &
  +dsin(psi(k-1))*dsin(th(k-1))*dsin(psi(k))*dcos(th(k)) &
  -dcos(th(k-1))*dsin(th(k))

      enddo
```

```
!define derivatives of b_{k+1,1},b_{k+1,2},b_{k+1,3},c_{k+1} wrt th(k) for k=0,...,n-1

      do k=0,n-1

      dbdth(k+1,k,1) = dsin(psi(k))*dcos(th(k))*dcos(th(k+1))+dsin(th(k))*dsin(psi(k+1))*dsin(th(k+1))

      dbdth(k+1,k,2) = dcos(psi(k))*dcos(th(k))*dcos(th(k+1))+dsin(th(k))*dcos(psi(k+1))*dsin(th(k+1))

      dbdth(k+1,k,3) = dcos(psi(k))*dcos(th(k))*dsin(psi(k+1))*dsin(th(k+1)) &
      -dsin(psi(k))*dcos(th(k))*dcos(psi(k+1))*dsin(th(k+1))

      dcdth(k+1,k) = dcos(psi(k))*dcos(th(k))*dcos(psi(k+1))*dsin(th(k+1)) &
    +dsin(psi(k))*dcos(th(k))*dsin(psi(k+1))*dsin(th(k+1)) &
    -dsin(th(k))*dcos(th(k+1))

      enddo

!define the derivative of R_{k} wrt psi(k) for k=1,...,n

      do k=1,n

      dRdpsi(k,k,1,1) = (1d0-h(k)*h(k)*b(k,1)*b(k,1))*dcdpsi(k,k)+2d0*h(k)*b(k,1)*dbdpsi(k,k,1)

      dRdpsi(k,k,1,2) = h(k)*b(k,1)*dbdpsi(k,k,2)+h(k)*b(k,2)*dbdpsi(k,k,1)-h(k)*h(k)*b(k,1)*b(k,2)*dcdpsi(k,k)-dbdpsi(k,k,3)

      dRdpsi(k,k,1,3) = h(k)*b(k,1)*dbdpsi(k,k,3)+h(k)*b(k,3)*dbdpsi(k,k,1)-h(k)*h(k)*b(k,1)*b(k,3)*dcdpsi(k,k)+dbdpsi(k,k,2)

      dRdpsi(k,k,2,1) = h(k)*b(k,1)*dbdpsi(k,k,2)+h(k)*b(k,2)*dbdpsi(k,k,1)-h(k)*h(k)*b(k,1)*b(k,2)*dcdpsi(k,k)+dbdpsi(k,k,3)

      dRdpsi(k,k,2,2) = (1d0-h(k)*h(k)*b(k,2)*b(k,2))*dcdpsi(k,k)+2d0*h(k)*b(k,2)*dbdpsi(k,k,2)

      dRdpsi(k,k,2,3) = h(k)*b(k,2)*dbdpsi(k,k,3)+h(k)*b(k,3)*dbdpsi(k,k,2)-h(k)*h(k)*b(k,2)*b(k,3)*dcdth(k,k)-dbdpsi(k,k,1)

      dRdpsi(k,k,3,1) = h(k)*b(k,1)*dbdpsi(k,k,3)+h(k)*b(k,3)*dbdpsi(k,k,1)-h(k)*h(k)*b(k,1)*b(k,3)*dcdth(k,k)-dbdpsi(k,k,2)

      dRdpsi(k,k,3,2) = h(k)*b(k,2)*dbdpsi(k,k,3)+h(k)*b(k,3)*dbdpsi(k,k,2)-h(k)*h(k)*b(k,2)*b(k,3)*dcdth(k,k)+dbdpsi(k,k,1)

      dRdpsi(k,k,3,3) = (1d0-h(k)*h(k)*b(k,3)*b(k,3))*dcdpsi(k,k)+2d0*h(k)*b(k,3)*dbdpsi(k,k,3)

      enddo

!define the derivative of R_{k+1} wrt psi(k) for k=0,...,n-1

      do k=0,n-1

      dRdpsi(k+1,k,1,1) = (1d0-h(k+1)*h(k+1)*b(k+1,1)*b(k+1,1))*dcdpsi(k+1,k)+2d0*h(k+1)*b(k+1,1)*dbdpsi(k+1,k,1)

      dRdpsi(k+1,k,1,2) = h(k+1)*b(k+1,1)*dbdpsi(k+1,k,2)+h(k+1)*b(k+1,2)*dbdpsi(k+1,k,1) &
 -h(k+1)*h(k+1)*b(k+1,1)*b(k+1,2)*dcdpsi(k+1,k)-dbdpsi(k+1,k,3)

      dRdpsi(k+1,k,1,3) = h(k+1)*b(k+1,1)*dbdpsi(k+1,k,3)+h(k+1)*b(k+1,3)*dbdpsi(k+1,k,1) &
 -h(k+1)*h(k+1)*b(k+1,1)*b(k+1,3)*dcdpsi(k+1,k)+dbdpsi(k+1,k,2)

      dRdpsi(k+1,k,2,1) = h(k+1)*b(k+1,1)*dbdpsi(k+1,k,2)+h(k+1)*b(k+1,2)*dbdpsi(k+1,k,1) &
 -h(k+1)*h(k+1)*b(k+1,1)*b(k+1,2)*dcdpsi(k+1,k)+dbdpsi(k+1,k,3)

      dRdpsi(k+1,k,2,2) = (1d0-h(k+1)*h(k+1)*b(k+1,2)*b(k+1,2))*dcdpsi(k+1,k)+2d0*h(k+1)*b(k+1,2)*dbdpsi(k+1,k,2)

      dRdpsi(k+1,k,2,3) = h(k+1)*b(k+1,2)*dbdpsi(k+1,k,3)+h(k+1)*b(k+1,3)*dbdpsi(k+1,k,2) &
 -h(k+1)*h(k+1)*b(k+1,2)*b(k+1,3)*dcdpsi(k+1,k)-dbdpsi(k+1,k,1)

      dRdpsi(k+1,k,3,1) = h(k+1)*b(k+1,1)*dbdpsi(k+1,k,3)+h(k+1)*b(k+1,3)*dbdpsi(k+1,k,1) &
 -h(k+1)*h(k+1)*b(k+1,1)*b(k+1,3)*dcdpsi(k+1,k)-dbdpsi(k+1,k,2)

      dRdpsi(k+1,k,3,2) = h(k+1)*b(k+1,2)*dbdpsi(k+1,k,3)+h(k+1)*b(k+1,3)*dbdpsi(k+1,k,2) &
 -h(k+1)*h(k+1)*b(k+1,2)*b(k+1,3)*dcdpsi(k+1,k)+dbdpsi(k+1,k,1)

      dRdpsi(k+1,k,3,3) = (1d0-h(k+1)*h(k+1)*b(k+1,3)*b(k+1,3))*dcdpsi(k+1,k)+2d0*h(k+1)*b(k+1,3)*dbdpsi(k+1,k,3)

      enddo

!define the derivative of R_{k} wrt th(k) for k=1,...,n
```

```
      do k=1,n

      dRdth(k,k,1,1) = (1d0-h(k)*h(k)*b(k,1)*b(k,1))*dcdth(k,k)+2d0*h(k)*b(k,1)*dbdth(k,k,1)

      dRdth(k,k,1,2) = h(k)*b(k,1)*dbdth(k,k,2)+h(k)*b(k,2)*dbdth(k,k,1)-h(k)*h(k)*b(k,1)*b(k,2)*dcdth(k,k)-dbdth(k,k,3)

      dRdth(k,k,1,3) = h(k)*b(k,1)*dbdth(k,k,3)+h(k)*b(k,3)*dbdth(k,k,1)-h(k)*h(k)*b(k,1)*b(k,3)*dcdth(k,k)+dbdth(k,k,2)

      dRdth(k,k,2,1) = h(k)*b(k,1)*dbdth(k,k,2)+h(k)*b(k,2)*dbdth(k,k,1)-h(k)*h(k)*b(k,1)*b(k,2)*dcdth(k,k)+dbdth(k,k,3)

      dRdth(k,k,2,2) = (1d0-h(k)*h(k)*b(k,2)*b(k,2))*dcdth(k,k)+2d0*h(k)*b(k,2)*dbdth(k,k,2)

      dRdth(k,k,2,3) = h(k)*b(k,2)*dbdth(k,k,3)+h(k)*b(k,3)*dbdth(k,k,2)-h(k)*h(k)*b(k,2)*b(k,3)*dcdth(k,k)-dbdth(k,k,1)

      dRdth(k,k,3,1) = h(k)*b(k,1)*dbdth(k,k,3)+h(k)*b(k,3)*dbdth(k,k,1)-h(k)*h(k)*b(k,1)*b(k,3)*dcdth(k,k)-dbdth(k,k,2)

      dRdth(k,k,3,2) = h(k)*b(k,2)*dbdth(k,k,3)+h(k)*b(k,3)*dbdth(k,k,2)-h(k)*h(k)*b(k,2)*b(k,3)*dcdth(k,k)+dbdth(k,k,1)

      dRdth(k,k,3,3) = (1d0-h(k)*h(k)*b(k,3)*b(k,3))*dcdth(k,k)+2d0*h(k)*b(k,3)*dbdth(k,k,3)

      enddo

!define the derivative of R_{k+1} wrt th(k) for k=0,...,n-1

      do k=0,n-1

      dRdth(k+1,k,1,1) = (1d0-h(k+1)*h(k+1)*b(k+1,1)*b(k+1,1))*dcdth(k+1,k)+2d0*h(k+1)*b(k+1,1)*dbdth(k+1,k,1)

      dRdth(k+1,k,1,2) = h(k+1)*b(k+1,1)*dbdth(k+1,k,2)+h(k+1)*b(k+1,2)*dbdth(k+1,k,1) &
-h(k+1)*h(k+1)*b(k+1,1)*b(k+1,2)*dcdth(k+1,k)-dbdth(k+1,k,3)

      dRdth(k+1,k,1,3) = h(k+1)*b(k+1,1)*dbdth(k+1,k,3)+h(k+1)*b(k+1,3)*dbdth(k+1,k,1) &
-h(k+1)*h(k+1)*b(k+1,1)*b(k+1,3)*dcdth(k+1,k)+dbdth(k+1,k,2)

      dRdth(k+1,k,2,1) = h(k+1)*b(k+1,1)*dbdth(k+1,k,2)+h(k+1)*b(k+1,2)*dbdth(k+1,k,1) &
-h(k+1)*h(k+1)*b(k+1,1)*b(k+1,2)*dcdth(k+1,k)+dbdth(k+1,k,3)

      dRdth(k+1,k,2,2) = (1d0-h(k+1)*h(k+1)*b(k+1,2)*b(k+1,2))*dcdth(k+1,k)+2d0*h(k+1)*b(k+1,2)*dbdth(k+1,k,2)

      dRdth(k+1,k,2,3) = h(k+1)*b(k+1,2)*dbdth(k+1,k,3)+h(k+1)*b(k+1,3)*dbdth(k+1,k,2) &
-h(k+1)*h(k+1)*b(k+1,2)*b(k+1,3)*dcdth(k+1,k)-dbdth(k+1,k,1)

      dRdth(k+1,k,3,1) = h(k+1)*b(k+1,1)*dbdth(k+1,k,3)+h(k+1)*b(k+1,3)*dbdth(k+1,k,1) &
-h(k+1)*h(k+1)*b(k+1,1)*b(k+1,3)*dcdth(k+1,k)-dbdth(k+1,k,2)

      dRdth(k+1,k,3,2) = h(k+1)*b(k+1,2)*dbdth(k+1,k,3)+h(k+1)*b(k+1,3)*dbdth(k+1,k,2) &
-h(k+1)*h(k+1)*b(k+1,2)*b(k+1,3)*dcdth(k+1,k)+dbdth(k+1,k,1)

      dRdth(k+1,k,3,3) = (1d0-h(k+1)*h(k+1)*b(k+1,3)*b(k+1,3))*dcdth(k+1,k)+2d0*h(k+1)*b(k+1,3)*dbdth(k+1,k,3)

      enddo

!define the derivative of P_{j} wrt psi(k) for j=0,...,n and k=0,...,n

      do j=0,n
      do k=0,n
      do xalpha=1,3
      do xbeta=1,3
      dPdpsi(j,k,xalpha,xbeta) = 0d0
      enddo
      enddo
      enddo
      enddo

!---------------------------------------------------------------------

      do xalpha=1,3
      do xbeta=1,3
      dPdpsi(0,0,xalpha,xbeta) = 0d0
      enddo
      enddo
```

```
      do k=1,n
      do xalpha=1,3
      do xbeta=1,3
      sum=0d0
      do xgamma=1,3
      xincdPdpsi0(xgamma) = dRdpsi(k,k,xalpha,xgamma)*P(k-1,xgamma,xbeta)
      sum = sum + xincdPdpsi0(xgamma)
      enddo
      dPdpsi(k,k,xalpha,xbeta) = sum
      enddo
      enddo
      enddo

!---------------------------------------------------------------------

      do k=0,n-1
      do xalpha=1,3
      do xbeta=1,3
      sum=0d0
      do xgamma=1,3
      xincdPdpsi1(xgamma) = dRdpsi(k+1,k,xalpha,xgamma)*P(k,xgamma,xbeta) &
   +R(k+1,xalpha,xgamma)*dPdpsi(k,k,xgamma,xbeta)
      sum = sum + xincdPdpsi1(xgamma)
      enddo
      dPdpsi(k,k+1,xalpha,xbeta) = sum
      enddo
      enddo
      enddo

!---------------------------------------------------------------------

      do xzeta=2,n
      do k=0,n-xzeta
      do xalpha=1,3
      do xbeta=1,3
      sum=0d0
      do xgamma=1,3
      xincdPdpsixzeta(xgamma) = R(k+xzeta,xalpha,xgamma)*dPdpsi(k+xzeta-1,k,xgamma,xbeta)
      sum = sum + xincdPdpsixzeta(xgamma)
      enddo
      dPdpsi(k+xzeta,k,xalpha,xbeta) = sum
      enddo
      enddo
      enddo
      enddo

!define the derivative of P_{j} wrt th(k) for j=0,...,n and k=0,...,n

      do j=0,n
      do k=0,n
      do xalpha=1,3
      do xbeta=1,3
      dPdth(j,k,xalpha,xbeta) = 0d0
      enddo
      enddo
      enddo
      enddo

!---------------------------------------------------------------------

      do xalpha=1,3
      do xbeta=1,3
      dPdth(0,0,xalpha,xbeta) = 0d0
      enddo
      enddo

      do k=1,n
      do xalpha=1,3
      do xbeta=1,3
      sum=0d0
      do xgamma=1,3
      xincdPdth0(xgamma) = dRdth(k,k,xalpha,xgamma)*P(k-1,xgamma,xbeta)
      sum = sum + xincdPdth0(xgamma)
```

```
      enddo
      dPdth(k,k,xalpha,xbeta) = sum
      enddo
      enddo
      enddo

!---------------------------------------------------------------------

      do k=0,n-1
      do xalpha=1,3
      do xbeta=1,3
      sum=0d0
      do xgamma=1,3
      xincdPdth1(xgamma) = dRdth(k+1,k,xalpha,xgamma)*P(k,xgamma,xbeta) &
  +R(k+1,xalpha,xgamma)*dPdth(k,k,xgamma,xbeta)
      sum = sum + xincdPdth1(xgamma)
      enddo
      dPdth(k,k+1,xalpha,xbeta) = sum
      enddo
      enddo
      enddo

!---------------------------------------------------------------------

      do xzeta=2,n
      do k=0,n-xzeta
      do xalpha=1,3
      do xbeta=1,3
      sum=0d0
      do xgamma=1,3
      xincdPdthxzeta(xgamma) = R(k+xzeta,xalpha,xgamma)*dPdth(k+xzeta-1,k,xgamma,xbeta)
      sum = sum + xincdPdthxzeta(xgamma)
      enddo
      dPdth(k+xzeta,k,xalpha,xbeta) = sum
      enddo
      enddo
      enddo
      enddo

!define derivatives of u^{0} wrt psi(k) for k=0,...,n

      do k=0,n
      do xalpha=1,3
      du0dpsi(k,xalpha) = 0d0
      enddo
      enddo

      do xalpha=1,3
      du0dpsi(0,xalpha) = dcos(th(0))*xv(0,xalpha)
      enddo

!define derivatives of u^{0} wrt th(k) for k=0,...,n

      do k=0,n
      do xalpha=1,3
      du0dth(k,xalpha) = 0d0
      enddo
      enddo

      do xalpha=1,3
      du0dth(0,xalpha) = -t(0,xalpha)
      enddo

!define derivatives of v^{0} wrt psi(k) for k=0,...,n

      do k=0,n
      do xalpha=1,3
      dv0dpsi(k,xalpha) = 0d0
      enddo
      enddo

      dv0dpsi(0,1) =-dcos(psi(0))
      dv0dpsi(0,2) =-dsin(psi(0))
```

```
      dv0dpsi(0,3) = 0d0


!define derivatives of v^{0} wrt th(k) for k=0,...,n

      do k=0,n
      do xalpha=1,3
      dv0dth(k,xalpha) = 0d0
      enddo
      enddo

!define the derivative of bigomega_{j} wrt psi(k) for j=1,...,n and k=0,...,n

      do j=1,n
      do k=0,n
      do xalpha=1,3

      dbigomegadpsi(j,k,xalpha) = 0d0

      enddo
      enddo
      enddo

!---------------------------------------------------------------------

      do k=1,n
      do xalpha=1,3

      dbigomegadpsi(k,k,xalpha) = (2d0/xl)*h(k)*(dbdpsi(k,k,xalpha)-h(k)*dcdpsi(k,k)*b(k,xalpha))

      enddo
      enddo

!---------------------------------------------------------------------

      do k=0,n-1
      do xalpha=1,3

      dbigomegadpsi(k+1,k,xalpha) = (2d0/xl)*h(k+1)*(dbdpsi(k+1,k,xalpha)-h(k+1)*dcdpsi(k+1,k)*b(k+1,xalpha))

      enddo
      enddo

!define the derivative of bigomega_{j} wrt th(k) for j=1,...,n and k=0,...,n

      do j=1,n
      do k=0,n
      do xalpha=1,3

      dbigomegadth(j,k,xalpha) = 0d0

      enddo
      enddo
      enddo

!---------------------------------------------------------------------

      do k=1,n
      do xalpha=1,3

      dbigomegadth(k,k,xalpha) = (2d0/xl)*h(k)*(dbdth(k,k,xalpha)-h(k)*dcdth(k,k)*b(k,xalpha))

      enddo
      enddo

!---------------------------------------------------------------------

      do k=0,n-1
      do xalpha=1,3

      dbigomegadth(k+1,k,xalpha) = (2d0/xl)*h(k+1)*(dbdth(k+1,k,xalpha)-h(k+1)*dcdth(k+1,k)*b(k+1,xalpha))

      enddo
```

```
      enddo

!define the derivative of w1^{j} wrt psi(k) for j=0,...,n

      do j=0,n
      do k=0,n
      do xalpha=1,3
      dw1dpsi(j,k,xalpha) = dcos(phi(j))*du0dpsi(k,xalpha)+dsin(phi(j))*dv0dpsi(k,xalpha)
      enddo
      enddo
      enddo

!define the derivative of w1^{j} wrt th(k) for j=0,...,n

      do j=0,n
      do k=0,n
      do xalpha=1,3
      dw1dth(j,k,xalpha) = dcos(phi(j))*du0dth(k,xalpha)+dsin(phi(j))*dv0dth(k,xalpha)
      enddo
      enddo
      enddo

!define the derivative of w2^{j} wrt psi(k) for j=0,...,n

      do j=0,n
      do k=0,n
      do xalpha=1,3
      dw2dpsi(j,k,xalpha) = -dsin(phi(j))*du0dpsi(k,xalpha)+dcos(phi(j))*dv0dpsi(k,xalpha)
      enddo
      enddo
      enddo

!define the derivative of w2^{j} wrt th(k) for j=0,...,n

      do j=0,n
      do k=0,n
      do xalpha=1,3
      dw2dth(j,k,xalpha) = -dsin(phi(j))*du0dth(k,xalpha)+dcos(phi(j))*dv0dth(k,xalpha)
      enddo
      enddo
      enddo

!define the derivative of m1^{j} wrt psi(k) for j=0,...,n and k=0,...,n

      do j=0,n
      do k=0,n
      do xalpha=1,3
      sum=0d0
      do xgamma=1,3
      xincdm1dpsi(xgamma) = dPdpsi(j,k,xalpha,xgamma)*w1(j,xgamma) &
   +P(j,xalpha,xgamma)*dw1dpsi(j,k,xgamma)
      sum = sum + xincdm1dpsi(xgamma)
      enddo
      dm1dpsi(j,k,xalpha) = sum
      enddo
      enddo
      enddo

!define the derivative of m1^{j} wrt th(k) for j=0,...,n and k=0,...,n

      do j=0,n
      do k=0,n
      do xalpha=1,3
      sum=0d0
      do xgamma=1,3
      xincdm1dth(xgamma) = dPdth(j,k,xalpha,xgamma)*w1(j,xgamma) &
   +P(j,xalpha,xgamma)*dw1dth(j,k,xgamma)
      sum = sum + xincdm1dth(xgamma)
      enddo
      dm1dth(j,k,xalpha) = sum
      enddo
      enddo
      enddo
```

```
!define the derivative of m2^{j} wrt psi(k) for j=0,...,n and k=0,...,n

      do j=0,n
      do k=0,n
      do xalpha=1,3
      sum=0d0
      do xgamma=1,3
      xincdm2dpsi(xgamma) = dPdpsi(j,k,xalpha,xgamma)*w2(j,xgamma) &
   +P(j,xalpha,xgamma)*dw2dpsi(j,k,xgamma)
      sum = sum + xincdm2dpsi(xgamma)
      enddo
      dm2dpsi(j,k,xalpha) = sum
      enddo
      enddo
      enddo

!define the derivative of m2^{j} wrt th(k) for j=0,...,n and k=0,...,n

      do j=0,n
      do k=0,n
      do xalpha=1,3
      sum=0d0
      do xgamma=1,3
      xincdm2dth(xgamma) = dPdth(j,k,xalpha,xgamma)*w2(j,xgamma) &
   +P(j,xalpha,xgamma)*dw2dth(j,k,xgamma)
      sum = sum + xincdm2dth(xgamma)
      enddo
      dm2dth(j,k,xalpha) = sum
      enddo
      enddo
      enddo

!define the derivative of omega1_{j} wrt psi(k) for j=1,...,n and k=0,...,n

      do j=1,n
      do k=0,n
      sum=0d0
      do xgamma=1,3
      xincdomega1dpsi(xgamma) = bigomega(j,xgamma)*(dm1dpsi(j-1,k,xgamma)+dm1dpsi(j,k,xgamma)) &
       +dbigomegadpsi(j,k,xgamma)*(xm1(j-1,xgamma)+xm1(j,xgamma))
      sum = sum + xincdomega1dpsi(xgamma)
      enddo
      domega1dpsi(j,k) = (sum)/(2d0)
      enddo
      enddo

!define the derivative of omega1_{j} wrt th(k) for j=1,...,n and k=0,...,n

      do j=1,n
      do k=0,n
      sum=0d0
      do xgamma=1,3
      xincdomega1dth(xgamma) = bigomega(j,xgamma)*(dm1dth(j-1,k,xgamma)+dm1dth(j,k,xgamma)) &
       +dbigomegadth(j,k,xgamma)*(xm1(j-1,xgamma)+xm1(j,xgamma))
      sum = sum + xincdomega1dth(xgamma)
      enddo
      domega1dth(j,k) = (sum)/(2d0)
      enddo
      enddo

!define the derivative of omega2_{j} wrt psi(k) for j=1,...,n and k=0,...,n

      do j=1,n
      do k=0,n
      sum=0d0
      do xgamma=1,3
      xincdomega2dpsi(xgamma) = bigomega(j,xgamma)*(dm2dpsi(j-1,k,xgamma)+dm2dpsi(j,k,xgamma)) &
       +dbigomegadpsi(j,k,xgamma)*(xm2(j-1,xgamma)+xm2(j,xgamma))
      sum = sum + xincdomega2dpsi(xgamma)
      enddo
      domega2dpsi(j,k) = (sum)/(2d0)
      enddo
```

```
      enddo

!define the derivative of omega2_{j} wrt th(k) for j=1,...,n and k=0,...,n

      do j=1,n
      do k=0,n
      sum=0d0
      do xgamma=1,3
      xincdomega2dth(xgamma) = bigomega(j,xgamma)*(dm2dth(j-1,k,xgamma)+dm2dth(j,k,xgamma)) &
       +dbigomegadth(j,k,xgamma)*(xm2(j-1,xgamma)+xm2(j,xgamma))
      sum = sum + xincdomega2dth(xgamma)
      enddo
      domega2dth(j,k) = (sum)/(2d0)
      enddo
      enddo

!define the derivative of E wrt psi(k) for k=0,...,n

      do k=0,n
      sum=0d0
      do j=1,n
      xincdEdpsi(j) = xB1*omega1(j)*domega1dpsi(j,k) &
     +xB2*omega2(j)*domega2dpsi(j,k)
      sum = sum + xincdEdpsi(j)
      enddo
      dEdpsi(k) = xl*(sum)
      enddo

!define the derivative of E wrt th(k) for k=0,...,n

      do k=0,n
      sum=0d0
      do j=1,n
      xincdEdth(j) = xB1*omega1(j)*domega1dth(j,k) &
    +xB2*omega2(j)*domega2dth(j,k)
      sum = sum + xincdEdth(j)
      enddo
      dEdth(k) = xl*(sum)
      enddo

!define the derivative of E wrt phi(k) for k=0,...,n

      do k=0,n
      sum=0d0
      do xalpha=1,3
      xincdEdphi(xalpha) = xB1*(omega1(k)*h(k)*b(k,xalpha)+omega1(k+1)*h(k+1)*b(k+1,xalpha))*xm2(k,xalpha) &
  -xB2*(omega2(k)*h(k)*b(k,xalpha)+omega2(k+1)*h(k+1)*b(k+1,xalpha))*xm1(k,xalpha)
      sum = sum +xincdEdphi(xalpha)
      enddo
      dEdphi(k) = sum + xC*(xm(k)-xm(k+1))
      enddo

!derivatives wrt the lagrage multipliers

      sum=0d0
      do j=0,n
      xincsumone(j)=xl*dcos(psi(j))*dsin(th(j))
      sum = sum + xincsumone(j)
      enddo
      sumone = sum

      sum=0d0
      do j=0,n
      xincsumtwo(j)=xl*dsin(psi(j))*dsin(th(j))
      sum = sum + xincsumtwo(j)
      enddo
      sumtwo = sum

      sum=0d0
      do j=0,n
      xincsumthree(j)=xl*dcos(th(j))
      sum = sum + xincsumthree(j)
      enddo
```

```
      sumthree = sum

!equations

      F(1) = sumone

      F(2) = sumtwo

      F(3) = sumthree - (n+1d0)*xl + xd

      do k=0,n
      F(4+k) = dEdpsi(k) &
      -xlambda1*xl*dsin(psi(k))*dsin(th(k)) &
      +xlambda2*xl*dcos(psi(k))*dsin(th(k))
      enddo

      do k=0,n
      F(n+5+k) = dEdth(k) &
        +xlambda1*xl*dcos(psi(k))*dcos(th(k)) &
        +xlambda2*xl*dcos(psi(k))*dsin(th(k)) &
-xlambda3*xl*dsin(th(k))
      enddo

      do k=0,n
      F(2*n+6+k) = dEdphi(k)
      enddo

      END SUBROUTINE FUNC

      SUBROUTINE STPNT(NDIM,U,PAR,T)
!     ---------- -----

      IMPLICIT DOUBLE PRECISION (A-H,Q-Z)
      PARAMETER (n=4)
      INTEGER NDIM
      DOUBLE PRECISION T, U(NDIM), PAR(*)

      par(1) = 0d0

      do j=0,n
      u(2*n+6+j) = 0d0
      enddo

      END SUBROUTINE STPNT

      SUBROUTINE BCND
      END SUBROUTINE BCND

      SUBROUTINE ICND(NDIM,U,PAR,T)
      END SUBROUTINE ICND

      SUBROUTINE FOPT
      END SUBROUTINE FOPT

      SUBROUTINE PVLS
      END SUBROUTINE PVLS
```

References

[1] P.Fratzl. 2008. Collagen, structure and mechanics.
Springer.

[2] T. Creighton 1992. Proteins: Structures and Molecular Properties.
W. H. Freeman

[3] K. Beck, B. Brodsky. 1998. Supercoiled protein motifs: The collagen triple-helix and the alpha helical coiled coil.
Journal of Structural Biology 122, 17-29.

[4] A. Gautieri, S. Vesentini, A. Redaelli, M. Buehler. 2010. Hierarchical structure and nanomechanics of collagen microfibrils from the atomistic scale up.
Nano Letters 11, 757-766.

[5] J. Graham, A. N. Vomund, C. Phillips, M. Grandbois. 2004. Structural changes in human type I collagen fibrils investigated by force spectroscopy.
Exp cell res 299,2, 335-342.

[6] J. Petruska, A. Hodge. 1964. A subunit model for the tropocollagen macromolecule.
PNAS 51,5, 871.

[7] J. Molnar, KS. Fong, QP. He, K. Hayashi, Y. Kim, SF. Fong, B. Fogelgren, KM. Szauter, M. Mink, K. Csiszar. 2003. Structural and funtional diversity of lysyl oxadise and the LOX-like proteins.
Biochim Biophys Acta 1647, 220-224.

[8] H. Londish, A. Berk, S. Zipursky, P. Matsudaira, D. Baltimore, J. Darnell. 1999. Molecular cell biology.
W. H. Freeman.

[9] M. Buehler. 2008. Nanomechanics of collagen fibrils under varying cross-link densities: Atomistic and continuum studies.
Journal of The Mechanical Behavior of Biomedical Materials 1, 59-67.

[10] P. Chen. 2012. Biological materials: Functional adaptations and bioinspired designs.
Progress in Materials Science. 57,8, 1492-1704

[11] J. Smith. 1968. Molecular pattern in native collagen.
Nature 219, 157-158.

[12] B. Trus, K. Piez. 1980. Compressed microfibril models of the native collagen fibril.
Nature 286, 300-301.

[13] D. Hulmes, T. Wess, D. Prockop, P. Fratzl. 1995. Radial packing, order, and disorder in collagen fibrils.
Biophys. J 68, 1661-1670.

[14] T. Wess, A. Hammersley, L. Wess, A. Miller. 1998. A consensus model for molecular packing of type 1 collagen.
Journal of Structural Biology 122, 92-100

[15] M. Buehler. 2006. Nature designs tough collagen: Explaining the nanostructure of collagen fibrils.
Acad. Sci. USA 103, 1228512290

[16] M. Raspanti, M. Reguzzoni, M. Protasoni, D. Martini. 2011. Evidence of a discrete axial structure in unimodal collagen fibrils
Biomacromolecules 12,12, 4344-4347

[17] J. Orgel, T. Irving, A. Miller, T. Wess. 2006. Microfibrillar structure of type I collagen in situ.
PNAS 103,24, 9001-9005

[18] I. Streeter, N. de Leeuw. 2010. Atomistic modeling of collagen proteins in their fibrillar environment.
J. Phys. Chem. B 114, 1326313270

[19] https://wiki.ucl.ac.uk/display/ ucesest/Cross-sectional+lattices+of+the+collagen+fibril

[20] A.Travers, J.Thompson. 2004. An introduction to the mechanics of DNA.
Phil. Trans. r. soc. lond 362, 1265-1279

[21] L. Bozec, G. van der Heijden, M. Horton. 2007. Collagen fibrils: nanoscale ropes.
Biophysical Journal 92, 70-75

[22] C. Heussinger, F. Schuller, R. Frey. 2010. Statics and dynamics of the wormlike bundle model.
Physical Review 81, 021904

[23] M. Wenger, L. Bozec, M. Horton, P. Mesquida. 2007. Mechanical properties of collage fibrils
J. Biophysical Journal 93(4), 1255-1263

[24] E. Doedel, B. Oldeman. 2009. AUTO-07P : Continuation and bifurcation software for ordinary differential equations.
Developer notes

[25] C. Fraser. 1991. Mathematical technique and physical conception in Eulers investigation of the elastica.
Centaurus 34,3, 211-246

[26] B. Horn. 1981. The curve of least energy.
Technical Report A.I. memo 612

[27] D. Bertsekas. 1996. Constrained optimization and Lagrange multiplier methods.
Athena Scientific 7

[28] P.Howell, G. Kozyreff, J. Ockendon. 2009. Applied Solid Mechanics.
Cambridge University Press

[29] T. Atanackovic. 1997. Stability theory of elastic rods.
World scientific

[30] A. Bruckstein, R. Holt, A. Netravali. 1996. Discrete elastica.
Lecture Notes in computer science 1176, 59-72

[31] H. Lamb 1897. An elementary course of infinitesimal calculus.
Cambridge University Press 406

[32] R. Bishop. 1975. There is more than one way to frame a curve.
The American Mathematical Monthly 82,3, 246-251

[33] J. Stoker. 2011. Differential Geometry.
Pure and Applied Mathematics 20, 82

[34] A. Pressley. 2010. Elementary differential geometry.
Springer

[35] M. Spivak. 1999. A Comprehensive Introduction to Differential Geometry (Volume Two).
Publish or Perish, Inc

[36] S. Sternberg. 1964. Lectures on Differential Geometry.
Publish or Perish, Inc

[37] A. Hanson, H. Ma. 1995. Parallel Transport Approach to Curve Framing.
Technical Report TR425

[38] M. Karacan, B. Bukcu. 2010. On natural curvatures of Bishop frame.
Journal of Vectorial Relativity 5,4

[39] A. Love. 1944. A Treatise on the Mathematical Theory of Elasticity.
Dover publications

[40] S. Timoshenko, J. Goodier. 1970. Theory of Elasticity.
New York, McGraw-Hill

[41] S.Antman. 2005. Nonlinear Problems of Elasticity.
Springer-Verlag

[42] G van der Heijden. 2000. Helical and localised buckling in twisted rods: a unified analysis of the symmetric case.
Nonlinear Dynamics 21, 71-99

[43] M. Langer, D. Singer. 1996. Lagrangian aspects of the Kirchhoff elastic rod.
SIAM Review 38,4

[44] A. Goriely. 2012. Elasticity/Plasticity.
Lecture notes

[45] A. Bobenko and Y. Suris. 2008. Discrete differential geometry.
American Mathematical Society

[46] M. Bergou, M. Wardetzky, S. Robinson, B. Audoly, E. Grinspun. 2007. Discrete elastic rods.
ACM Transactions on Graphics 27,3

[47] T.Moller, J. Hughes. 2000. Efficiently building a matrix to rotate one vector to another.
Journal of Graphics Tools 4,4